School of Science & Engineering
Department of Chemistry

Electrochemical Detection of Biomolecules at Liquid-liquid Interfaces

Shane O'Sullivan

This thesis is presented for the Degree of
Doctor of Philosophy
of
Curtin University

February 2014

Declaration

To the best of my knowledge and belief this thesis contains no material previously published by any other person except where due acknowledgment has been made. This thesis contains no material which has been accepted for the award of any other degree or diploma in any university

Signed: _____

Table of contents

Acknowledgements

First of all I will start by thanking Professor Damien Arrigan. Damien decided he had enough of the Cork weather and moved about as far away as possible, to a very hot and sunny Perth. Fortunately for me, I was able to follow him and join the Irish contingent in Australia. I'm very grateful to have had the opportunity to work with Damien over the course of my PhD. His professionalism in scientific research is something that I have (hopefully) learned from, and will take with me into any future endeavours. Damien allowed me the freedom to work independently, while always being happy to provide any support I may have needed throughout my PhD. It has been a pleasure to work with Damien and I would like to wish him all the best in his future here in Australia.

Next up I would like to thank our research group, which has expanded quite a bit from the early days. Despite being in the isolated city of Perth we seem to be gathering every other nationality to our group besides Aussies! So I'll start with those who were here from the beginning, Eva, Debbie and Mickael. Then we were joined by Salmah and Mazniza, adopted Wade (Junnie) at some point and Krish enjoyed his honours year so much he decided to stay on for a PhD. Recently there have been two more arrivals with Yang and Ghulam joining us. Of course I cannot forget all those Honours and project students we have had in our lab also. It has been a great group to work with over the past few years.

Another thank you to all the people I have worked with outside of our group; my fellow HDR students, all the teaching staff, the admin staff, the technical staff, and those who I have collaborated with both at Curtin University and at the Tyndall National Institute. There are far too many names to mention all of them, and no doubt I would have missed some, so hopefully that list covers everyone. I also wish to thank Curtin University for funding me throughout my PhD.

Finally I would like to thank my family, in particular my mom and dad. Without their support my long career as a professional student wouldn't have been possible. Although they were probably quite content to ship me away to the other side of the world for a few years break from me. I would also like to thank my nan for her support. And last but not least, I would like to thank my partner Jamila (who did not frequently remind me to include her) for her support throughout my PhD. She packs my lunch, she's the best! ☺

Glossary of Major Symbols

Roman symbols

Symbol	Meaning	Units
A	Area	cm^2
a_i	Activity of species i	-
AMI	Acute myocardial infarction	-
C	Capacitance	F
Cdl	Double layer capacitance	F
C_i	Concentration of species i	mol cm^{-3}
d	Centre-to-centre separation in microdiscs or micropores	cm
D	Diffusion coefficient	cm^2 s^{-1}
Da	Daltons	-
e^-	Electrons	-
E	Potential	V
E_{eq}	Equilibrium potential	V
E^0	Standard potential	V
F	Faraday constant	C
G	Gibbs free energy	J mol^{-1}
G^0	Standard Gibbs free energy	J mol^{-1}
i	Current	A

I_{lim}	Limiting current	A
i_{ss}	Steady state current	A
Ji	Flux of species *i*	mol s^{-1} cm^{-2}
ln	Natural Logarithm	-
M	Molarity	mol L^{-1}
m	Mass	g mol^{-1}
n	Number of electrons	-
N	Number of moles	-
o	Organic phase at liquid – liquid interfaces	-
O	Oxidised species in redox reactions	--
q	Charge	C
r	Radius	cm
R	Reduced species in redox reactions	-
	Resistance	Ω
	Resistivity	Ω
	Universal gas constant	J K^{-1} mol^{-1}
t	Time	s
T	Temperature	K
V	Potential difference	V
w	Water / aqueous phase at liquid – liquid interfaces	-
z_i	Charge of species i	-

Greek symbols

Symbol	Meaning	Units
α	Aqueous phase of a liquid – liquid system	-
β	Organic phase of a liquid – liquid system	-
Γ	Surface coverage	-
Δ	Difference	-
δ	Diffusion zone	-
η	Overpotential	V
μ	Micro	-
$\bar{\mu}_i^{\alpha}$	Electrochemical potential of species i in phase α	kJ mol^{-1}
μ_i^{α}	Chemical potential of species i in phase α	kJ mol^{-1}
$\mu_i^{\alpha,0}$	Standard chemical potential of species i in phase α	kJ mol^{-1}
v	Scan rate in voltammetry	V s^{-1}
	Hydrodynamic velocity	cm s^{-1}
ϕ	Standard Galvani potential difference	V

Abbreviations

Abbreviation	Meaning
Aβ	Amyloid beta protein
AD	Alzheimer's disease

AdSV	Adsorptive stripping voltammetry
Ag/AgCl	Silver/silver chloride electrode
AOT	Bis(2-ethylhexyl) sulfosuccinate
ATP	Adenosine triphosphate
BioMEMS	Biomicroelectrochemical system
BTPPA	Bis(triphenylphosphoranyliden)ammonium, organic cation
BSA	Bovine serum albumin
CE	Capillary electrophoresis
	Counter electrode
Cl^-	Chloride ion
Cs^+	Caesium ion
CV	Cyclic voltammetry
Cyt c	Cytochrome c
DCE	Dichloroethane
1,6-DCH	1,6-dichlorohexane
DiMFc	Dimethyl ferricinium
$DMFeCp_2$	1,1'-dimethylferrocence
DNA	Deoxyribonucleic acid
DNNS	Dinonylnaphthalenesulfonate
DRIE	Deep reactive ion etching
ELISA	Enzyme linked immunosorbent assay

hA	Human amylin
Hb	Haemoglobin
HCl	Hydrochloric acid
HEWL	Hen-egg-white-lysozyme
IAAP	Islet amyloid polypeptide
IgG	Immunoglobulin G
IHP	Inner Helmholtz plane
ITIES	Interface between two immiscible electrolyte solutions
KOH	Potassium hydroxide
LiCl	Lithium Chloride
LSV	Linear sweep voltammetry
Mb	Myoglobin
MD	Molecular dynamics
MVN	Modified Verwey – Niessen model
NaCl	Sodium chloride
NB	Nitrobenzene
OHP	Outer Helmholtz plane
PBS	Phosphate buffered saline
pI	Iso-electric point
Pt	Platinum
PVC	Polyvinyl chloride

QELS	Quasi laser light scattering
rA	Rat amylin
RE	Reference electrode
SECM	Scanning electrochemical microscopy
SV	Stripping voltammetry
TBA^+	Tetrabutyl ammonium ion
TEA^+	Tetraethyl ammonium ion
TPB^-	Tetraphenylborate ion
$TPBCl^-$	Tetrakis(4-chlorophenyl)borate ion
$TPFB^-$	Tetrakis(4-fluorophenul)borate ion
UV/vis	Ultraviolet visible

Abstract

The work presented in this thesis relates to the electrochemistry of biomolecules at the polarised liquid – liquid interface. The work aims to enhance the knowledge of the fundamental behaviour of proteins at the interface between two immiscible electrolyte solutions. This understanding is vital for utilisation of the interface between two immiscible electrolyte solutions (ITIES) as a platform for biomolecular sensing.

The electrochemistry of myoglobin was investigated at the aqueous – organic interface. Using cyclic voltammetry it was found to show a linear current response to concentration of protein in the aqueous phase. Myoglobin was shown to produce a voltammetric response only when protonated. It was found that increasing the ionic strength of the aqueous phase resulted in larger and more distinct peaks, attributed to the salting out effect, which can be related to the Hofmeister series. The adsorption – desorption mechanism proposed was investigated by investigating simple ion transfer in the presence of the protein, where it was found that the protein distorted tetraethyl ammonium transfer.

The issue of selective detection of proteins and peptides was investigated using three different approaches.

The first approach relates to the investigation of amylin. It was found that due to the properties of the polypeptide that it could be detected at physiological pH, where it is charged due to its iso-electric point. Although a slight reduction in sensitivity is observed when using physiological pH a linear response to concentration was observed. Amylin was detected in a protein mixture containing haemoglobin and myoglobin at physiological pH. This study indicated that simply adjusting the pH can tune the electrochemistry to achieve selectivity.

Another approach was employed to the detection of insulin in the presence of albumin. Adsorptive stripping voltammetry was used to characterise the adsorption behaviour of the proteins. It was found that insulin and albumin have different optimum adsorption potentials. This allowed for the detection of insulin in the presence of albumin by selection of the appropriate adsorption potential, where one protein was adsorbed over another in solution of both proteins.

An initial investigation into the behaviour of anti – albumin antibodies and its interactions with albumin were undertaken. It was shown that at physiological pH no electrochemistry was observable, although adsorption of the protein and antibody at the liquid – liquid interface is expected. At pH of 2 the antibody showed little response as did the albumin. When the albumin and antibody are allowed to interact at pH 2 there is an observable increase in ion transfer at the positive end of the potential window. This may be due to non specific interactions between the protein and the antibody.

The interactions between an anionic surfactant and proteins were investigated at an array of microinterfaces. It was found that the presence of the surfactant in the organic phase enhanced the adsorption of the protein resulting in an increase in observed peak currents when compared to the same experiments without surfactant present. The mechanism of interaction between the surfactant and protein was investigated using the surfactant anion as the anion as an electrolyte which showed a new adsorption process that was dependant on the presence of surfactant. It was found that for cytochrome *c*, repeated voltammetric cycling increased the amount of adsorbed protein and therefore the peak currents observed.

Adsorptive stripping voltammetry was used to characterise the adsorption characteristics of cytochrome *c* at the interface between two immiscible electrolyte solutions. The effects of adsorption time and bulk concentration were investigated and showed that upon reaching a certain interfacial

concentration of protein a saturation point is reached, as observed in a plateau in electrochemical response. It was found that upon accumulation of protein over longer periods of time the voltammetric response changed from a single peaked response to a double and triple peak. It is hypothesised that the protein is forming aggregates under the conditions of low pH and molecular crowding at the interface as a result of the applied potential.

The results presented provide a deeper understanding into the electrochemical behaviour of biomolecules at the interface between two immiscible electrolyte solutions.

Chapter 1

Introduction

1.1 Principles of electrochemistry

1.1.1 Solid state electrochemistry

Electrochemistry can be defined as the study of the relationship between chemical and electrical processes.[1] There are many processes which can occur but will generally fall into either one of two possible categories. These are (1) the study of the physical or chemical processes which occur due to the flow of current or (2) the study of the electrical phenomena produced by chemical reactions. [1, 2]

Typically electrochemistry will be carried out at the interface between a solid electrode and a conductive electrolyte solution, where charge transfer processes such as oxidation and reduction occur at the solid liquid interface. Under conditions where the potential difference between the electronic conductor (electrode) and the ionic conductor (electrolyte) is great enough, electrons can transfer from one species to another. The case of electrons moving from the electrode to electrolyte is referred to as a reduction current; when the electrons are transferred from the electrolyte to the electrode, this is referred to as an oxidation current.[1, 2]

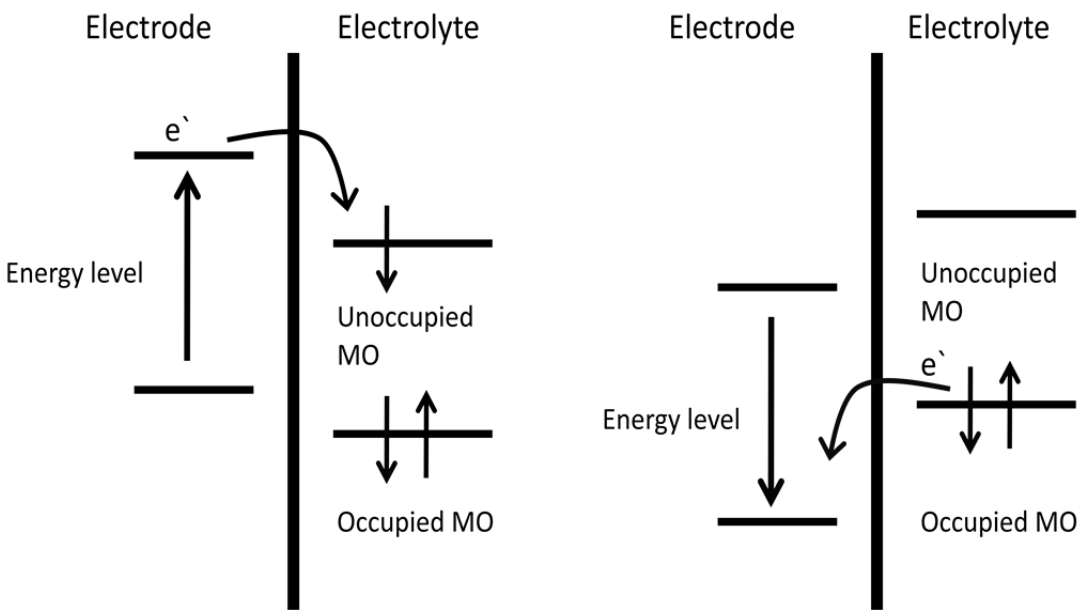

Figure: 1.1.1: Illustration of the electron transfer process which occur at solid-liquid interfaces. The electron is transferred from a high energy level in the solid to a lower unoccupied molecular orbital of a species in solution (reduction) or the species in solution transfers an electron to the lower energy electrode surface (oxidation)

This is illustrated in Figure 1.1.1, where it can be seen that when the potential difference is varied, which can be achieved by using an external power source, the relative energy level of the electrons in the electrode are changed, so that they may have a higher relative energy to that of unoccupied molecular orbitals in the electrolyte, promoting electron transfer to that species, or in the case where the energy of electrons in the electrode is reduced relative to that of the electrolyte, electrons will transfer from electrolyte to electrode. These processes can be related to the standard potentials for reaction occurring in an electrochemical cell , E^{0}.[1-3] In a reaction where a species O is reduced to a species

$$(O + ne^{-} \rightleftharpoons R_1) \text{ Eqn 1.1.1}$$

R_1, such as in Eqn 1.1.1 where O is the oxidised species, R is the reduced species and ne^{-} is the number of electrons involved in the reaction. The

relationship between the activities of O and R can be related to free energy of the system, as in Eqn 1.1.2.

$$\Delta G = \Delta G^0 + RTln\frac{a_o}{a_R} \quad \text{Eqn 1.1.2}$$

Where ΔG (J mol^{-1}) is the Gibbs free energy, $\Delta G°$ is the standard free energy (J mol^{-1}), R is the gas constant (8.314 J mol^{-1}K^{-1}), T is temperature (K) a_o and a_R and the activities of species O and R respectively (mol L^{-1}). From this relation between the concentrations of oxidised and reduced species and the Gibbs free energy the potential, E (V) can be found.

$$\Delta G^0 = -nFE^0 \quad \text{Eqn 1.1.3}$$

Shown in equation 1.1.3 is the relationship between $\Delta G°$ the standard free energy (J mol^{-1}), and the standard potential difference E^0 (V), n is the number of electrons and F is the Faraday constant (96,485 C mol^{-1}). The standard potential difference is in reference to a system where there is no external voltage or current source present. These relationships are the basis for the formation of the Nernst equation,[1-3] Eqn 1.1.4, where E is potential difference (V).

$$E = E^0 + \frac{RT}{nF}ln\frac{a_o}{a_R} \quad \text{Eqn 1.1.4}$$

This important equation shows how the concentrations of the electroactive species O and R can be related to the potential difference of a cell.

1.1.2 Faradaic and non-faradaic processes

The electrical processes occurring in an electrochemical cell can be defined in distinct categories, faradaic and non faradaic processes. Faradaic processes are those concerned with chemical reactions taking place (oxidation and reduction) which produce an electrical response. These processes are governed by Faraday's law, Eqn 1.1.5.

$$Q = nFN \quad \text{Eqn 1.1.5}$$

Where Q is total charge passed (C), n is the number of electrons, F is the Faraday constant (96,485 C mol^{-1}) and N is moles (mol).This equation relates the charge produced to the amount of product.

Whereas non faradaic processes are all other processes which occur besides redox reactions, these non faradaic processes follow Ohm's law, Eqn 1.1.6. where V is voltage (V), R is resistance (Ω) and i is current (A).

$$V = Ri \quad \text{Eqn 1.1.6}$$

Adsorption of charged molecules at the solid – liquid interface and electrolyte composition are examples of factors which affect non-faradaic processes.

1.1.3 Polarisable and non polarisable interfaces

For non-spontaneous processes which will not occur at equilibrium, a potential difference must be applied. The difference between the applied potential (E) and the equilibrium potential (E_{eq}) is referred to as the overpotential (η), as shown in Eqn 1.1.17.

$$\eta = E - E_{eq} \quad \text{Eqn 1.1.17}$$

An ideally polarisable electrode is one in which there are no charge transfer currents produced with any given applied potential. In reality no electrode will behave this way, but can have a potential region in which this behaviour is observed.[1, 2] On the other hand an ideally non-polarisable electrode is one which shows no change in potential with the passage of current.

1.1.4 Electrical double layer

As the electrochemistry observed is dependent on the interface between the solid electrode and the electrolyte it is useful to be able to describe its structure. The electrolyte region can be considered as several distinct layers,

the inner Helmholtz plane, the outer Helmholtz plane and the diffuse layer, as can be seen from Figure 1.1.2(a).

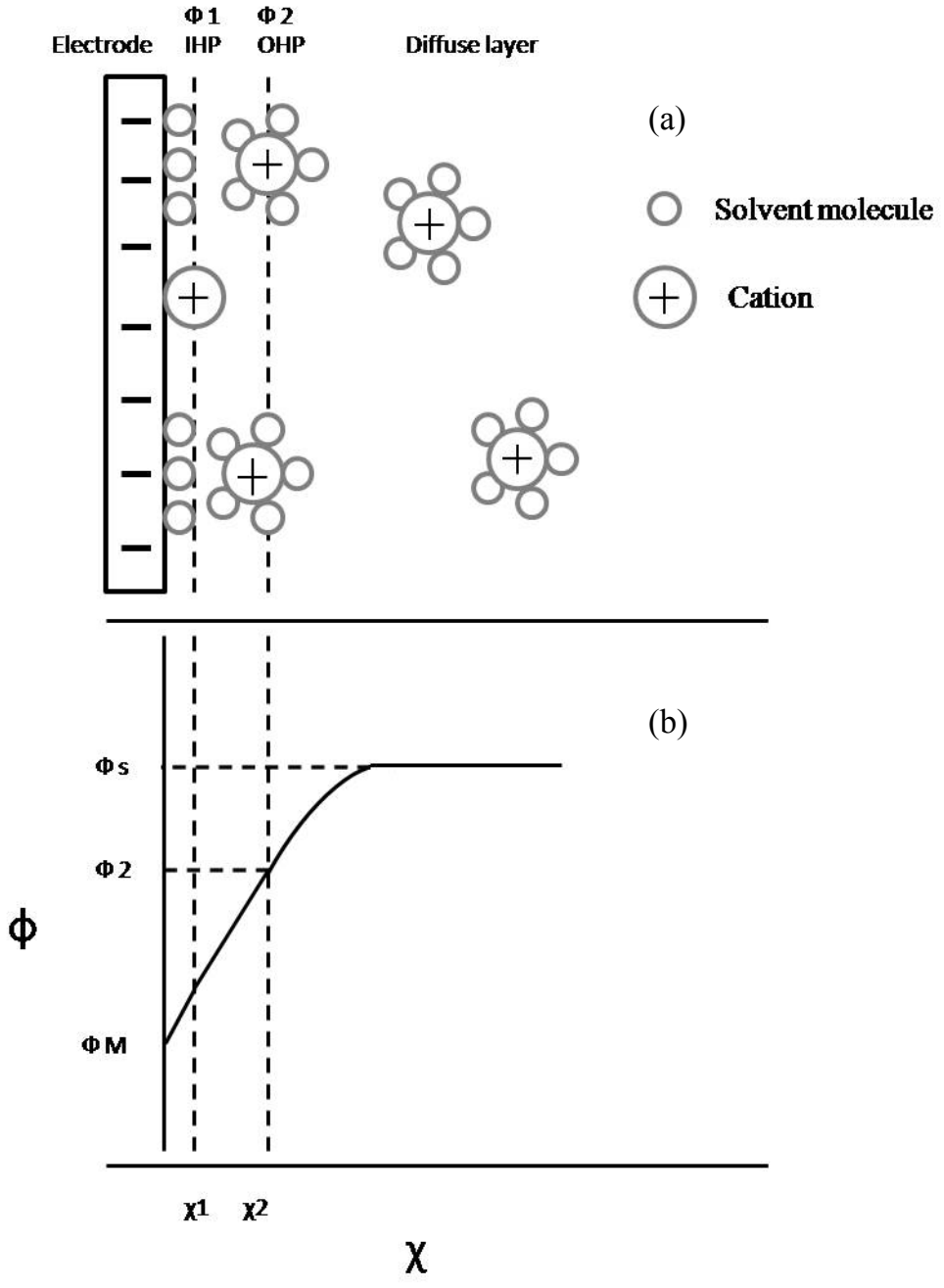

Figure 1.1.2: Showing the representation of the electrode – solution interface, where the inner Helmholtz plane (ϕ1) and outer Helmholtz plane (ϕ2) and the diffuse layer are shown in figure (a). ϕM, ϕ2 and ϕS refer to galvani potential of the metal, solvated cation and the electrolyte respectively, shown in figure (b).

The first distinct region is called the inner Helmholtz plane (IHP). This is where there are molecules closest to the electrode, consisting of solvent molecules or specifically adsorbed ions which are attracted to the electrode through electrostatic forces.[1-3] The locus of the IHP is found at distance $\chi 1$ from the interface. The ions found at the IHP are non- solvated, whereas solvated ions are found no closer than a distance $\chi 2$, which is referred to as the outer Helmholtz plane (OHP). The interactions between ions and the electrode are formed through long range electrostatic forces which are independent of chemical structure. The solvated ions are referred to as being non-specifically adsorbed. The IHP and OHP can be referred to as the compact layer, there is a strong interaction between this layer and the electrode. Beyond the OHP, extending into the bulk solution is the diffuse layer containing non-specifically adsorbed solvated ions. The diffuse layer is considered in three dimensions and its length is dependent on potential difference and electrolyte concentration.[1-3] Since electro-neutrality must be maintained, the excess charge on the electrode surface must equal the charge of surrounding layers of ions in the solution. This results in two distinct potential/distance profiles corresponding to the compact layer and the diffuse layer. The compact layer potential follows a linear relationship with distance, whereas the diffuse layer potential has an exponential relation to distance, as can be seen in Figure 1.1.2(b). The electric double layer can be thought of as a capacitor. An ideal capacitor follows Eqn 1.1.8, where q is charge stored by the capacitor (C), E is the potential across the capacitor and C is the capacitance (F).

$$q = CE \quad \text{Eqn 1.1.8}$$

The capacitance of the electrical double layer or C_{dl} is given by the combination of the capacitance of the compact and diffuse layers and can be defined by equation 1.1.9,

$$q = C_{dl}A\left(E - E_{pzc}\right) \quad \text{Eqn 1.1.9}$$

where A is the area (cm^2) and E_{pzc} is the potential of zero charge . It is this double layer capacitance which contributes to charging current (background current), which is a non-faradaic process. In general the faradaic currents are those which are utilised for analytical purposes.

1.1.4 Mass transport

For a given electrochemical reaction, assuming a simple case where no additional chemical or physical processes occur, the reaction is governed by mass transport of the electroactive species to the electrode, its electron transfer at the electrode surface and its transport away from the electrode after the redox reaction. When reaction rates are controlled by the rate at which the electroactive species arrives to the electrode, the reaction is considered to be mass transport limited. [1-3]

There are three ways in which mass transport can occur.

1) Diffusion – this is the movement of a species due to concentration gradients.
2) Convection – this mass transport is due to natural density gradients or physical forces such as stirring of the solution.
3) Migration – where mass transport occurs due to the influence of an electric field (potential gradient)

Mass transport to an electrode, in which the dimensions and shape of the electrode become important, obeys the Nernst – Planck equation, Eqn 1.1.10,

$$J_i(x) = -D_i \frac{\partial C_i(x)}{\partial x} - \frac{z_i F}{RT} D_i C_i \frac{\partial \phi(x)}{\partial x} + C_i v(x) \quad \text{Eqn 1.1.10}$$

where $J_i(x)$ is the flux of species i (mol s^{-1} cm^{-2}) at a distance x from the electrode surface, D_i is the diffusion coefficient (cm^2 s^{-1}), $\frac{\partial C_i(x)}{\partial x}$ is the concentration gradient at distance x, z_i is the charge (dimensionless) on the species i, C_i is the concentration (mol cm^{-3}), $\frac{\partial \phi(x)}{\partial x}$ is the potential gradient

along the x-axis and $v(x)$ is the hydrodynamic velocity (cm s^{-1}). The three terms in the equation for flux (J_i) are related to diffusion, migration and convection, respectively. The migration term can be removed by addition of a supporting electrolyte far in excess of analyte concentrations and the convection term can be removed by having a non-stirred solution at a fixed temperature, thus simplifying the equation as shown in Eqn 1.1.11,

$$J_i(x,t) = -D_i \frac{\partial C_i(x,t)}{\partial x} \quad \text{Eqn 1.1.11}$$

where t is the time. This is Fick's first law of diffusion and describes the flux of a species at a given time and position in relation to concentration.[2] With the removal of the migration and convection terms the current and flux can be related by Eqn 1.1.12, where A is the area of the electrode surface (cm^{-2})

$$i = -nFAJ \quad \text{Eqn 1.1.12}$$

By combining Eqn 1.1.10 and 1.1.11 a general equation for current response in a diffusion limited system is given (Eqn 1.1.13).

$$i = nFAD \frac{\partial C_i(x,t)}{\partial x} \quad \text{Eqn 1.1.13}$$

The resulting term for time dependant diffusional flux is governed by Fick's second law, given in eqn 1.1.14.

$$\frac{\partial C_i(x,t)}{\partial t} = D \frac{\partial^2(x,t)}{\partial x^2} \quad \text{Eqn 1.1.14}$$

Fick's second law describes the concentration profile of a species with respect to time between two given points.[2, 3] In this case it is assumed to be between two parallel planes which are perpendicular to the direction of diffusion, thus describing linear diffusion to a surface. In an electrochemical experiment the diffusion profile is dependent on the geometry of the electrode, therefore the equations need to be modified to correctly represent the geometry used. This can be achieved through the use of a mathematical approach using Laplace transformations which can account for diffusion to different geometries.

1.2 Electrochemistry at the interface between two immiscible electrolyte solutions (ITIES)

1.2.1 Background of electrochemistry at the ITIES

The core of the work in this thesis is based on electrochemistry at the interface between two immiscible electrolyte solutions (ITIES). The ITIES is formed when two immiscible solutions come into contact, ideally these solutions have no miscibility, but in reality they will have a very low miscibility.[4] Typically this interface is formed between an organic and an aqueous phase, each containing a dissolved electrolyte. Generally the organic solvent is polar and must have a large enough dielectric permittivity to dissociate, or at least partially dissociate, the electrolyte.[4, 5] It is this polarisable interface where the electrochemistry of interest occurs, typically in the form of ion transfer from one phase to another,[6-9] although less commonly observed, redox reactions at the liquid –liquid interface are also possible.[10, 11] There are several key advantages of using the ITIES for electrochemistry. Unlike conventional redox chemistry, electrochemistry at the ITIES enables the analysis of analytes which are not redox active or which have complications associated with their redox chemistry such as surface fouling.[5] The only requirement is that the analyte has a charge (or can be charged), so often controlling the pH allows for varying the electrochemical behaviour observed. A particular advantage in the area of bioanalytical measurements is that the ITIES can be used for label free detection of biomolecules. This has received particular interest and will be further discussed in section 1.2.8. The ITIES is also amenable to miniaturisation which is a major driving force behind electrochemical sensor technology. Originally, macro - scaled experiments were used, [6, 12] followed by the development of a micro - sized ITIES[7, 13-15] and nanoscale ITIES.[16-20] Since the development of the ITIES in the late 1970s where Koryta et al. showed that the ITIES could be used as an ideally polarised electrode to observe ion transfer[21], and the subsequent development

of the first 4-electrode electrochemical ITIES[22], the area has developed considerably. The liquid – liquid interface has been used to study simple ion transfer,[9, 23] assisted ion transfer, [8, 24]and a range of analytes such as aminoglycoside antibiotics,[25] DNA,[26-28] neurotransmitters such as dopamine and noradrenaline[29 30, 31] and protons.[32] As well as a large variety of analytes being used and the miniaturisation of the liquid – liquid interface, the ITIES has also been integrated with other techniques such as flow cells for flow injection analysis,[33, 34] capillary electrophoresis[35, 36] and ion chromatography.[37]

1.2.2 Structure of the ITIES

The earliest structural model of the ITIES was developed by Verwey and Niessen,[38] which considered the interface to be equivalent to back - to - back diffuse layers, which is based on the Gouy-Chapman theory. This model proposed that one side of the interface contained excess positive charge and the other contained an excess negative charge as shown in Figure 1.2.1 (A). Gavach et al. modified this theory to include a non-ionic layer between the two charged phases. This interfacial layer is said to contain orientated solvent molecules. This model is known as the modified Verwey – Niessen (MVN) model, shown in Figure 1.2.1 (B).[4, 39] Girault et al. further probed the interfacial structure, in particular showing that the interface was unlikely to be a region with a rigid divide between the two unmixed layers, rather that it would be a mixed-solvent layer which would have a constantly changing composition.[40] The molecular dynamics (MD) simulations carried out by Benjamin[41] showed that although the interface is molecularly sharp it has distortions from capillary waves which give it a rough shape, as depicted in Figure 1.2.1 (C).

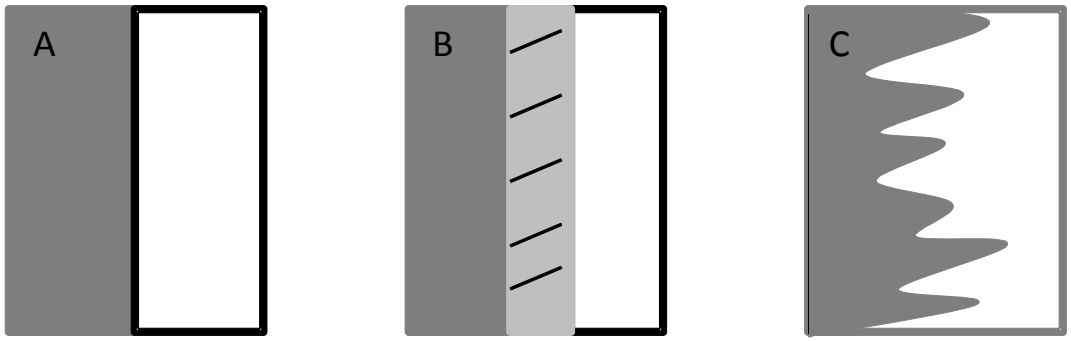

Figure 1.2.1: Schematic representations of the interfacial structure represented by the Verwey – Niessen model (A), the modified Verwey – Niessen model (B) and the molecular dynamics model (C).

Strutwolf et al. investigated the liquid – liquid interfacial structure using neutron reflectivity, where it was shown that interface had a root mean square roughness of less than 10 Å.[42] Further evidence for the theory of a rough interface was provided by Richmond et al. by the combination of vibrational spectroscopy with molecular dynamics simulations. It was shown that the experimentally generated spectra, which provide information about the interfacial structure, are in good agreement with spectra generated from molecular dynamics simulations.[43] Schlossman et al. used synchrotron X-ray reflectivity to study the distribution of ions at an aqueous – organic interface.[44] It was found that the experimental results differed from what is predicted when using the Gouy – Chapman theory and modified Verwey – Niessen theories as these descriptions do not sufficiently account for the interfacial liquid structure, which impacts the distribution of ions across it[45].

1.2.3 Theory of liquid – liquid electrochemistry

When two immiscible electrolyte solutions come into contact it is the distribution of ions across this interface which gives rise to a potential difference, as shown in equation 1.2.1.

$$\Delta_o^w \phi = \phi(w) - \phi(o) \quad \text{Eqn 1.2.1}$$

Where ϕ is the Galvani interfacial potential difference for the aqueous (w) and organic phases (o)[2]

At equilibrium and under constant temperature and pressure the electrochemical potential in the solution phases follows the relationship in Equation 1.2.2.

$$\bar{\mu}_i(w) = \bar{\mu}_i(o) \quad \text{Eqn 1.2.2}$$

Where $\bar{\mu}_i$ is the electrochemical potential of an ion, i, in either the aqueous (w) or organic (o) phase.

The electrochemical potential for a given component in a phase is given by equation 1.2.3 where $\bar{\mu}_i^o$ is the standard chemical potential of component i in phase (α), a is the activity of ion i, z is the charge of the ion and ϕ is the electrical potential of the phase.

$$\bar{\mu}_i^\alpha = \bar{\mu}_i^{o,\alpha} + RTlna_i^\alpha + z_iF\phi^\alpha \quad \text{Eqn 1.2.3}$$

Under equilibrium conditions where equation 1.2.2 applies, the electrochemical potentials can be described by equation 1.2.4 for a two phase system, with phases α and β.

$$\bar{\mu}_i^{o,} + RTlna_i^\alpha + z_iF\phi^\alpha = \bar{\mu}_i^{o,\beta} + RTlna_i^\beta + z_iF\phi^\beta \quad \text{Eqn 1.2.4}$$

This relationship allows the expression of the Galvani interfacial potential difference between phases α and β as a Nernst - type equation, shown in equation 1.2.5.

$$\Delta_\beta^\alpha\phi = \phi^\alpha - \phi^\beta = \Delta_\beta^\alpha\phi_i^o + \frac{RT}{z_iF} ln \frac{a_i^\beta}{a_i^\alpha} \quad \text{Eqn 1.2.5}$$

Where $\Delta_\beta^\alpha\phi_i^o$ is the standard Galvani potential difference for ion transfer and can be defined by equation 1.2.6.

$$\Delta_\beta^\alpha\phi_i^o = \frac{\Delta_\beta^\alpha G_i^o}{z_iF} = \frac{\mu_i^{o,\beta} - \mu_i^{o,\alpha}}{z_iF} \quad \text{Eqn 1.2.6}$$

From equation 1.2.6 $\Delta_{\beta}^{\alpha}G_i^o$ is the Gibbs energy of ion transfer from phase (α) to phase (β). If an ion has a large positive value for $\Delta_{\beta}^{\alpha}G_i^o$ it is said to be hydrophilic and those with large negative values are said to be hydrophobic. As the standard potential for ion transfer, $\Delta_{\beta}^{\alpha}\phi_i^o$, is constant, the interfacial potential difference, $\Delta_{\beta}^{\alpha}\phi$, is directly related to the activity or concentration of the species i in each phase, $a_i^{\beta} / a_i^{\alpha}$. Therefore, by manipulation of the interfacial potential difference, the equilibrium can be shifted and ions transferred from one phase to another. This is the fundamental basis for performing electrochemical experiments at the ITIES, whereby application of a potential difference across the liquid – liquid interface, driven by an external source, induces ion transfer across the ITIES, producing an electric current. It is also worth noting that the potential difference across the interface, $\Delta_{\beta}^{\alpha}\phi$, can be altered without an external power source by changing the concentrations of ions in each phase, thereby altering the $a_i^{\beta} / a_i^{\alpha}$ term in equation 1.2.5 .

1.2.4 Polarisable and non-polarisable ITIES

An ideally polarisable ITIES is one in which will not undergo faradaic charge transfer when a potential difference is applied across the interface. This is achieved by having an aqueous phase with a sufficiently hydrophilic electrolyte, $A^{1+}B^{1-}$ and an organic phase with a sufficiently hydrophobic electrolyte, $A^{2+}B^{2-}$, which in theory will not transfer across the interface under any applied potential difference. In reality these electrolytes do transfer across the interface when sufficient energy is applied and the relevant Gibbs transfer energy is exceeded. It is these transfer potentials of the background electrolyte which govern the potential window available experimentally. A non-polarisable ITIES is one where current is allowed to pass through the interface but the potential difference remains at its equilibrium value. An ideally non polarisable ITIES is achieved by having a common ion for the electrolyte used in each phase, for example a common cation A^{3+} in each phase with different

anions would result in a partition between $A^{3+}B^{1-}$ and $A^{3+}B^{2-}$. In this case B^{1-} and B^{2-} are hydrophilic and hydrophobic enough to remain in the aqueous and organic phases respectively and A^{3+} is free to transfer between the two phases, which will mean that the Galvani potential difference of the interface in now dependant on the activity of A^{3+} following equation 1.2.7.

$$\Delta_{\beta}^{\alpha}\phi = \Delta_{\beta}^{\alpha}\phi_{A^3}^{o} + \frac{RT}{F} ln \frac{a_{A^{3+}}^{\beta}}{a_{A^{3+}}^{\alpha}} \quad \text{Eqn 1.2.7}$$

1.2.5 Ion transfer at the ITIES

To demonstrate how the electrochemical signals are generated at the ITIES, two examples will be used. Firstly, cyclic voltammetry (CV) of an electrochemical cell containing only background electrolyte will be considered, followed by a cell containing a simple ion such as tetraethyl ammonium (TEA^+), also containing background electrolyte. The background electrolyte considered will be hydrochloric acid (HCl) for the aqueous phase and bis(triphenylphosphoranylidene)ammonium tetrakis(4-chlorophenyl)borate ($BTPPA^+TPBCl^-$) in the organic phase, which will be 1,6-dichlorohexane (1,6-DCH). The direction of polarisation will be in the positive direction, meaning that the aqueous phase will be more positive at a more positive potential difference. By convention it is given that positive currents are produced by positive ions transferring from the aqueous to the organic phase and negative ions transferring from the organic to the aqueous. The opposite applies for negative currents which are attributed to anions transferring from the aqueous to the organic phase and for cations transferring from the organic to the aqueous phase.

Shown in Figure 1.2.2 is a typical CV of background electrolyte, also referred to as a blank CV. The region from 0 V to 0.2 V shows change in current with potential difference. Upon application of 0 V the $BTPPA^+$ transfers to the aqueous phase and Cl^- to the organic phase. Approaching 0.2 V the $BTPPA^+$ and Cl^- transfer back to the organic and aqueous phases respectively. The flat

region from 0.2 V to 0.8 V is the polarisation region, where no faradaic current is observed across the ITIES, non faradaic currents are still present and are what contribute to the observed charging currents in this voltage region. At the voltage region between 0.8 V and 1.0 V again background electrolyte is transferred, H^+ is transferred to the organic phase producing positive currents and the $TPBCl^-$ s transferred to the aqueous phase producing negative currents. If suitable electrolytes are chosen and no additional reactions occur, then this process can be cycled from 0 V to 1 V and back to 0 V repetitively with very reproducible voltammograms being obtained.

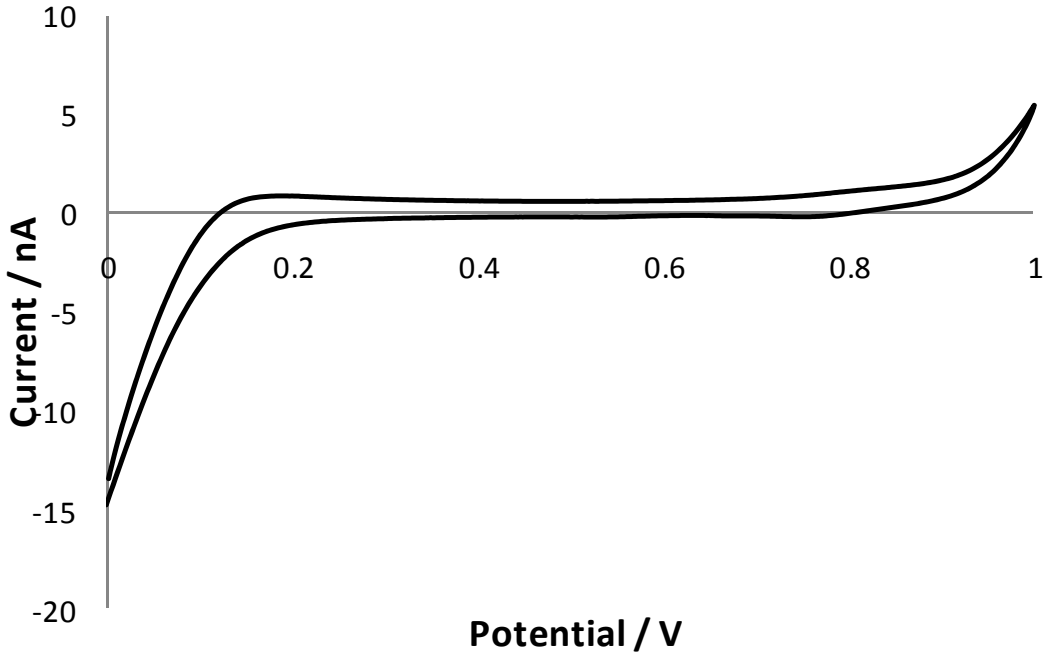

Figure 1.2.2: Cyclic voltammetry of background electrolytes, aqueous 10 mM HCl and 10 mM $BTPPA^+TPBCl^-$ in 1,6-DCH, using an 8 pore array, with a pore diameter of 20 μm.

The region of most significance from an experimental viewpoint is the polarisation window, in this case from approximately 0.2 V to 0.8 V where no background electrolyte transfer occurs. In this region the transfer of ions can be observed if the potential difference allows the ion to overcome its Gibbs energy of transfer, as shown in equation 1.2.6 and will not have their signal

interfered with due to background currents, although the current produced must be large enough to be observed above the background charging current. In Figure 1.2.3 the simple ion transfer of TEA^+ is shown, which is added to the aqueous phase as a chloride salt, therefore no additional peaks due to anion transfer will be observed in the polarisation window. At ~0.6 V on the forward scan the TEA^+ begins to transfer which is observed as an increase in positive current, at ~ 0.75 V it reaches a steady state current. This is due to the geometry of the microinterfaces used in the experiments and will be discussed in section 1.2.6. On the reverse scan, as the potential becomes more negative the TEA^+ starts to transfer back to the organic phase at ~0.75 V this time with a peak shape response with a negative current. The transfer potentials are related to the Gibbs energy of transfer as discussed previously and the magnitude of the peaks are often useful analytically as they can be related to concentration of an analyte.

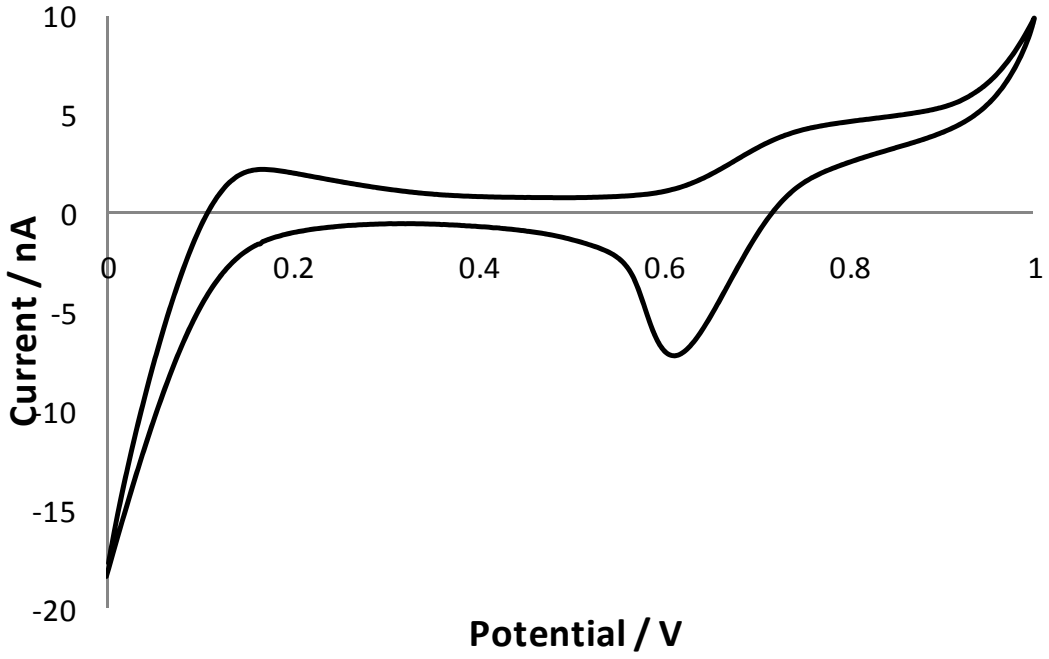

Figure 1.2.3: Cyclic voltammetry of 10 μM TEA^+ in background electrolytes, aqueous 10 mM HCl and 10 mM $BTPPA^+TPBCl^-$ in 1,6-DCH.

1.2.6 Micro ITIES (μ-ITIES)

Although the origins of liquid-liquid electrochemistry date back to the beginning of the 20th century with the work of Nernst and Risenfield[46] the first occurrence of what would become the typical platform for liquid-liquid electrochemical experiments came from the development of a 4 electrode potentiostat by Samec *et al.*[6, 47] This setup used a 0.01 M LiCl aqueous solution and a nitrobenzene (NB) organic solution of 0.05 M tetrabutylammonium tetraphenylborate (TBA TPB). Two Ag/AgCl reference electrodes were used, one in contact with the aqueous phase and the other with the organic phase. This was achieved by use of Luggin capillaries to aqueous and organic phases. To ensure only the water/nitrobenzene interface was polarisable the Luggin capillary in contact with the aqueous phase was filled with 0.01 M aqueous LiCl and the capillary in contact with the nitrobenzene phase was filled with 0.05 M aqueous tetrabutylammonium chloride. A large Pt counter electrode was immersed in each phase, where the connecting wire was protected from its surroundings with a glass casing. This experimental setup can be used to observe charge transfer events across the liquid-liquid interface. Although there is a trend towards using micro sized or smaller interfaces since the pioneering work of Girualt,[7, 14] the 4-electrode setup is still being employed by researchers worldwide. [28, 48, 49]

As with conventional electrochemical methods, miniaturisation of the ITIES offer a number of benefits over their macro counterparts, such as smaller size and portability, increased mass transport rates, reduced ohmic drop and charging currents, ease of data analysis and integration into complimentary techniques.[50, 51] As stated above the ITIES was first miniaturised to micro scale by Girault and co-workers where the organic electrolyte was held inside a glass pipette with a micron sized tip, which formed a micro ITIES when immersed in an aqueous electrolyte.[7] This miniature interface produced radial or spherical diffusion of analyte to the interface, analogous to that of a solid state microelectrode.[52, 53] By definition microelectrodes contain at least one

dimension less than 50 µm, referred to as the critical dimension, which is smaller than the diffusion layer thickness, resulting in radial diffusion to the interface and the resulting steady state voltammetry.[8, 52-54] An alternative method for developing micro scale ITIES was also developed by Girault et al. where an ultraviolet eximer laser was used to photo ablate a thin polymer membrane resulting in circular holes of ~ 20 µm in diameter.[14] Thus there are two options for preparation of µ-ITIES, either by use of a micro scaled pulled glass pipette,[7, 8, 24, 55, 56] or with a porous membrane[13, 14, 57, 58]. For the experiments used in this work micro interface arrays was used. The arrays are fabricated from silicon wafers, using photolithographic patterning, potassium hydroxide (KOH) etching and deep reactive ion etching (DRIE). This results in an etched pore with a hydrophobic interior wall, allowing the organic phase to enter the pores and result in an inlaid geometry.[57] An example of a 30-pore array is illustrated in Figure 1.2.4. The pores are ~ 20 µm in diameter and have a pore to pore separation of ~ 200 µm with a depth of ~ 100 µm.

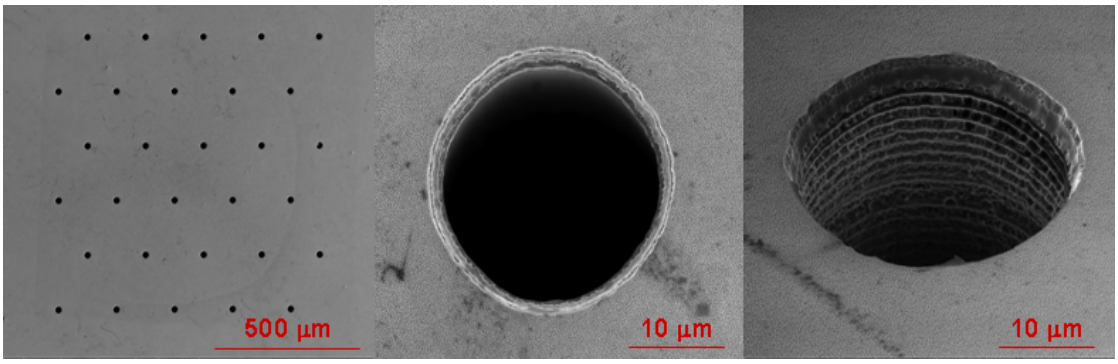

Figure 1.2.4: Scanning electron microscope (SEM) images of a silicon micropore array containing 30 pores with a diameter of ~ 20 µm, a pore to pore separation of ~ 200 µm and a depth of ~ 100 µm. Images taken at Tyndall National Institute.

1.2.7 Advancements in electrochemistry at the ITIES

The work by Vanýsek et al.in 1984 was among the earliest work involving protein behaviour at the ITIES. In this work the charge transfer of Cs^+ ions across the macro scale ITIES was investigated in the presence of proteins, namely ovalbumin, colicines and bovine serum albumin (BSA).[59] It was shown through CV and impedance studies that the proteins adsorbed at the interface hindered the otherwise reversible transfer of Cs^+ ions. It was also noted that upon adsorption of the proteins to the water - nitrobenzene interface, contact denaturation occurred and a white precipitate was observed. At this point the protein itself was not directly observed by voltammetry, rather a shortening of the available potential window was observed upon addition of the protein to the aqueous phase due to adsorption at the interface.

In 1990 this work was extended with further impedance and voltammetric studies of BSA adsorbed at the water/nitrobenzene interface, where it was shown through capacitance measurements that the adsorbed protein formed a monolayer depending on bulk concentrations and that the adsorbed protein affected the distribution of ions at the interface.[60]

In the late 1990s the transfer of oligopeptides at the ITIES was investigated by Osakai and Sawada.[61] In this work the transfer of oligopeptides was shown to be possible under acidic conditions, where the amino group would be protonated and that the transfer potential could be related to the hydrophobicity of the peptides. The facilitated transfer of the oligopeptides was also investigated, by adding an ionophore (dibenzo-18-crown-6) to the organic phase. The protonated oligopeptides were also shown to undergo a facilitated transfer in the presence of the ionophores, which was indicated by lower transfer potentials relative to the unassisted simple ion transfer.

The work by Williams group in 2000 investigated the electron transfer reactions of the enzyme glucose oxidase at the water/1,2-Dichloroethane interface by SECM.[62] The glucose – glucose oxidase reaction was mediated

by dimethyl ferricinium (DiMFc) in the organic phase. The glucose oxidase was adsorbed at the interface where neutral surfactant was present to prevent denaturation of the enzyme. The DiMFc was recycled in organic phase electrochemically by the SECM tip.

Dryfe and colleagues investigated the charge transfer properties of cytochrome *c* mediated by 1,1'-dimethylferrocene ($DMFeCp_2$) at the ITIES.[10] It was shown that when the aqueous phase protein was in its oxidised form that a heterogeneous electron transfer reaction with $DMFeCp_2$ could be induced electrochemically, giving an observable response by using CV. This electron transfer process across the ITIES resembles charge transfer processes which occur in vivo, hence the interest in this platform as a simple model of a biological membrane.

The transfer of an anionic surfactant across the oil – water interface was investigated by Kakiuchi et al. in 2002.[63] The results showed that in the presence of such surface active molecules, unusual and chaotic currents are produced, by the transfer of surfactants across the ITIES. This was attributed to an electrochemical instability, caused by the presence of the ionic surfactant. These results were in agreement with the proposed thermodynamic model presented in a previous paper that year.[64]

In 2004 Sugihara et al. also investigated the glucose oxidase catalysed reaction with mediators present in the organic phase.[11] It was found that the enzyme reaction could be controlled when an ionic mediator, $DiMFc^+$ was present in the organic phase. This was due to the ability to electrochemically control the transfer of $DiMFc^+$ to the aqueous phase, where it undergoes spontaneous reduction in the presence of the glucose oxidase enzyme.

The first reported electrochemically driven transfer of a protein across the ITIES was reported by Karyakin's group.[65] The non redox active protein, α-chymotrypsin, was found to be solubilised by the formation of reverse micelles in the organic phase, although this was only observed as an increase

in an already present background current, attributed to the transfer of cations in the aqueous phase to reverse micelles formed under applied potentials.

The first case of unassisted ion transfer of a protein or polypeptide came in 2003 with the work of Amemiya et al. where the electrochemistry of protamines was investigated, in this case a micro - sized interface was achieved through the use of micro pipettes .[66] The protamines are highly arginine rich, which gives a large positive charge (~20) at physiological pH or below. It was shown that the protamines exhibited steady state current responses on the forward voltammetric sweep, indicating radial transfer, similar to that of a model cation tetraethyl ammonium, TEA^+. The effects of varying the organic phase polarity was also investigated. On moving from nitrobenzene to a more relatively non polar solvent, 1,6-dichlorohexane, the voltammetric response of the protamines varied significantly. The steady state behaviour of the forward sweep was replaced by a pair of peaks. These peaks were attributed to the adsorption of protamines to the interface followed by a transfer process. The large reverse peak was attributed to release of the accumulated charge back to the aqueous phase on the reverse sweep. Although it is clear that the nature of the organic phase plays a role in the behaviour of the polypeptide, the details of the mechanisms would still need further investigation to clarify the processes occurring at or near the interface.

Further work by the group was published in 2004 showing the selective detection of protamine by facilitated ion transfer with the surfactant dinonylnaphthalenesulfonate (DNNS).[67] The reaction mechanism was investigated through the use of micropipettes where the voltammetry can be more easily interpreted by the shape of the volatmmetric responses obtained. It was proposed that firstly the DNNS adsorbs at the interface, after which interfacial complexation with the charged protamine occurs. This complex then transfers into the organic phase from the interface.

Kakiuchi and co-workers extended their work in the area of electrochemical instability of the ITIES due to ion transfer of surfactants in 2004. The work showed that even when there is a positive surface tension, the transfer of cationic surfactants still resulted in an electrochemical instability.[68] It was also shown that the complexation of metal ions with an anionic surfactant, Triton X-405, resulted in interfacial instability. Thus showing that not only ion transfer, but also complexation processes, induce the electrochemical instability of the interface.[69]

In 2005 the group investigated the polysaccharide, heparin, at the micro liquid-liquid interface.[70] The selective detection of heparin was found to be possible when a suitably hydrophobic quaternary ammonium species was present in the organic phase. It was found that the heparin undergoes a facilitated ion transfer process with the quaternary ammonium ions due to interfacial complexation. This work also addressed the points of sensitivity, in terms of relevant clinical concentrations, and selectivity in complex media. In buffered solution, a detection limit of 0.012 unit/mL was achieved, an order of magnitude lower than therapeutic heparin concentrations. Experiments were also carried out in sheep blood plasma where interferences due to dissolved salts and plasma proteins were observed. However heparin detection was still found to be possible; with stripping voltammetry (SV) a detection limit of 0.13 unit/mL was achieved, which is still lower than the therapeutic concentrations of heparin which are >0.2 unit/mL.

Also in 2005 Vagin et al. investigated a series of proteins and surfactants interactions at the interface between an aqueous and redox - polymer containing organic phase which was immobilised on a carbon electrode. It was shown that proteins could be transferred in reverse micelles to the organic phase to counter balance the charge produced by the redox activity of the polymer in the organic phase.[71]

In 2006 Osakai's group investigated the electroactivity of proteins in the presence of surfactants, although unlike previous studies by Vagin et al. the surfactant was added as a hydrophobic tetrapently ammonium salt which prevented spontaneous micelle formation.[72] This study showed that it was possible to achieve a response for the facilitated transfer of a protein by the surfactant, which was observed as a separate response to the process associated with micelle formation. It was found that at acidic pH values of 3.4, the protein, cytochrome *c* was found to aggregate at the interface, while at a pH of 7 cytochrome *c* appeared to form stable complexes with the reverse micelles in the organic phase. The authors also investigated the behaviour of the protein in the absence of surfactant and found that an electrochemical response was observed when running the CV at an acidic pH. It was proposed that the adsorbed cationic protein facilitated the transfer of the organic ion, resulting in the voltammetric response.

Samec's group published work in 2007 where counter ion binding to protamine was investigated using conductometry, cyclic voltametry and quasi-elastic light scattering (QELS). It was concluded that ion pairing between the organic anion and protamine results in the facilitated transfer of the positively charged protamine to the organic phase, but the authors suggest that the ion pair forms on the aqueous side of the interface.[73]

Further work in the area of electrochemical instability at the liquid – liquid interface was carried out by Kitazumi et at. in 2007. It was shown that the instability caused by the transfer of decylammonium ions across a micropipette interface, which produces irregular but reproducible currents, was dependant on the size of the interface used and the concentration of the ammonium ions in solution.[74]

In 2008 Osakai's group extended their earlier work by further investigating the mechanism of cytochrome *c* extraction of micelles, it was found that the

addition of the surfactant increased the interfacial potential, which reduced the interfacial tension allowing protein containing reverse micelles to be formed.[75]

The electrochemistry of a synthetic heparin mimic, Arixtra, was investigated by Amemiya's group using micropipette interfaces. The formal potentials and rate constants were found to be dependent on the ionophore used. It was also shown that using a primary ammonium group provided selective detection of the heparin mimetic at physiological pH in the presence of a major interfering anion, Cl^-. The primary ammonium ionophores were found to have more preferable binding properties as compared to the quaternary ammonium groups typically employed in other traditional potentiometric based methods.[76]

In 2008 Arrigan's group investigated haemoglobin behaviour at the ITIES, where it was found that at pH > pI of the protein, where it would be neutral or anionic, no charge transfer events were observable. After bulk ionolysis of the haemoglobin and subsequent measurements of the organic phase by UV/vis spectrophotometry it was found that no protein was present. The authors suggested that rather than the anion facilitating the transfer of the protein, it was the protein which was facilitating the transfer of the anion to the aqueous phase.[77] Similar behaviour was observed in the investigation of insulin by the group, where a detection limit of 2.5 μM was achieved by CV and 1 μM by square wave stripping voltametry.[78] Lysozyme was also studied in terms of its behaviour at the ITIES, the relationship between forward peak current and charge on the protein was investigated and agreed very well with the model predicted using the modified Randles-Sevcik equation, which uses the charge on the ion, rather than the number of electrons. Again, this was pointing towards facilitated transfer of the anion which is dependent on the charge of the protein.[79]

In 2010 Osakai and colleagues investigated the interactions of several proteins with various surfactants at the water/DCE interface.[80] In this work an adsorption/desorption mechanism was suggested while the aqueous phase was

relatively acidic. The authors proposed a model of protein/surfactant interaction based on the charge of the protein and its hydrophobicity. These parameters were correlated with the potential at which the voltammetric wave begins, although it was clear that many other parameters could affect the observed voltametry due to its underlying complexity.

Herzog et al. investigated the electrochemistry of protein digest at the μ-ITIES using enzymes. It was found that each protein studied gave a unique electrochemical response after digestion and also that the choice of enzyme also altered the response of the digested protein.[81] This provided an alternative approach to electrochemical detection of biomolecules at the ITIES. Also in 2010 Herzog et al. looked at the dependence of tertiary structure of haemoglobin on its electroactivity at the liquid-liquid interface by chemically denaturing the protein prior to undergoing CV.[82] It was found that although a current response was still achievable the denatured protein showed a much more diminished response, indicating the importance of tertiary structure to protein electrochemistry at the ITIES.

In 2010 Kakiuchi et al. further developed the theory of electrochemical instability, by developing an improved theoretical model.[83] The theoretical electrocapillary curves were found to be in good agreement with the experimental data.

The behaviour of lysozyme and insulin was evaluated by voltammetry at the interface between an aqueous phase and a gellified organic phase contained within a micropore array by Scanlon et al. [84], where it was determined that the same mechanistic principles apply to such interfaces as with its macro counterpart. It was shown that the proteins adsorb at the aqueous side of the interface, which was evident from the disruption of the normal steady state behaviour of the tetraethyl ammonium cation (TEA^+) which occurs due to the radial diffusion from the aqueous to organic phases at an inlaid micro-interface.

In 2011 Herzog and colleagues extended previous work where the electroactivity of denatured haemoglobin was investigated at the ITIES and used this principle to monitor unfolding of the protein by CV and extract thermodynamic properties such as free energy of folding and protein compactness from experimental data.[85] This work highlighted the usefulness of the ITIES as a simple platform not only for sensing but also for biophysical investigations.

The work of Zhai et al. investigated the conformational changes that occur for α-lactalbumin upon adsorption to the oil/water interface using synchrotron radiation circular dichroism spectroscopy, front-face tryptophan fluorescence spectroscopy and dual polarisation interferometry, [86] which indicated that the hydrophobic core becomes unfolded and a new non-native secondary structure is present. These findings agree with the proposed mechanism for facilitated ion transfer where interactions between hydrophobic regions of the protein and the hydrophobic electrolyte occur.[84]

The formation of dielectric layers and charge regulation of proteins in adsorbed layers at the ITIES was studied by Jensen's group.[87] A model was developed to evaluate the net charge of a protein adsorbed at the ITIES as compared to that of the bulk solution, which is said to be generally lower as the adsorbed protein undergoes charge regulation at the interface.

In an effort to improve detection limits towards more biologically relevant concentrations, an adsorptive stripping approach was developed by Alvarez et.al [88], where detection limits as low as 30 nM were achieved. This approach involved preconcentrating or accumulating protein at the interface by a fixed applied potential, which was tuned for optimal adsorption of lysozyme. This technique gave a 10-fold improvement over previously reported detection limits of lysozyme, although for many proteins of clinical relevance, lower limits of detection are still necessary.

A method for detection of albumin in urine was developed by Osakai's group, where a flow cell was used which had porous tubing to allow contact with an organic phase containing an anionic surfactant, $DNNS^-$.[89]It was found that after some pre treatment by dialysis and dilutions, that albumin could be detected down to 1.2 μM, which is in the region of clinically relevant concentrations. However as the authors state, interfering effects in a real sample are still likely as other proteins will be present and the system is not likely selective for albumin.

1.2.8 Aims of this work

The aim of this work is to further develop the understanding of the electrochemistry of biomacromolecules at the polarised liquid – liquid interface. Increasing knowledge in this area may lead to future development in biosensor technology. The two main themes in this thesis are (I) the study of the fundamental behaviour of biomacromolecules at the interface between two immiscible electrolyte solutions and (II) an investigation into methods to improve sensitivity and selectivity of biomacromolecular detection using liquid –liquid electrochemistry.

The specific objectives of the work presented in this thesis are:

- Uncovering the fundamental behaviour of myoglobin at the μ-ITIES, where the ion transfer electrochemistry of the protein is characterised by voltammetric methods. (Chapter 3)

- Investigating the issue of selective detection of biomacromolecules at the ITIES. Several different approaches were utilised in the exploration of this topic. (Chapter 4)

- The effects of addition of a surfactant to the organic phase on protein detection. The mechanism of interaction between the protein and the surfactant is studied. The work also investigates the effects of the surfactant on the analytical performance of protein detection at the ITIES. (Chapter 5)

- The exploration of the fundamental behaviour of proteins under conditions of prolonged adsorption at the interface due to the use of adsorptive stripping voltammetry. (Chapter 6)

Chapter 2

Experimental materials and methods

2.1 Liquid – liquid electrochemical set-up

2.1.1: The electrochemical cell

In this section the experimental set-up of the liquid – liquid electrochemical cell will be discussed. The experiments performed at the μ-ITIES utilise a two electrode set-up, which becomes possible due to the low currents observed as a result of the micro sized interfaces.[7] Although the electrochemistry of interest is performed at the interface between the organic phase and the aqueous phase, there are four interfaces in total which contribute to the working electrochemical cell used (interfaces such as those formed between the glass or the membrane and its surroundings are not considered). The four interfaces are: (1) The aqueous phase is in contact with the solid electrode forming a solid – aqueous interface, (2) the aqueous – organic interface, (3) the organic – organic reference solution interface and (4) the solution for the organic reference electrode – electrode interface. This liquid – liquid electrochemical arrangement is as shown in the schematic in Figure 2.1.1. The composition of the electrodes and the solutions used will be detailed in section 2.1.2. It is the aqueous - organic phase interface which is the only polarisable interface in the electrochemical cell. The potential difference at this interface is controlled by application of an external voltage through two silver/silver chloride (Ag/AgCl) electrodes which are connected to the potentiostat with crocodile clips. The other interfaces are non-polarisable. For all experiments the electrochemical cell is housed in a Faraday cage. All electrochemical experiments are performed at room temperature and in unstirred solutions.

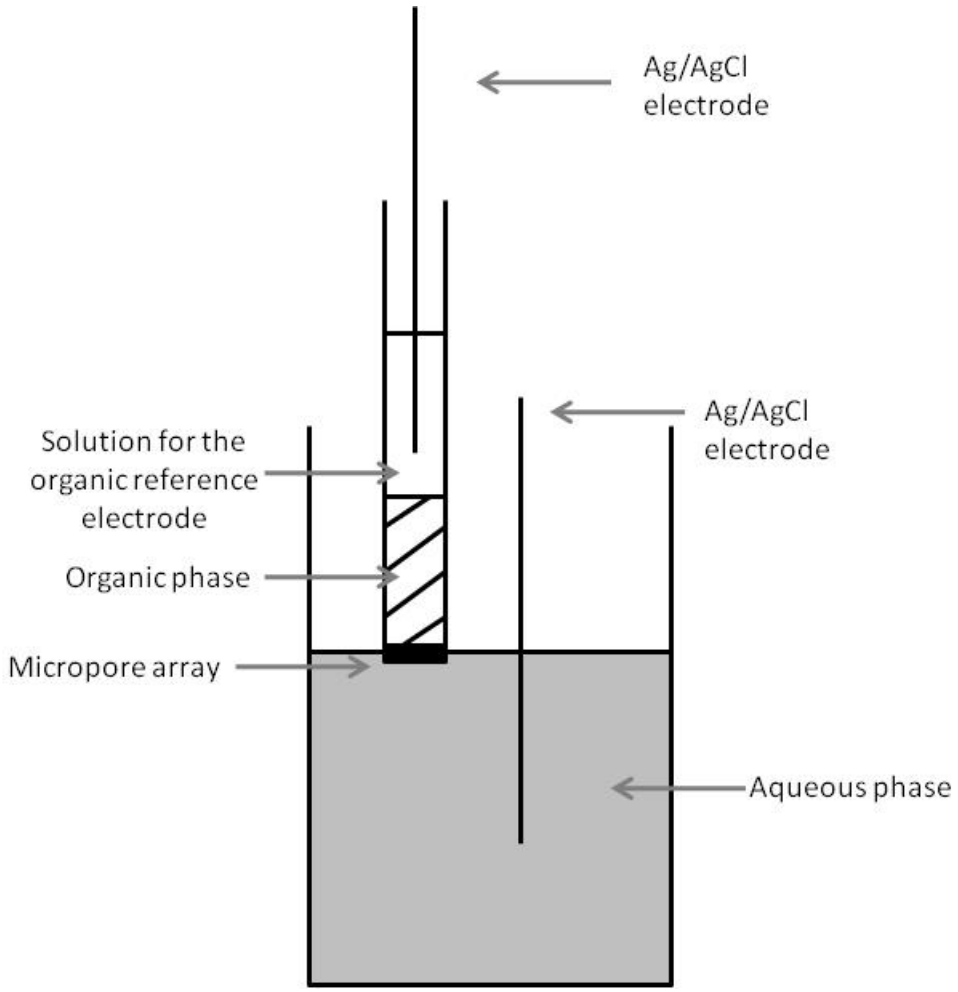

Figure 2.1.1: Schematic of the μ-ITIES array experimental set-up.

2.1.2: The electrodes and electrolytes

There are only two electrodes used in the μ-ITIES experiment as compared to its macro counterpart which typically uses a four electrode cell, with two counter electrodes and two reference electrodes developed by Samec et al.[22] The micro interfaces provide a greater current density, but overall a smaller magnitude in current is observed, in the region of nano amps (nA) is typical. This allows for the use of a two electrode set-up where the counter electrodes that are normally used to compensate ohmic drop are no longer necessary and the reference electrode can suffice on its own.

The electrodes used are Ag/AgCl, which is produced by oxidising silver wire in a solution of ferric chloride ($FeCl_3$). The Ag/AgCl electrodes are non-

polarisable due to the presence of chloride as a common ion, following equation 2.1.1.

$$AgCl_{(s)} + e^{-} \rightleftharpoons Ag_{(s)} + Cl^{-} \quad \text{Eqn 2.1.1}$$

The Ag/AgCl electrode has a standard potential, E^0, of 0.22249 V against the standard hydrogen electrode, as given by the IUPAC definition.[90]

The aqueous phase will have an electrolyte which is a chloride salt, such as lithium chloride (LiCl) or hydrochloric acid (HCl). This provides a non – polarisable interface between the Ag/AgCl electrode and the aqueous solution. The other Ag/AgCl electrode is immersed in the solution for the organic reference electrode. This aqueous solution contains a chloride salt also, as to form another non-polarisable interface with the electrode. The salt is typically bis(triphenylphosphoranylidene)ammonium chloride ($BTPPA^+Cl^-$), which importantly has a common ion not only with the Ag/AgCl electrode but also with the organic phase which contains $BTPPA^+$ $TPBCl^-$ to ensure no polarisable interfaces are formed.

The remaining interface is the one between the aqueous, containing an electrolyte such as HCl, and the organic phase containing an electrolyte such as bis(triphenylphosphoranylidene)ammonium tetrakis(4-chlorophenyl)borate ($BTPPA^+$ $TPBCl^-$), where there are no common ions on either side. Therefore this polarisable interface will follow equation 1.2.5, where the concentration of ions on either side of the interface is determined by the potential difference across the interface. It should be noted that the potential of transfer of an ion across the interface is not equivalent to its standard transfer potential as the potential difference applied is a sum of the potential differences at the two Ag/AgCl electrodes, the reference phase potential and the aqueous – organic phase potential.[91]

2.1.3 μ-ITIES set-up

The μ – ITIES was formed by utilising a silicon membrane array with eight or thirty micropores. The pores are arranged in a hexagonal pattern with diameter of 22 μm and a pore to pore separation of 400 μm for the eight pore design and a diameter of 22.4 μm and a pore-to-pore separation of 200 μm for the thirty pore design as can be seen in Figures 2.1.2 and 2.1.3 respectively

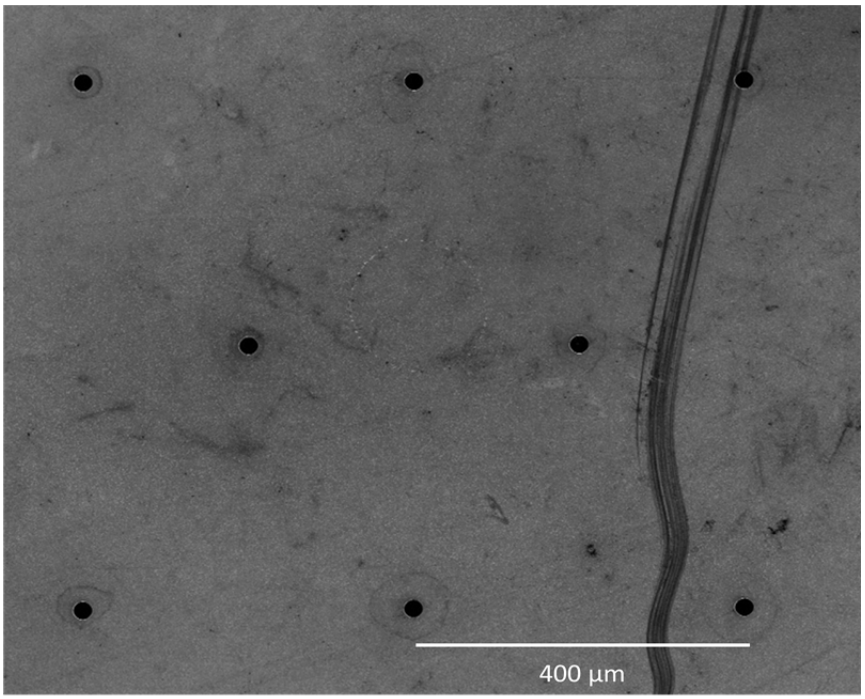

Figure 2.1.2: SEM image of an 8 micropore array.

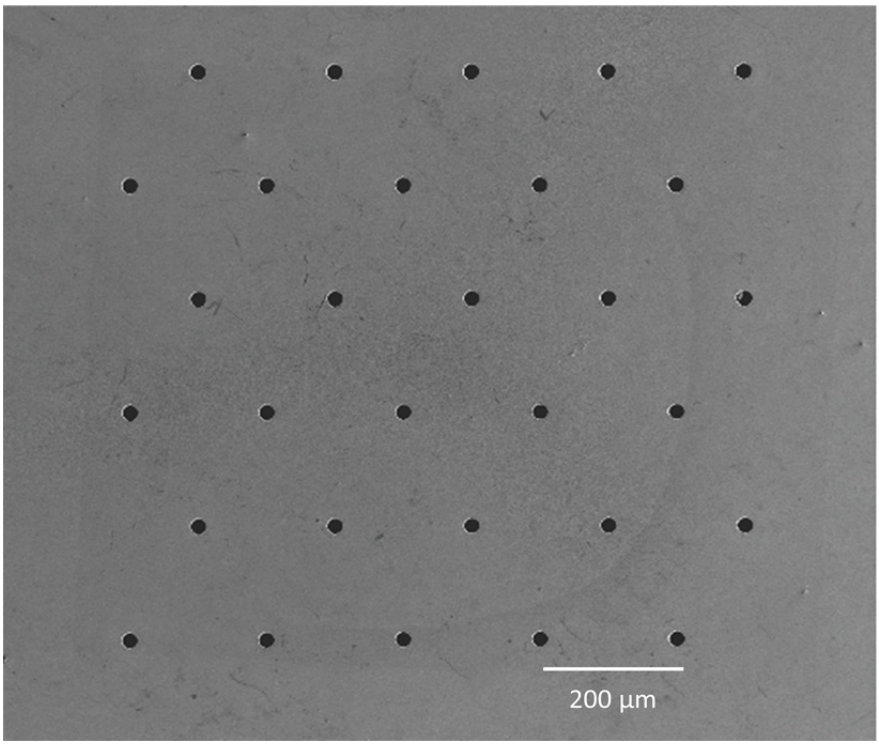

Figure 2.1.3: SEM image of a 30 micropore array

The membrane is attached to the end of a glass tube with silicone rubber (Acetic acid curing Selleys glass silicone, Selleys Australia and New Zealand). The organic phase of 1,6-DCH was gellified for mechanical stability and prepared as follows:

- A 10 mM solution of $BTPPA^+$ $TPBCl^-$ (preparation of the electrolyte is describe in appendix A) is prepared in 1,6-DCH in a 10 mL beaker.
- The solution is allowed to dissolve by stirring on a hotplate with a magnetic stirrer. The beaker is sealed with Parafilm to ensure no loss of solvent.
- Once dissolved the solution is heated to 60 °C and 10 % w/v of low molecular weight poly(vinyl chloride) (PVC) is added slowly.
- The solution is stirred on the hotplate until the PVC is fully dissolved, which will result in a clear gel.
- The organic gel is the added to the inside of the tube with the attached micropore array using a glass Pasteur pipette which has been heated on the hot plate to ensure the gel does not solidify before reaching the micropore interface array.

- Once the gel is added to the micropore array, it is allowed to set for 1 hour prior to use.

Once the gel has set it can be used for electrochemical experiments. The organic reference solution is added into the glass tube above the gelled organic phase, into which a Ag/AgCl electrode is immersed. The Ag/AgCl electrode must not penetrate the organic gel. The glass tube is immersed into a 10 mL beaker containing 10 mM electrolyte (typically HCl) and the second Ag/AgCl electrode is immersed into the aqueous phase. Once the two electrodes are connected to the potentiostat the cell is complete, as shown in Figure 2.1.1.

2.1.4 Diffusion profiles at micro interfaces

The diffusion profiles of micro ITIES were first described by Girault et al. in the 1980's,[7, 92] where it was observed that steady state peaks were obtained for ion transfer on the forward voltammetric sweep and peak shape responses were obtained on the reverse sweep. This was attributed to the geometry of the interface where radial or spherical diffusion occurs from the aqueous phase to the organic phase due to the inlaid geometry formed when the organic phase fills the micron sized pipette tip. The linear diffusion on the reverse sweep is attributed to the geometry, in which the ions are confined within the walls of the pipette tip and diffusion is limited to one direction. The same description applies to micropores also, as illustrated in Figure 2.1.4, where the organic phase fills the pore and forms an inlaid geometry. This feature of varying diffusion profiles causes the asymmetry observed for the voltammetric responses at such interfaces as seen in Figure 1.2.3.

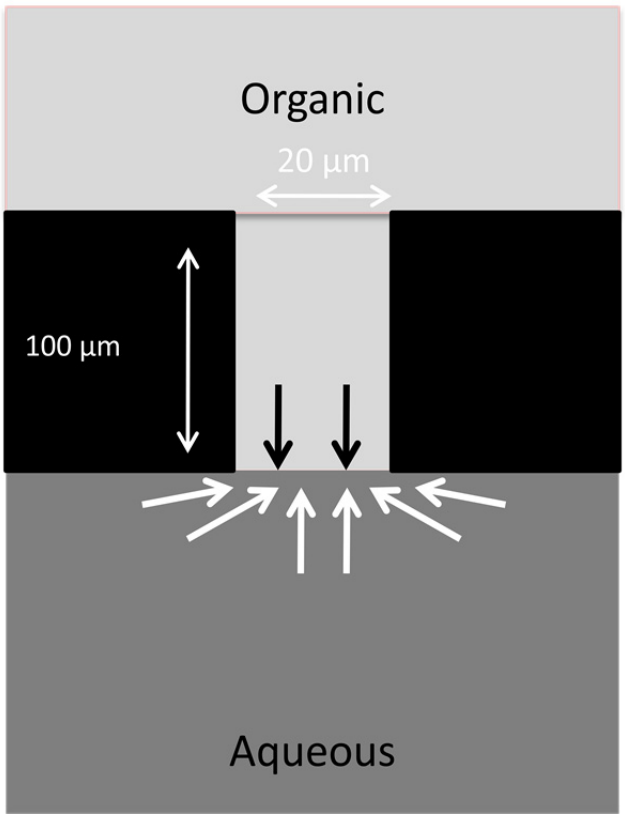

Figure 2.1.4: Illustration of diffusion profiles at an interface located at the mouth of a micropore showing radial diffusion from the aqueous phase and linear diffusion from the organic phase. The arrows indicate the direction of diffusion.

The electrochemical response of the µ-ITIES is analogous to that of a microdisc electrode[93-95] and follows equation 1.2.8 for the steady sate current.

$$i_{ss} = 4zFDCr \quad \text{Eqn 2.1.2}$$

Where i_{ss} is the steady state current (A), z, D and C are the charge (dimensionless), diffusion coefficient ($cm^2\ s^{-1}$) and bulk concentration (mol cm^{-3}) of the ion, respectively and r is the radius of the electrode (cm). The value of the first term, which is 4 in this case, is related to the type of interface. This is the value corresponding to a disc - shaped microelectrode, whereas the value for a micropipette will be 3.35π.[50] For an array of micro interfaces, not only the size of the pore but the spacing between them becomes important in determining the diffusional behaviour observed. If the electrodes,

or interfaces in this case, are spaced too close together the diffusion regimes will overlap and linear diffusion will be observed rather than radial, as illustrated in Figure 2.1.5. If the spacing is far enough apart the pores will have independent diffusion and radial diffusion will be achieved as seen in Figure 2.1.6.[52, 54, 96]

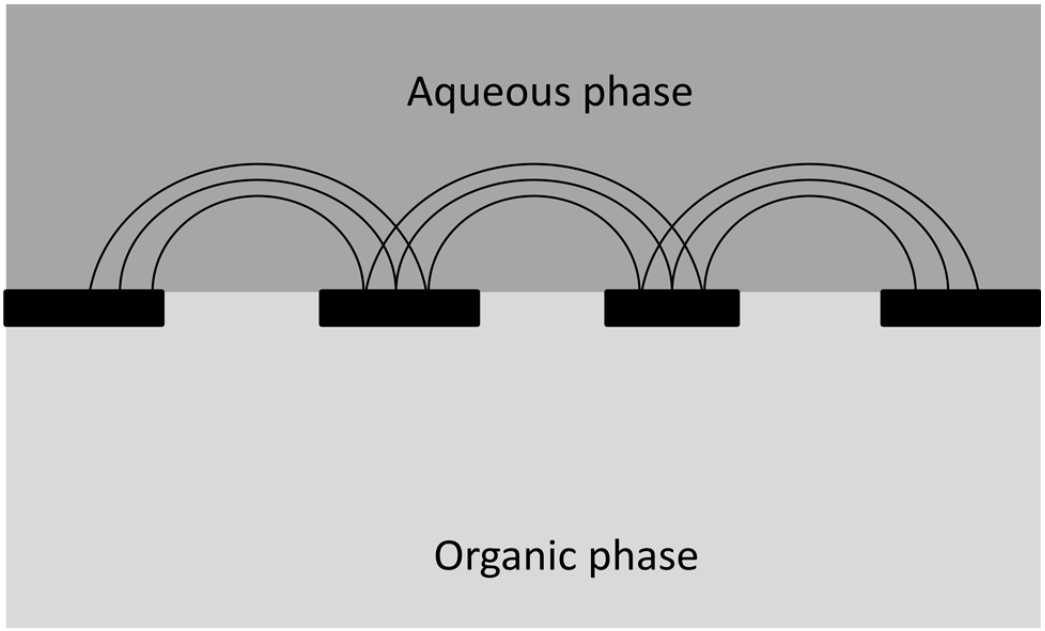

Figure 2.1.5: Schematic of a micropore array which has diffusional overlap causing linear diffusion from the aqueous side.

The optimal conditions are those in which each pore behaves independent of the others with respect to diffusional overlap, but the greatest number of pores per unit area is still achieved so as to produce the largest current.[53] To achieve optimal conditions the pore to pore distances must satisfy equation 2.1.3.

$$0.5r_c > \delta \quad \text{Eqn 2.1.3}$$

Where r_c is the pore centre to centre separation, and δ is the greatest extension of the diffusion zone from a micropore.

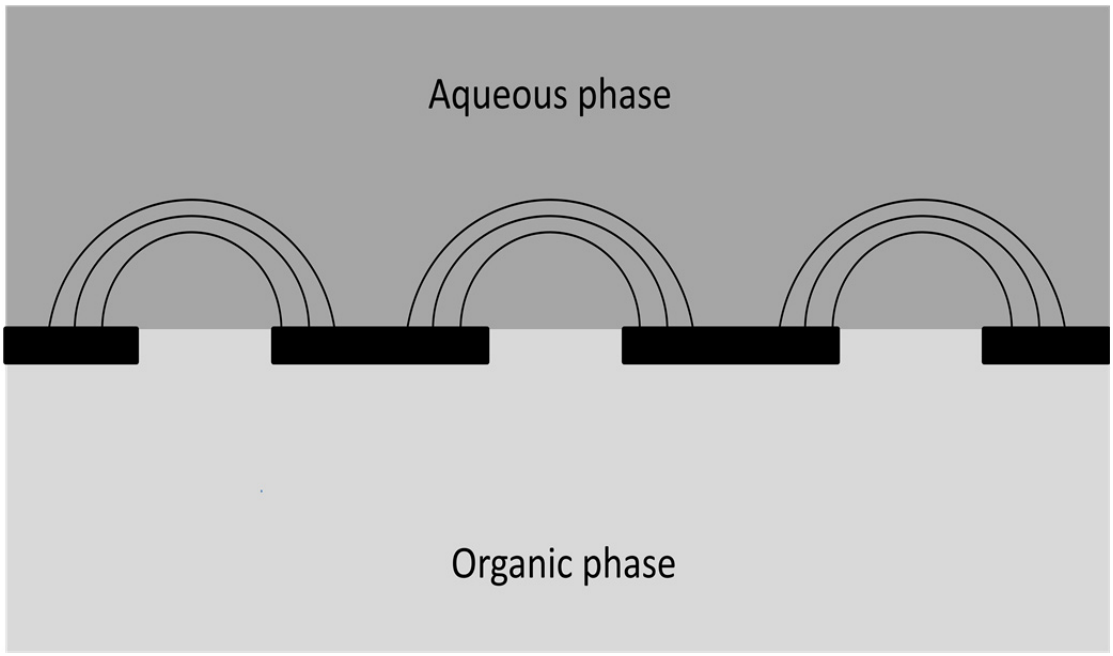

Figure 2.1.6: Schematic of a micropore array which has diffusional independence causing spherical diffusion from the aqueous side.

The size of the diffusion zone is dependent on the time scale of the experiment and the diffusion coefficient[1] as shown in equation 2.1.4.

$$\delta = \sqrt{Dt} \quad \text{Eqn 2.1.4}$$

Where D is the diffusion coefficient ($cm^2\ s^{-1}$) and t is time (s^{-1}). Therefore as the time scale of the experiment changes, so too does the diffusion zone. There have been several attempts to define the parameters which will result in a steady state response at a microelectrode array. Saito[97] was first to describe the relationship by relating the pore to pore separation, r_c, with pore radius, r_a, following equation 2.1.5

$$r_c > 12r_a \quad \text{Eqn 2.1.5}$$

This relationship was later proven to be unsatisfactory by Lee et al. by the use of finite element simulation, which were compared to experimental data.[98]

Another relationship was proposed by Horne et al.[99] which follows equation 2.1.6.

$$r_c \geq 20r_a \quad \text{Eqn 2.1.6}$$

Again this was found to be an insufficient description of the parameters which produce a steady state current. This is in part due to the complexity and the number of parameters involved, as the voltammetric response is not only dependant on pore size and pore to pore separation, but also time scale of the experiment, diffusion coefficient of the analyte. Davies et al. proposed an alternative relationship[100] shown in equation 2.1.7

$$r_c > \sqrt[2]{2D\frac{\Delta E}{v}} \quad \text{Eqn 2.1.7}$$

Where ΔE is the potential range from the foot of the peak to the reverse point and v is the scan rate (V s^{-1}). This equation includes the parameters for diffusion coefficient and scan rate but still does not account for pore radius. In 2008 Strutwolf et al. performed finite element simulations using microITIES arrays and found that the proposed models correlate well with experimental data[101] thus providing a useful method for array design.

2.2 Electrochemical techniques

All electrochemical measurements were carried out using an AUTOLAB PGSTAT302N electrochemical analyser (Metrohm Autolab, Utrecht, The Netherlands) with the supplied NOVA software for analysis.

2.2.1 Cyclic voltammetry and linear sweep voltammetry

Cyclic voltametry (CV) is a very widely used technique in electrochemistry. It can provide information on both the thermodynamics and kinetics of electrochemical processes. Cyclic voltammetry is performed by scanning a linear potential range from an initial potential, E_1, to a final potential,

E_2. Once E_2 is reached the potential is scanned in the reverse direction, often back to E_1, but not necessarily. The current is monitored as a function of applied potential and the resulting plot is a cyclic voltammogram. The number of potential cycles may be repeated depending on the objective of the experiment, but can be more than one. The potential cycling follows a triangular waveform as shown in Figure 2.2.1

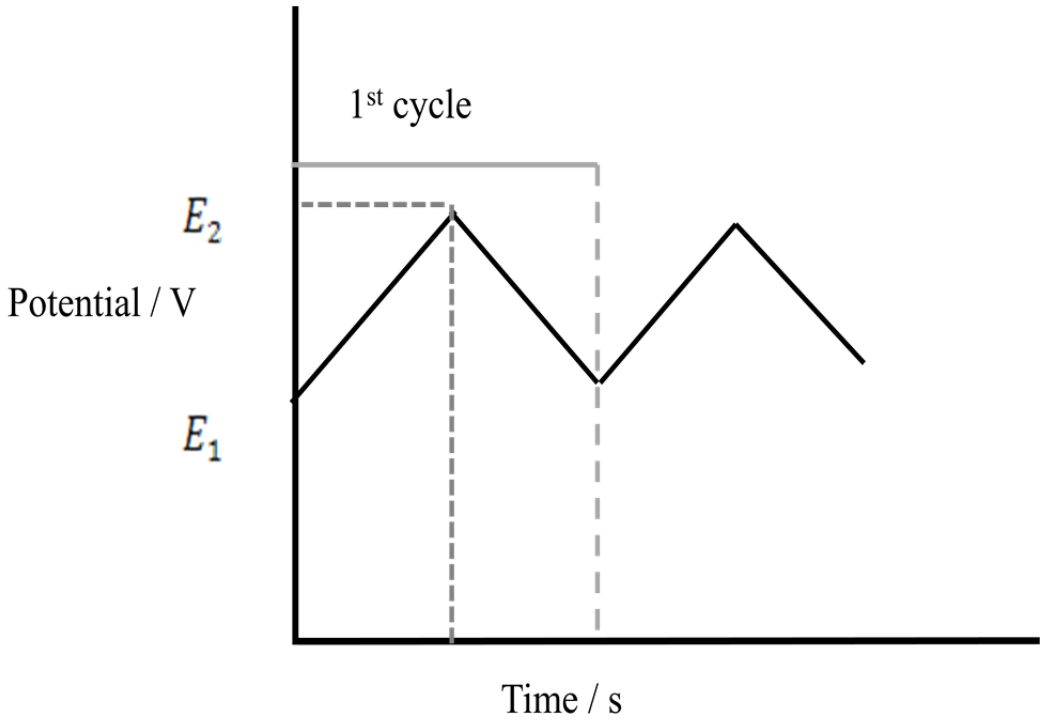

Figure 2.2.1: The potential – time signal used in cyclic voltammetry.

The first half of the scan from E_1 to E_2 is referred to as the forward scan and from E_2 to E_1 is the reverse scan.

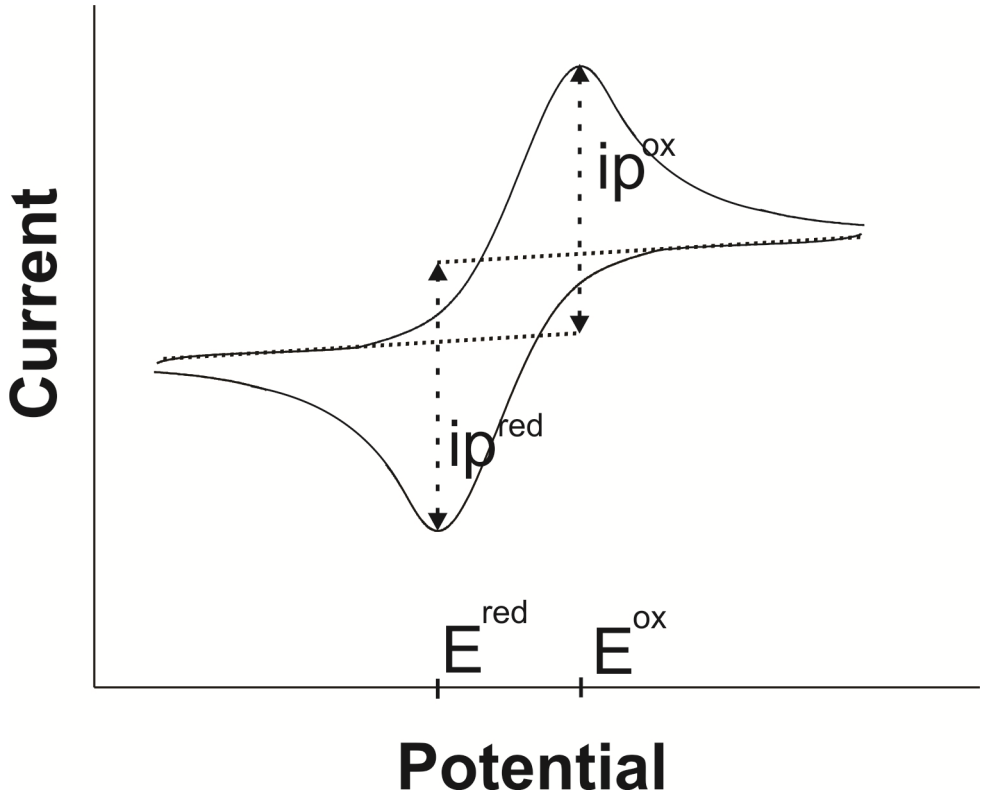

Figure 2.2.2: Cyclic voltammogram for the transfer of a cationic species from aqueous to the organic phase, resulting in peak current, i_p^{Ox} at a potential E_p^{Ox} on the forward scan. On the reverse scan the cationic species transfers from the organic phase to the aqueous resulting in a peak current, i_p^{Red} at a potential E_p^{Red}.

Often the peak currents and the corresponding potentials are the most valuable information obtained from a CV. A typical CV for cation transfer across the aqueous – organic interface is shown in Figure 2.2.2, where a peak current is produced at a given potential during the voltammetric scan. For a reversible process a peak will be observed on the forward and the reverse scan, indicated by E_p^{Ox} and E_p^{Red}, i_p^{Ox} and i_p^{Red} are the respective peak currents. Where 1-dimensional or linear diffusion is occurring the peak current follows the Randles – Ševčik[2] equation given by equation 2.2.1.

$$i_p = (2.69 \times 10^5) z_i^{3/2} A C D^{1/2} v^{1/2} \quad \text{Eqn 2.2.1}$$

Where i_p is the peak current and v is the scan rate. From this relationship it can be seen that the peak current, i_p, is proportional to the square root of the scan rate, $v^{1/2}$. This equation is analogous to that for the case of electron transfer, where the charge of the ion, z_i, is replaced by the number of electrons n.[3] A similar analogy to electron transfer processes can be used to test the reversibility of the system. The ratio of the forward and reverse peak currents, i_p^{Ox} / i_p^{Red} should equal to 1. Also the difference in peak potentials should equal to 59 mV/z_i for a reversible process of a single-charged ion,[3] in this case the term z_i has replaced n, as seen in equation 2.2.2.

$$\Delta E_p = E_p(fw) - E_p(rev) = \frac{0.059}{z_i} \text{ V} \quad \text{Eqn 2.2.2}$$

Values for ΔE_p that deviate from this value are said to be quasi-reversible processes. Where no reverse peak current is present, the process is said to be irreversible. When peak currents, i_p, are proportional to scan rate v, this is indicative of non-faradaic charge transfer which includes adsorption events.

The voltammetric responses described here are representative of simple ion transfer at the ITIES where linear diffusion is dominant, typical of a macro sized interface with a flat boundary between the two phases. Due to the use of micro ITIES and more complicated molecules such as proteins, deviations from this behaviour are observed. Simple ion transfer at the μ-ITIES produces voltammetry as described in section 1.2.5.

Linear sweep voltammetry (LSV) follows the same principles as cyclic voltammetry, but represents one half of the cycle where the potential is scanned in one direction only. From Figure 2.1.1 this would be represented by a linear potential change of a fixed scan rate, v, from E_1 to E_2. This produces a voltammetric response equivalent to half of Figure 2.2.2 where only the forward or reverse peak is observed, depending on the initial starting potential and direction of scan.

For molecules which undergo adsorption – desorption to the interface the peak current is directly proportional to surface coverage, Γ, given by equation 2.2.3.

$$i_p = \frac{n^2F^2\Gamma Av}{4RT} \quad \text{Eqn 2.2.3}$$

The surface coverage, Γ, can also be related to the to charge transfered for a process, Q by equation 2.2.4.

$$Q = z_i FA\Gamma \quad \text{Eqn 2.2.4}$$

Again the term z_i has replaced the term n to represent ion transfer rather than electron transfer. The value for total charge, Q, can be obtained for a given process by integration of the area under the voltammetric peak of interest.

2.2.2 Stripping voltammetry

Stripping voltametry or stripping analysis is an electrochemical technique often used to achieve lower detection limits.[102] The technique has been used widely, but is most commonly associated with trace metal analysis.[103] Stripping voltametry is essentially a two part technique, where firstly the analyte is accumulated on a surface, followed by a stripping of the analyte from the surface and recording the resulting voltammetric response. It is the accumulation of the analyte onto the surface which contribute to the low detection limits, which can be as low as 10^{-10} M.[103]

Although this technique is typically used for redox processes, the concepts can be applied directly to electrochemistry at the ITIES. Rather than accumulate a metal on an electrode surface by holding at a potential more negative than its reduction potential, an ion can be accumulated in one phase by holding at an applied potential which is greater than the ions transfer potential. Once the analyte has been accumulated, the potential can be scanned back using a linear sweep method, when the reverse transfer potential is reached the ion will

transfer back to the original phase and produce a voltammetric response, which is magnified due to the larger concentration of analyte transferring.

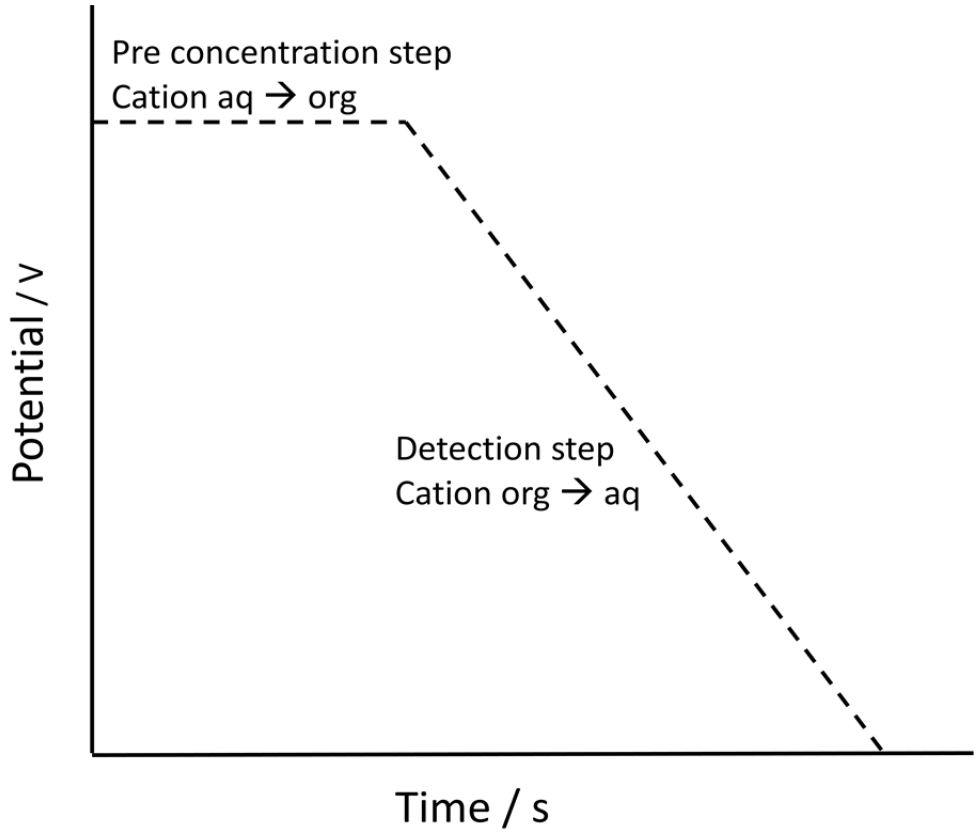

Figure 2.2.3: Stripping voltammetry potential – time sequence. On application of a fixed potential, the cation transfers from the aqueous phase (aq) to the organic phase (org). After a period of time at the fixed potential, the potential is decreased and the cation transfers back to the aqueous phase while the voltammetric response is recorded.

This process is illustrated in Figure 2.2.3, where a cation is accumulated in the organic phase by holding a fixed potential and is subsequently stripped back to the aqueous phase when the potential is lowered, resulting in a voltammetric response. This accumulation process is effectively a pre-concentration step coupled with LSV, which provides improved detection responses over conventional voltammetry.

Chapter 3

Electrochemical behaviour of myoglobin at an array of microscopic liquid-liquid interfaces

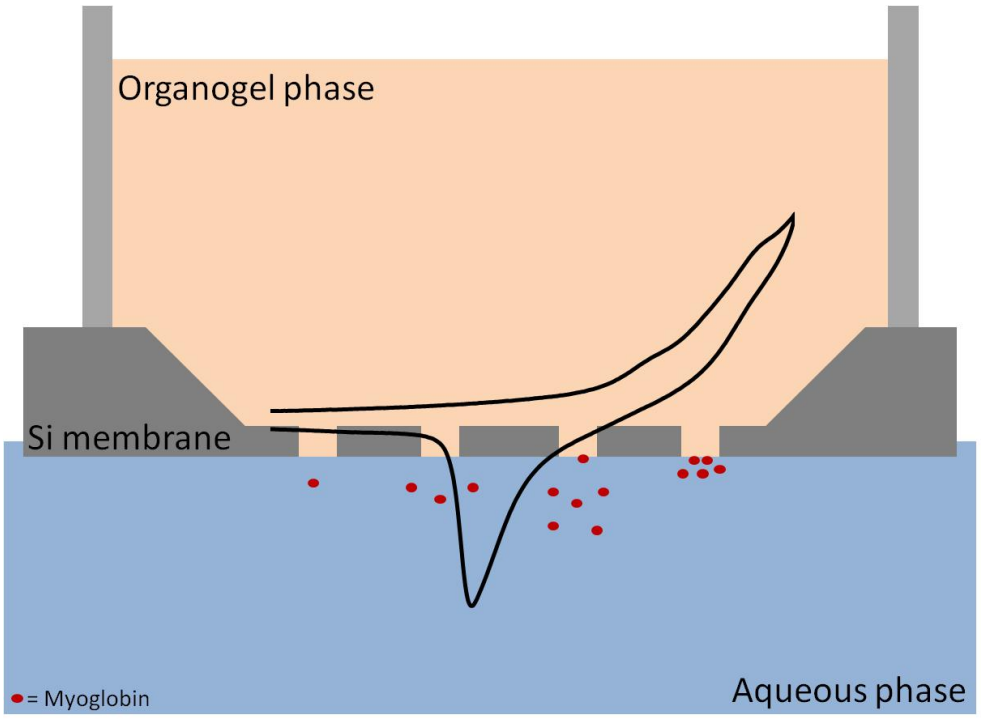

3.1 Introduction

In this chapter, the electroactivity of myoglobin (Mb) at the interface between two immiscible electrolyte solutions (ITIES) [4] is presented. Mb is a globular protein containing a haem group, comprised of a single chain of 153 amino acids with a molecular mass of 16.7 kDa and an iso-electric point of ~7.3 [104]. It was the first protein to have its 3D crystal structure determined, in 1958 [105]. Mb is an oxygen-binding protein used in the transportation and storage of 0_2 in muscle cells [106]. The detection of Mb may be a route to the diagnosis of acute myocardial infarction (AMI), as elevated concentrations of Mb are present in the blood following the onset of the disease [107, 108]. Elevated concentrations of Mb (4 – 11 nM) are present as early as 1-3 hours after AMI [109], which implies that a rapid, accurate and reliable testing method is needed. The detection of Mb within these first few hours allows Mb to be used as an early confirmation of AMI and has the potential to impact fundamentally on preventative medicine [110]. More generally, the presence of Mb in blood may be indicative of muscle damage.

Electrochemistry at the ITIES provides a strategy for the label-free detection of molecules that are not easily detected by conventional redox methods at solid electrodes [5, 111]. To improve the performance characteristics of electrochemistry at the ITIES, the miniaturisation of the interface has been a topic of interest since the use of the first micron-sized ITIES by Taylor and Girault in 1986 [7]. The use of μITIES minimises problems occurring at larger (mm or cm) interfaces such as charging current and ohmic potential drop while also significantly increasing mass transport rates [51, 112]. The development of nanoscale interfaces has received much attention recently, in an attempt to further improve the electrochemical response at the ITIES [19, 112, 113]. Methods for development of the micro/nano ITIES vary from pulled glass pipettes [7], laser ablation of a substrate [14] to various chemical etching methods [114]. The results reported here utilised a μITIES array fabricated from a silicon

membrane containing an array of micropores [57]. In recent years there have been many reports on the behaviour and detection of biomolecules at the ITIES. The detection of a range of biomolecules including amino acids[115], heparin[70, 116], protamine[67, 73], haemoglobin[77, 82], lysozyme[79, 84], insulin[78], dopamine[15, 29, 31], noradrenaline[29] and DNA[28] have been reported at the ITIES.

The effect of varying the organic phase anion on the electrochemistry of protamine at the ITIES was extensively studied by Trojanek *et al*. using conductometry, voltammetry and quasi-elastic light scattering [73]. The interactions of cationic proteins with the hydrophobic anions has been verified also by on-line acoustic sensor[117] and mass spectrometric[118] methods.

The aim of the work presented in this chapter was to investigate the behaviour of Mb at the μITIES array and to make comparisons to previous work. In particular, it was of interest to see if the previously proposed mechanism for protein detection was generic: the adsorption of protein and facilitated ion-transfer of hydrophobic anion applies to haemoglobin[77, 82], lysozyme[79, 84, 118] and insulin[78 84] will it also apply to Mb? Although some behaviour of Mb at the ITIES was reported[80] that work was based on experiments in the presence of organic phase surfactant. In the present work, the behaviour of Mb was characterised by cyclic voltammetry at the interface between the liquid aqueous phase and the gelled organic phase. The organogel was located within the pores of the silicon membrane used, so that the interface was inlaid. This arrangement results in radial diffusion to the interface from the aqueous side of the interface and linear diffusion from the organic side of the interface [57, 119].

3.2. Experimental details

3.2.1 Reagents

All the reagents were purchased from Sigma-Aldrich Australia Ltd. and used as received, unless indicated otherwise. The gellified organic phase was prepared using bis(triphenylphosphoranylidene) tetrakis(4-chlorophenyl)borate (BTPPA+TPBCl-, 10 mM) in 1,6-dichlorohexane (1,6-DCH) and low molecular weight poly(vinyl chloride) (PVC) [120]. The organic phase electrolyte salt $BTPPA^{+}TPBCl^{-}$ was prepared by metathesis of bis(triphenylphosphoranylidene)ammonium chloride ($BTPPA^{+}Cl^{-}$) and potassium tetrakis(4-chlorophenyl) borate ($K^{+}TPBCl^{-}$)[121]. The electrolyte ($BTPPA^{+}$ $TFPB^{-}$) was prepared by metathesis of bis(triphenylphosphoranylidene)ammonium chloride ($BTPPA^{+}Cl^{-}$) and sodium tetrakis(4-flourorophenyl) borate ($Na^{+}TFPB^{-}$). Aqueous stock solutions of Myoglobin (from equine heart) were prepared in 10 mM HCl or in mixtures of 1, 10 or 100 mM LiCl in 10 mM HCl (pH 2) on a daily basis and stored at +4 ºC. For variable pH experiments, the pH was adjusted using solutions of 10 mM HCl and 10mM NaOH. Tetraethyl ammonium (TEA^{+}) chloride solutions were prepared in a background electrolyte of 10 mM HCl. All the aqueous solutions were prepared in purified water (resistivity: 18 MΩ cm) from a USF Purelab Plus UV.

3.2.2 Experimental set-up

Once prepared as described in Section 2.1.3., the silicon micropore membrane was then inserted into the aqueous phase (10 mM HCl, Myoglobin in 10 mM HCl or 1, 10 or 100 mM LiCl and/or TEA+ in 10 mM HCl). Ultraviolet/visible (UV/vis) absorbance spectroscopy was carried out using a Perkin-Elmer Lambda 35 instrument. The instrument was scanned in the range of 250 nm to 500 nm at the rate of 480 nm min^{-1}. The slit width was 1 nm with a resolution of 1 nm. The sample was run in a 1 x 1 cm quartz cuvette.

The setup used for the experiments comprised of a two electrode cell [122], with one Ag|AgCl electrode in the organic phase and one in the aqueous phase. The cell utilised in these experiments is shown in Figure 3.2.1, where x refers to the concentration of Mb or the tetraethyl ammonium ion (TEA^+). All potentials are reported with respect to the experimentally-used reference electrodes. An eight micropore array was employed for all experiments (described in section 2.1.3)

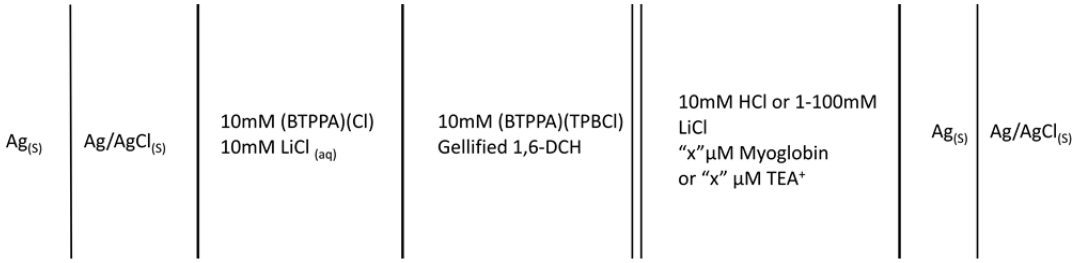

Figure 3.2.1: The electrochemical cell employed in these experiments.

3.3 Results and discussion

3.3.1 Cyclic voltammetry of Myoglobin

The electrochemical behaviour of Mb at the ITIES was investigated using cyclic voltammetry. Figure 3.3.1 (a) shows the voltammograms obtained when scanning from 0.0 V to 1.0 V relative to the Ag|AgCl electrodes. The protein's iso-electric point is 7.3 [104] and hence it is positively charged at pH 2 and assumed to be fully protonated, in which case it has a charge of +32, based on its amino acid sequence.[123, 124] The forward scan shows an increase in current in the presence of the protein as the scan reaches towards the end of

the electrochemical window (0.75 V). This is a feature of facilitated transfer of the organic phase anion in the presence of adsorbed positively charged protein at the ITIES [78, 84]. Although it is difficult to distinguish a transfer wave from background electrolyte transfer so close to the limit of the potential window, it can still be seen that the current increases with the concentration of Mb present in the aqueous phase. The reverse scan shows a well-defined peak at 0.68 V which is attributed to desorption of the protein from the interface, as seen in previous studies with other proteins [84]. Figure 3.3.1 (b) shows the peak currents from the reverse peaks in the concentration range 1 – 6 μM Mb. Blank scans (i.e. zero Mb present in the aqueous phase) were recorded in between scans with Mb present in order to ensure that no protein remained absorbed on the interface and carried over from one experiment to the next. These blank scans were featureless in the potential regions where Mb exhibited voltammetric behaviour as can be seen in Figure 3.3.1 (c). In the 1 – 6 μM concentration range there was a linear response between the reverse peak current and the concentration of Mb.

The surface coverage of Mb at the μITIES array can be determined from the charge under the reverse scan peaks using equation 2.2.4 [125].

$$Q = z_i FA\Gamma \qquad \text{Eqn 2.2.4}$$

Here, Q is the charge corresponding to the desorption peak (C), z_i is the charge on the protein, F is Faraday's constant (C mol^{-1}), A is the total geometric area of the microinterfaces (cm^2) in the array, and Γ is the surface coverage. The charges for the reverse peaks in Figure 3.3.1(a) correspond to surface coverages in the region of 10 - 50 pmol cm^{-2}. The surface coverage varied with aqueous phase concentration of Mb similar to that of the peak current, in that no saturation effect was observed in the concentration range studied. The adsorption of Mb monolayers at the ITIES was investigated by the Girault's group using optical second harmonic generation [126]. The surface area occupied by a single Mb molecule was taken from its crystallographic

data and assumed to be 10 nm^2 [127]. It was shown that a full monolayer coverage corresponds to 10^{17} molecules/m^2 (or 1.66 x 10^{-11} mol cm^{-2}). Using the surface coverage data obtained from Figure 3.3.1(a), it was found that there was a minimum of 0.6 of a monolayer formed at a surface coverage of 10 pmol cm^{-2} and a maximum of 2.9 of a monolayer formed at 50 pmol cm^{-2}. These results are consistent with the finding that a multilayer of haemoglobin formed at the liquid-liquid interfaces under cyclic voltammetric conditions[119]. It should be noted also that the experimental data obtained from cyclic voltammetry are not obtained at equilibrium, unlike the optical SHG studies[126] and much longer adsorption times may be needed to achieve surface saturation and equilibration.

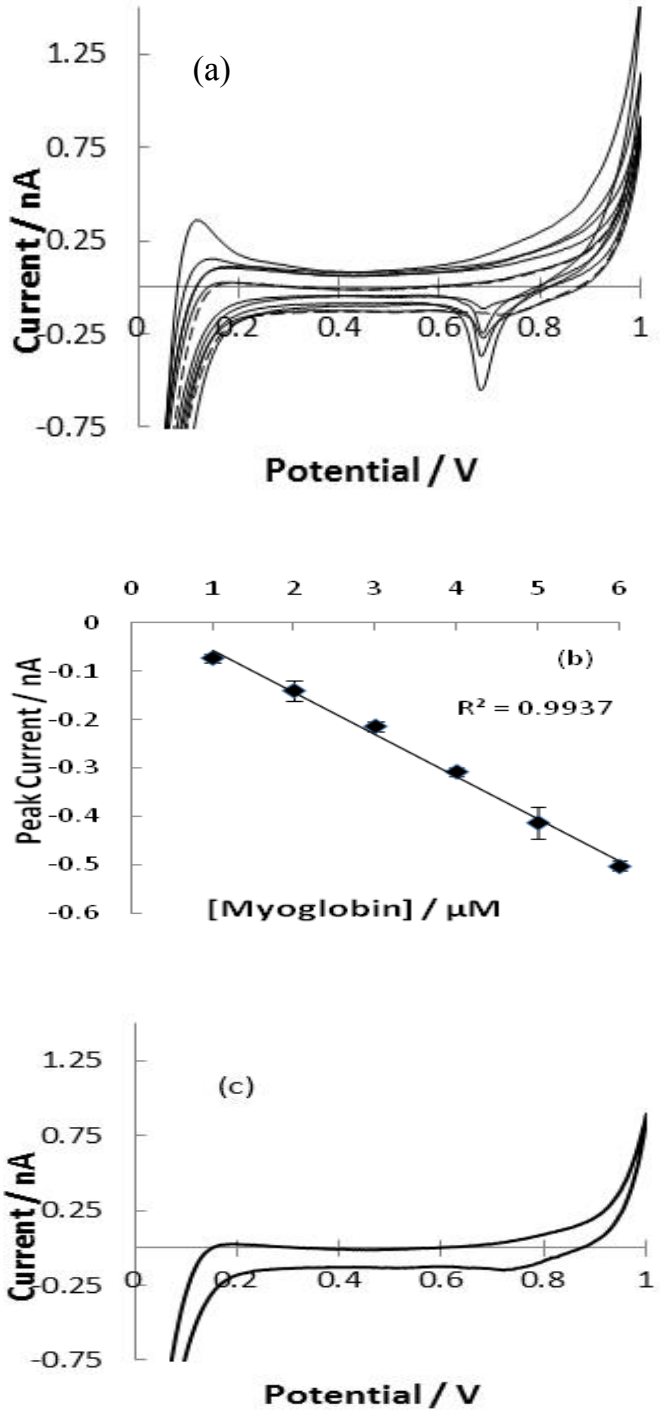

Figure 3.3.1: (a) CVs of 1, 2, 3, 4, 5 and 6 µM Mb, scan rate 5 mVs^{-1}. The dashed line represents 0 µM Mb. (b) Plot of reverse peak current versus myoglobin concentration. (c) Blank CV run between Mb scans, with only HCl present. The electrochemical cell is as outlined as in Figure 3.2.1.

3.3.2 Scan rate studies

To investigate the nature of the processes (diffusion, adsorption) occurring at the interface, cyclic voltammetry at a fixed Mb concentration (5 μM) was carried out with varying scan rates, in the range 5 – 75 mVs^{-1} (Figure 3.3.2(a)). The forward and reverse peak currents show a linear response to scan rate (correlation coefficient of R = 0.998 and R = 0.994, for the forward and reverse scans respectively) as seen in Figure 3.3.2 (b). It should be noted that on the forward sweep the current was taken consistently at 0.875 V for both Figure 3.3.2 (b) and (c). For a diffusion controlled process, a linear correlation between square root of scan rate and peak current is expected, as can be seen from Figure 3.3.2 (c) this is not the case. This dependence of both the forward and reverse peak current on scan rate indicates that the behaviour is not diffusion-controlled but is due to desorption of the protein from the interface. Although the peak current increased with scan rate, at the higher scan rates the peaks became broader and less distinguishable from the background electrolyte transfer and capacitive charging current and hence it was more difficult to measure the peak magnitude. As a result, the current versus scan rate plot exhibited a large intercept on the current axis, of ca. 1 μA. These results agree with the previous model proposed for a facilitated ion transfer (FIT) mechanism for protein detection at the ITIES [79, 84]. The protein adsorbs to the interface and facilitates the transfer of the organic phase anion resulting in the broad forward wave and the formation of a protein-organic phase anion complex at the aqueous side of the interface. On the reverse scan, the complex dissociates, with accompanying protein desorption and anion reverse transfer to the organic phase, resulting in the reverse peak recorded in the voltammogram.

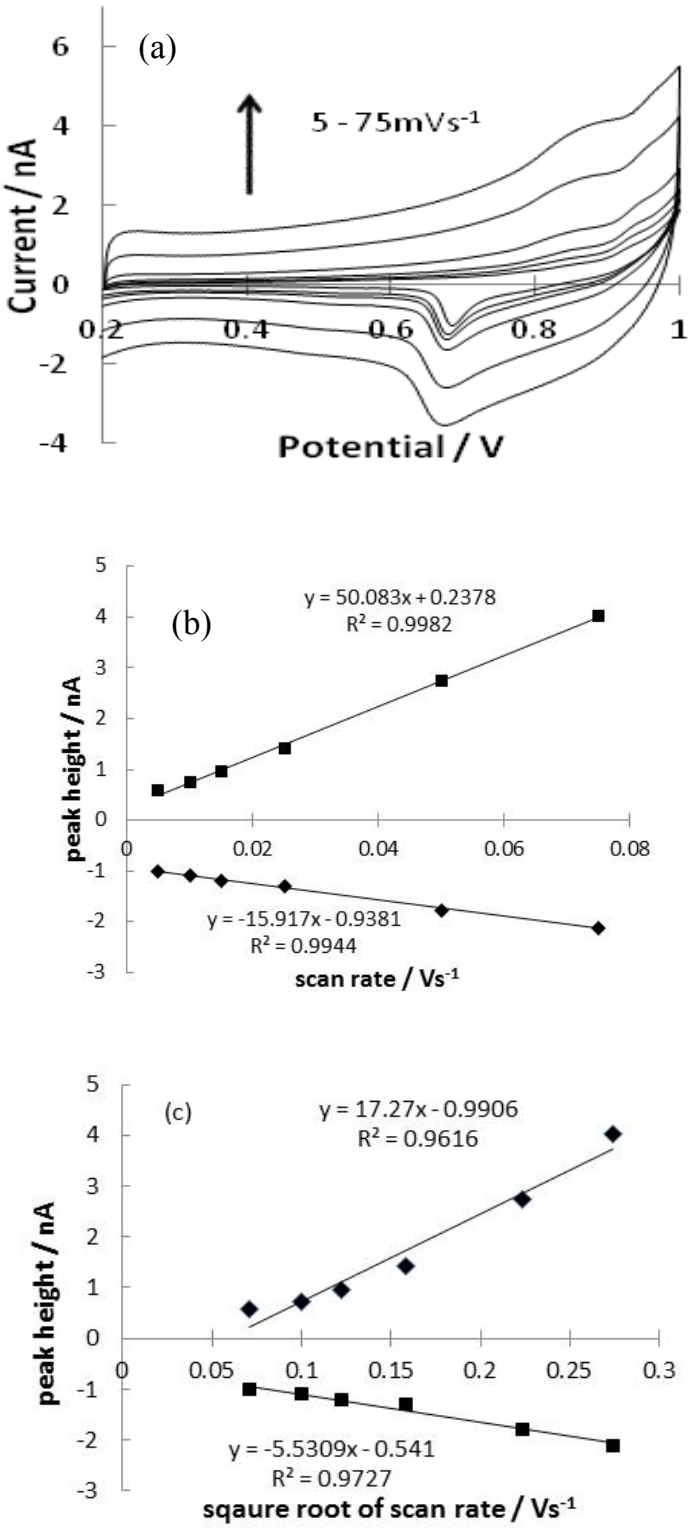

Figure 3.3.2: (a) CVs of 5 µM Mb at scan rates of 5, 10, 15, 25, 50 and 75 mVs^{-1}. (b) Plot of peak currents versus scan rate, relating to the CV's in (a). (c) Plot of peak currents versus square root of scan rate, relating to the CV's in (a). The electrochemical cell is as outlined in Figure 3.2.1.

3.3.3 Influence of the aqueous phase ionic strength

The effects of varying ionic strength on the voltammetry of Mb at a fixed concentration (5 μM) was investigated. This concentration was chosen as it was shown to give a reasonably large response, under the conditions used in Figure 3.3.1 (a). The ionic strength was varied by changing the concentration of LiCl in the aqueous phase from 1 mM to 10 mM to 100 mM. The aqueous phase was maintained at pH 2 by using 10 mM HCl in addition to the variable LiCl concentrations. The ionic strengths were calculated from equation 3.3.1, where I_c is the total ionic strength of the electrolyte solution (M), c_i is the molar concentration of the ion i (M), and z_i is the charge on that ion i. The sum is then taken over all ions in solution.

$$I_c = \frac{1}{2}\sum_i^n c_i z_i^2 \qquad \text{Eqn 3.3.1}$$

The corresponding ionic strengths for 1, 10 and 100 mM LiCl solutions in a background of 10 mM HCl were 0.011, 0.02 and 0.11 M, respectively. Figure 3.3.3 shows the resulting cyclic voltammograms related to increasing ionic strength of the aqueous phase. Previous work at the ITIES indicated that increasing ionic strength results in a marked decrease in the magnitude of peaks due to the presence of a protein [79], in that case hen egg white lysozyme (HEWL). It was suggested that the protein was further solvated by the ions in solution and this caused a decrease in protein concentration available to adsorb at the interface. Interestingly, the results presented here show that as the ionic strength increases (Figure 3.3.3(a-c)), the peaks attributed to protein adsorption/desorption become sharper and better defined as well as producing greater currents. A possible reason for the increase in the peak currents is the salting out effect [128]. This effect is used to precipitate proteins in solutions by adjusting the salt concentration. The effects of various ions on protein stability is characterised by the Hofmeister series [129]. Salt ions are categorised according to whether they denature or stabilise a protein [130]. At high salt concentrations, protein-protein interactions become favourable over

electrostatic repulsion and this is the driving force for precipitation [131, 132] and aggregation [133]. It has also been reported that at low pH, protein-protein interactions become more favourable [134]. It is likely that this combination of effects served to pre-concentrate the protein at or near the interface at the highest LiCl concentration. It was noted that during the preparation of the LiCl/Mb solutions at higher concentrations of LiCl, the protein tended to form a precipitate and aggregate in the aqueous solution. While this may improve the qualitative ability to detect Mb at the ITIES, it has implications for using the data obtained as a quantitative measurement of the protein present. As the protein solution is no longer homogeneous, representative sampling becomes a problem.

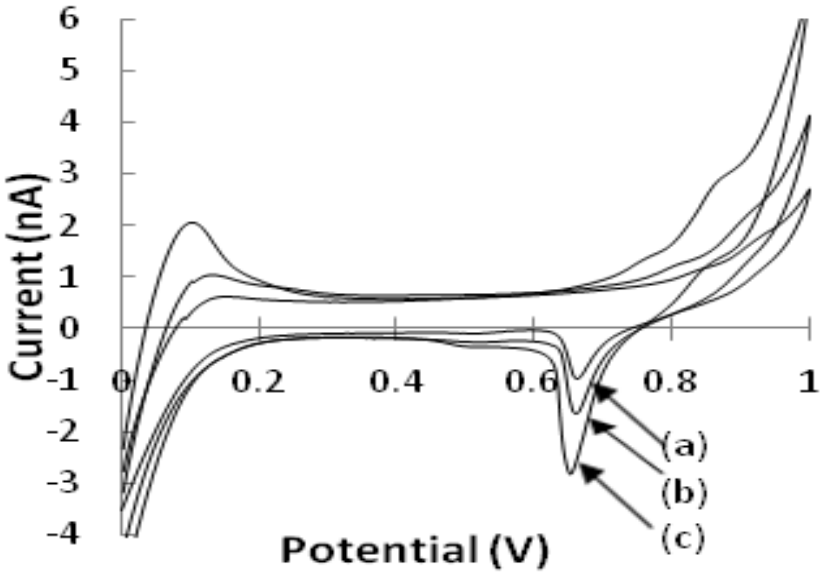

Figure 3.3.3: CV of 5 μM Mb with increasing ionic strength of the aqueous phase. (a) (b) and (c) correspond to 1, 10 and 100 mM LiCl in 10 mM HCl, respectively. Scan rate 5 mV s^{-1}.The electrochemical cell is as outlined in Figure 3.2.1.

3.3.4 Effects of the aqueous phase pH

The mechanism of FIT of the hydrophobic organic phase anion by the cationic protein species in the aqueous phase can be further validated by investigating the influence of the aqueous phase pH. Figure 3.3.4 shows the cyclic voltammetry of 9 μM Mb when the aqueous phase is adjusted to pH values of 7, 12 and 2, (Figures 3.3.4 (a), (b) and (c), respectively). The voltammograms show that the ion transfer process only occurs when the protein is in a cationic state (in an aqueous phase whose pH is lower than the protein's pI, which is 7.3 for Mb[104]); no electrochemical response was seen at the pI or above. This trend is typical of what has been seen in previous studies at the ITIES [78, 79]. Although the CVs in the absence and presence of Mb at aqueous phase pH values greater than the protein's pI are similar, there is a slight shift in the capacitative current (Figures 3.3.4 (a) and (b)) which may be a result of adsorption. But no peaks that can be associated with cation or anion transfer within the available potential window were observed.

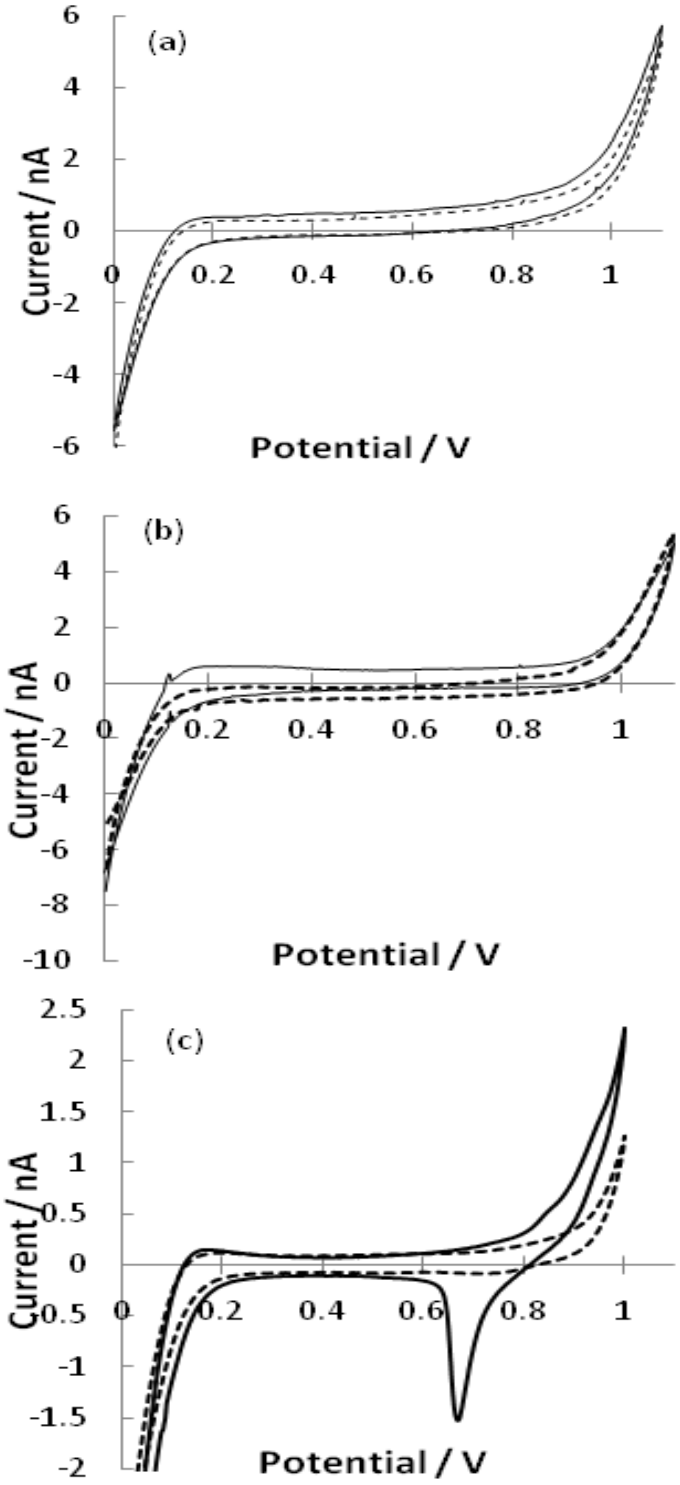

Figure 3.3.4: CV of 9 μM Mb in (a) pH 7, (b) pH 12, (c) pH 2 aqueous phase, scan rate 5 mVs-1. The blank scan (absence of Mb) is represented by the dashed line and the 9 μM Mb by the solid line. The electrochemical cell is as outlined in Figure 3.2.1.

3.3.5 Effect of organic electrolyte anion

The electrochemistry of Mb was investigated in the presence of another organic anion, $TFPB^-$. With the cation remaining unchanged the direct effects of the anion on the observed electrochemistry can be evaluated. It is know that the nature of the organic anion has an effect on the voltammetry observed,[77, 79] where the more hydrophobic anions shift the peak potentials for the protein response to more positive values. It can be seen from Figure 3.3.5 that the reverse peak current is observed at 0.76 V on the reverse scan, as compared to 0.68 V when the $TPBCl^-$ is used. Since the $TPBCl^-$ is more hydrophilic than its $TFPB^-$ counterpart, it would follow that $TPBCl^-$ requires a less positive potential for its transfer into the aqueous phase. Similar experiments have been carried out by Samec et al.[73] investigating the ion pairing between protamine and three different organic counterions, $TFPB^-$, $TPBCl^-$ and TPB^-. Although the same trend was observed, where the peak currents associated protamine and the organic counterion vary with the counterion, the trend was associated with counterion size, rather than hydrophobicity.

The peak current observed with $TFPB^-$ as the anion is ~ 0.4 nA, which is smaller than compared to ~ 1.2 nA for when $TPBCl^-$ is used. This may be due to a number of reasons, such as differing solubility of the ions in the aqueous phase, varying strengths of interaction with the Mb molecules or a combination of these factors. From comparison of previous results with insulin[78], haemoglobin[77], lysozyme[79] and protamine,[73] it is clear that the nature of the cationic species plays a significant role. In particular protamine shows the highest affinity for the TPB^- anion, whereas for all proteins studied, the affinity for TPB^- is the weakest. This may be due to the hydrophobic pockets of the protein becoming exposed due to some denaturation, either in the acidic solution or through adsorption. These hydrophobic pockets would interact more favourably with the $TPBCl^-$ and $TFPB^-$ ions. In the case of Mb, it would appear that the interactions are more favourable for the $TPBCl^-$ ion, indicating that protein structure is a key factor in the ion pairing. A greater understanding

of the interactions between these anions and the proteins may be of use in attaining selective detection of proteins, if for example an anion exhibits selectivity for one protein over another.

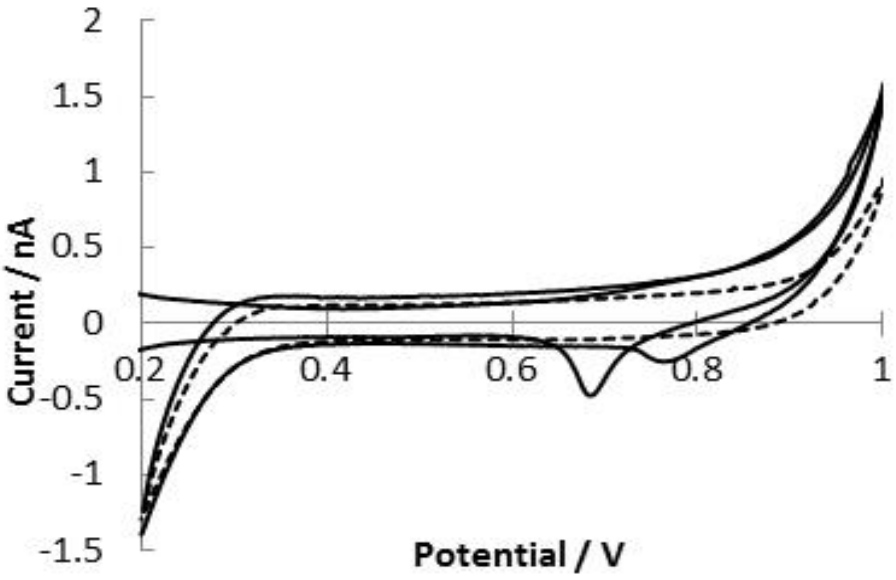

Figure 3.3.5: CV of 5 µM Mb in 10 mM HCl with $BTPPA^{+}TPBCl^{-}$ (peak at ~ 0.68 V on the reverse sweep) and $BTPPA^{+}TFPB^{-}$ (peak at ~ 0.76 V on the reverse sweep) as the organic electrolytes. The blank CV without Mb is represented as the dashed line. Scan rate is 5 mV s^{-1}.

3.3.6 Influence of Myoglobin on TEA^{+} transfer at the µITIES array

Further evidence for adsorption/desorption of Mb at the interface can be seen by comparing voltammograms in the presence and absence of the tetraethyl ammonium (TEA^{+}) cation. Simple ion transfer of an ion such as TEA^{+} at the µITIES array results in a steady-state current on the forward sweep and a peak-shaped current on the reverse sweep. The asymmetric voltammograms are the result of radial and linear diffusion profiles during the forward and reverse scans, respectively [8, 13, 119]. Figure 3.3.6 (a) shows the voltammogram

for TEA^+ transfer in the absence of Mb. The steady-state current for TEA^+ is 1.81 nA, with a half wave potential of 0.68 V. The steady-state forward response results from radial diffusion to the interface from the aqueous phase and the peak-shaped reverse response is due to linear diffusion of the analyte molecules, from the organic phase held within the membrane micropores, back to the aqueous phase. In the presence of aqueous phase Mb, the steady-state response to TEA^+ is disrupted on the forward scan (Figure 3.3.6(b)) once a potential has been reached that is sufficient to induce adsorption of the protein (> 0.6 V). This results in a decreased steady state current for TEA^+ transfer of 0.7 nA. This drop in current indicates that the transfer of the TEA^+ is affected by protein adsorbed at the interface, but also that Mb adsorption is less disruptive than lysozyme [84, 88]. In the presence of lysozyme a much more severe disruption of the TEA^+ transfer wave is observed. This is likely due to the adsorption potential of lysozyme being significantly lower than the transfer potential of TEA^+, whereas Mb would appear to adsorb after the transfer of TEA^+ begins. The reverse peak current for TEA^+ back-transfer was decreased in the presence of Mb from 1.8 nA to 1.5 nA, indicating that less TEA^+ was transferred into the organic phase due to adsorbed Mb. When the voltammogram for TEA^+ transfer (Figure 3.3.6(a)) is compared to the analogous voltammogram in the presence of protein (Figure 3.3.6 (b)) it can clearly be seen that the steady-state current on the forward sweep is diminished, while the reverse peak current is also decreased, albeit less substantially. This indicates that although the adsorbed Mb disrupts ion transfer at the interface, it does not however stop ion transfer completely, unlike the case observed with lysozyme [27,54]. This phenomenon may be a result of different adsorptive strengths for different proteins at the gelled ITIES.

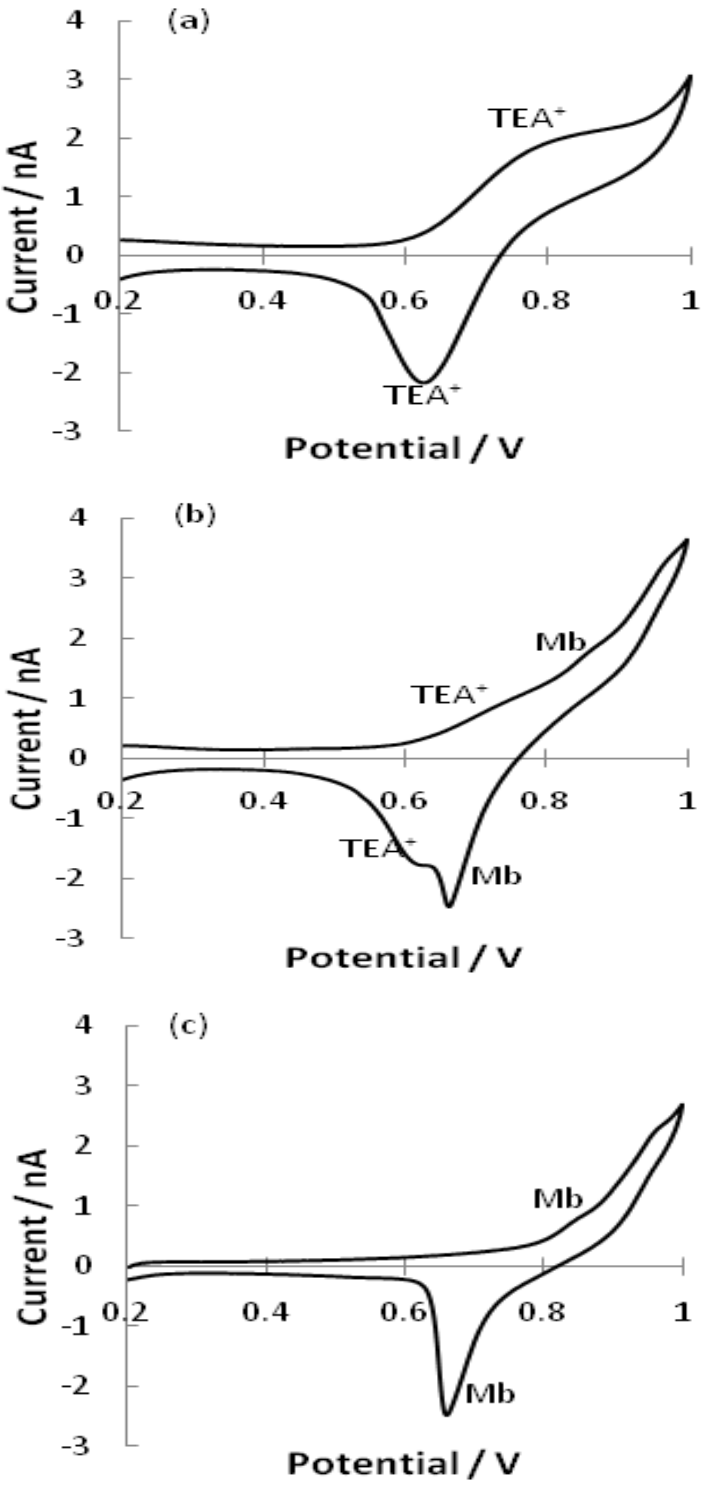

Figure 3.3.6. (a) CV of 15 μM TEA^+, (b) CV of 15 μM TEA^+ plus 9 μM Mb, and (c) CV of 9 μM Mb, scan rate 5 mVs^{-1}. The electrochemical cell is as outlined in Figure 3.2.1.

3.3.7 Effect of aqueous solution composition on Myoglobin conformation

UV/Vis absorbance spectroscopy was used to investigate whether there were any conformational changes within the Mb structure due to the effects of the aqueous phase solutions used in the above studies. UV/Vis has been used to directly investigate the effect of the environment on Mb tertiary structure. This is possible as the absorbance spectra of the haem group is directly affected by its physical environment.[135] Five different solutions were used in the sample preparation: purified H_2O, 10 mM LiCl, 10 mM PBS, 10 mM HCl and 10 mM LiCl at pH 2. The wavelength range scanned in the UV/Vis experiments was chosen to include the Soret band at *ca*. 410 nm [136], which is due the haem centre, and also the band at 280 nm, which is due to the aromatic amino acids [137]. It can be seen from Figure 3.3.7 that the Soret band is diminished in the presence of an acid solution (10 mM LiCl at pH 2 and 10mM HCl). However, in the higher pH solutions (no added acid), the Soret band remains unaffected. This is indicative of some denaturation/unfolding of the protein tertiary structure by the acidic aqueous phase electrolyte solution [135], although the extent of this process cannot be known from the UV/Vis spectra alone. The band due to the aromatic amino acids remains relatively unaffected in all aqueous solutions studied.

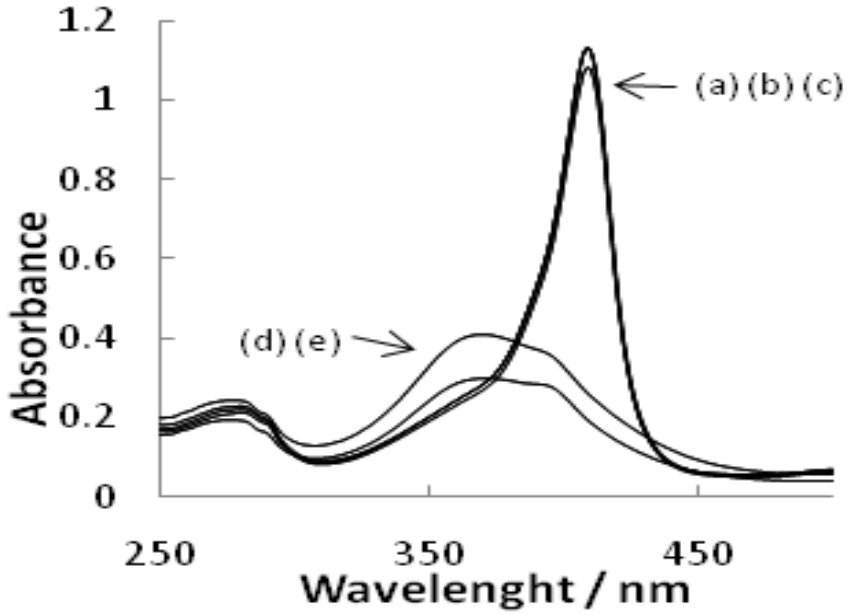

Figure 3.3.7: UV/Vis absorbance spectra of 10 μM Mb in (a) H_20, (b) 10 mM LiCl and (c) 10 mM phosphate buffered saline (PBS). (d) and (e) correspond to 10 μM Mb in aqueous solutions of 10 mM LiCl pH 2 and 10 mM HCl.

3.4 Conclusions

The aim of this work was to investigate whether myoglobin was electroactive at the μITIES array, to characterize its behaviour and to compare it to other reports of protein behaviour at this interface. The results indicate that the peak currents produced for myoglobin have a linear response to concentration in the range of 1 – 6 μM. The basis of the detection mechanism was investigated by varying the voltammetric scan rate, the organic phase anion, the aqueous phase pH and by comparing the presence of myoglobin on the simple ion TEA^+. Based on the results obtained, the detection of Mb is attributed to an interfacial adsorption/desorption process accompanied by organic phase anion transfer and association with cationic protein. It was shown that the behaviour of myoglobin was similar to previous studies of lysozyme,[79] insulin[78] and haemoglobin[77] in terms of its FIT mechanism and dependence on a cationic state of the protein in the aqueous phase. It was also shown that the presence

of a more hydrophobic anion shifted peak currents towards a more positive potential with a decrease in magnitude of the peak produced. The reverse peak showed a dependence on scan rate which indicates a desorption process. The appearance of a peak is dependent on the aqueous phase pH in that the protein needs to be in a charged state below the pI for detection to be possible. However, the need for the positively-charged protein species in the current system requires the use of low pH aqueous solutions, which have been shown, by the UV/Vis spectrophotometry of the myoglobin solutions, to denature the protein structure. The increasing peak currents due to increasing ionic strength concentration can best be explained if viewed as a type of pre-concentration step, where the protein aggregates due to precipitation. The results provide the basis for label-free detection of proteins at liquid-liquid interfaces by electrochemical methods.

Chapter 4

Methods for selective detection of proteins at the ITIES (I)

Selective detection of rat amylin in a protein mixture

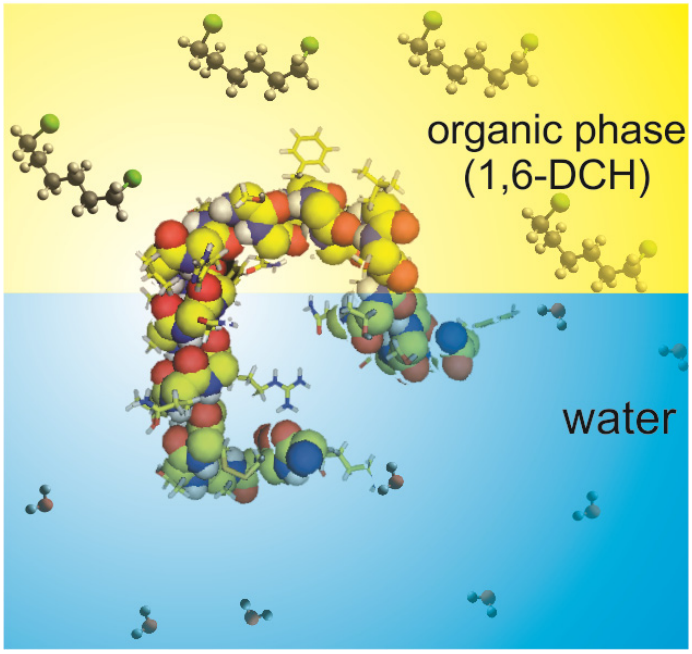

4.1 Chapter description

This chapter is split in three sections, each concerning selective detection of proteins at the ITIES but using a different approach. Selectivity is one of the major challenges concerning bimolecular detection at the ITIES. To date there has been little success in achieving selectivity aside from a few notable cases. This chapter discusses three different approaches for protein selectivity, namely adjusting the ionisation of the protein, selective voltammetric adsorption, and interactions with antibodies. Although there are many challenges still ahead in terms of selective detection of biomolecules, this work aims to show that it is an achievable target.

* I would like to acknowledge the contributions of Eva Alvarez de Eulate, Sharon Fletcher, Yiu Hang Yuen, Erik Helmerhorst and Philip Newsholme for their contributions towards the work relating to rat amylin and insulin.

4.1.1 Introduction

Alzheimer's disease (AD) is an irreversible, progressive brain disease that slowly destroys memory and cognitive skills. The disease is characterized by synaptic loss, extracellular amyloid plaques and intra-neuronal neurofibrillary tangles. Considerable genetic, animal modelling and biochemical data suggest that the principal component of amyloid plaques, the amyloid beta-protein (Aß), plays a central role in initiating AD.[138] A common characteristic of AD and type-2 diabetes is the formation of islet amyloid deposits by the 37–amino acid peptide amylin (known also as islet amyloid polypeptide, IAPP).[139] Amylin is a physiological component of islet beta-cell granules, from where it is co-secreted with insulin onto the cell surface via a regulated secretory pathway. Blood concentrations of amylin are estimated at 5 – 20 pM,[140] although the concentration at sites of release, such as the pancreatic islet, may rise to low nanomolar. It readily forms amyloid fibrils in vitro, and the deposition of fibrillar amylin has been correlated with the pathology of type 2

diabetes. Importantly, human amylin (hA), unlike its rodent homologs, has physicochemical properties that predispose it to aggregate and form amyloid fibrils. However, rat amylin (rA), which has a different amino acid sequence[141] (see Scheme 4.1.1.1) in the amyloidogenic molecular segment, does not aggregate and can form random conformations in physiological conditions. rA is known to bind to the surface of lipid micelles, such as dodecylphosphocholine,[141] which may be indicative of its biological mode of action in associating with cell membranes. The non-aggregating nature of rA makes it a simpler model polypeptide for electrochemical studies than hA.

Human: KCNTATCATQ RLANFLV**H**SS NN**F**G**AI**L**SS**T NVGSNTY

Rat: KCNTATCATQ RLANFLV**R**SS NN**L**G**PV**L**PP**T NVGSNTY

Scheme 4.1.1.1: The amino acid sequences of human and rat amylin. Differences are highlighted in bold font.

A previous study on the electrochemistry of amylin employed oxidation of tyrosine residues within hA to monitor its concentration and possible aggregation. This method involved placing a solution of the polypeptide onto the surface of a carbon electrode and allowing the solvent to evaporate prior to the electrochemical measurements.[142] However, the use of redox-active functionality within polypeptides and proteins for their detection can be problematic, resulting in issues such as fouling of the electrode surface by reaction products and an inability to rapidly transfer electrons between the electrode and a buried redox-active prosthetic group.[143] In contrast, electrochemistry of polypeptides and proteins at interfaces between immiscible electrolyte solutions (ITIES) (or at liquid-liquid interfaces formed between aqueous and organic electrolyte solutions) has been of intense interest in recent years because it provides a route to bioanalytical detection of these compounds via non-redox electrochemistry and hence circumventing the problems associated with oxidation/reduction processes at electrode surfaces,[5, 26, 66, 70, 80, 89, 144, 145] as well as providing information about the stability of

protein pharmaceutical formulations.[87, 118] Previous reports on the electrochemistry of the polypeptides protamine[66] and insulin[78] have demonstrated their detection at concentrations down to *ca*. micromolar levels. The ability to detect amylin via a non-redox electrochemistry has not been studied previously and may be beneficial in study of its function in biological processes.

In this work, the electrochemical behaviour of rA at the microinterface array between aqueous and gelled organic phases (or μITIES array) was examined. The main objective of this work was to evaluate the electrochemical behaviour of rA in an effort to develop a strategy for selective detection in a protein mixture. Selective detection of proteins is one of the major challenges faced when using electrochemistry at the ITIES as the detection method. The results detailed below show that rA is electroactive, that it transfers across the water-organogel interface, and that this transfer process is of analytical utility. This work indicates that the tuning of the charge on the analyte protein, by adjusting the pH, may provide a useful strategy to selective detection in a protein mixture. The differing of iso-electric points of the proteins provides the basis for the use of such a strategy. By adjusting the pH so that only the protein analyte has a positive charge, while the background proteins are neutral or anionic, it is possible to achieve selective detection of the target analyte. While the simplicity and ease of this method are advantageous, this technique will not work for all cases. However, when the iso-electric points of all proteins are known, the optimisation of protein charge should be considered as a method to improve for selective detection of one protein over another.

4.1.2 Experimental Details

4.1.2.1 Reagents

All reagents were purchased from Sigma-Aldrich Australia Pty Ltd and used as received, except rA, which was purchased from Bachem AG (Bubendorf, Switzerland). The gellified organic phase was prepared using bis(triphenylphosphoranylidene) tetrakis(4-chlorophenyl)borate (BTPPA+TPBCl-, 10 mM) in 1,6-dichlorohexane (1,6-DCH) and low molecular weight poly(vinyl chloride) (PVC) [120]. The organic phase electrolyte salt $BTPPA^{+}TPBCl^{-}$ was prepared by metathesis of bis(triphenylphosphoranylidene)ammonium chloride ($BTPPA^{+}Cl^{-}$) and potassium tetrakis(4-chlorophenyl) borate ($K^{+}TPBCl^{-}$)[121]. Aqueous solutions of rA were prepared in 10 mM HCl or 1 mM PBS on a daily basis and stored at +4 ºC. All the aqueous solutions were prepared in purified water (resistivity: 18 MΩ cm) from a USF Purelab Plus UV.

4.1.2.2 Experimental set-up

Once prepared as described in Section 2.1.3. the silicon micropore membrane was then inserted into the aqueous phase (10 mM HCl, 1 mM PBS or rA in 10 mM HCl or 1 mM PBS. Voltammetric experiments were then performed. The setup used for the experiments comprised of a two electrode cell [122], with one Ag|AgCl electrode in the organic phase and one in the aqueous phase. The cell utilised in these experiments is shown in Figure 4.1.2.1, where x refers to the concentration of rA. All potentials are reported with respect to the experimentally-used reference electrodes. A thirty micropore array was employed for all experiments (described in section 2.1.3)

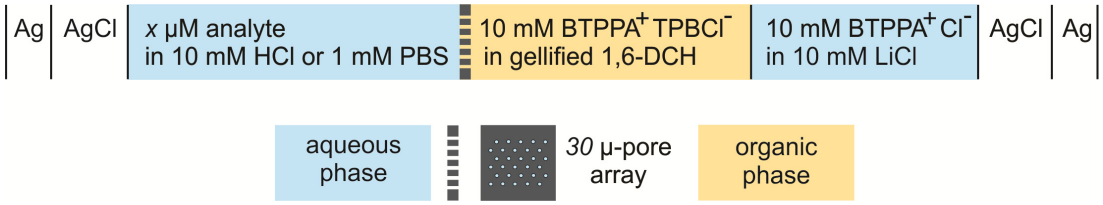

Figure 4.1.2.1: Electrochemical cell employed in this work. A thirty pore microarray was employed.

4.1.3 Results and Discussion

4.1.3.1 Detection of rat amylin at physiological pH

The iso-electric point (pI) of rA is 9, so that it is cationic at physiological pH with a charge z_i of 2+.[146] This allowed for an investigation into rA electroactivity at physiological pH, in contrast to proteins such as haemoglobin and myoglobin where it was not possible to detect them at physiological pH. Electroactivity at physiological pH suggests that there is an opportunity for applications in analysis of biological samples, because neutral or anionic proteins are not electrochemically active at this pH with the presently-employed constitution of the µITIES array. Figure 4.1.3.1 shows the CVs for rA obtained in aqueous phases of 1 mM phosphate buffered saline (PBS) at pH 7.3 (Figure 4.1.3.1 A) and in 10 mM HCl pH 2 (Figure 4.1.3.1 B). It can be seen that the rA transfers occur on the forward and reverse sweeps at similar potentials under physiological conditions as under acidic conditions. The steady-state currents on the forward sweeps (taken at ~ 0.84 V) are 3.46 nA and 2.59 nA and the reverse peak currents are 2.06 and 1.66 nA (taken at ~ 0.80 V) for rA in aqueous 1 mM PBS (z_i = 2+) and 10 mM HCl (z_i = 3+), respectively, at a concentration of 10 µM. The difference in the

observed currents can be attributed to a contribution from the molecular charge z_i and the diffusion coefficient of the polypeptide at each pH. The diffusion coefficient of rA in the aqueous phase was determined using equation 4.1.3.1

$$I_{lim} = n4z_iFDCr \qquad \text{Eqn 4.1.3.1}$$

where n is the number of μITIES in the array, z_i is the formal charge of the ion, F is the Faraday constant (C mol^{-1}), D the diffusion coefficient (cm^2 s^{-1}), C is the bulk concentration (mol $cm^{-3)}$, r is the radius (cm) of an individual microinterface and the current values from Figure 4.1.3.1, taking into account the charge of the polypeptide at the corresponding pH values. The values obtained were 6.4 10^{-6} cm^2 s^{-1} and 5.3 10^{-6} cm^2 s^{-1} for pH values of 7.3 and 2.0, respectively, which are comparable to the diffusion coefficient of TEA^+, 9.8 10^{-6} cm^2 s^{-1}.[101]

The electrical charge of the reverse peaks (integrated current with respect to time) are also influenced by the aqueous phase conditions. Comparison of the reverse peak charges for 10 μM rA in different aqueous phase conditions give values of 14.8 nC (pH 7.3) and 28.2 nC (pH 2). Taking into account the molecular charge at each pH and using Faraday's law in conjunction with the geometric area of the interface array, these peak charges correspond to interfacial coverages of 0.6 nmol cm^{-2} (pH 7.3) and 0.8 nmol cm^{-2} (pH 2). These coverages are an order of magnitude greater than a monolayer surface coverage.

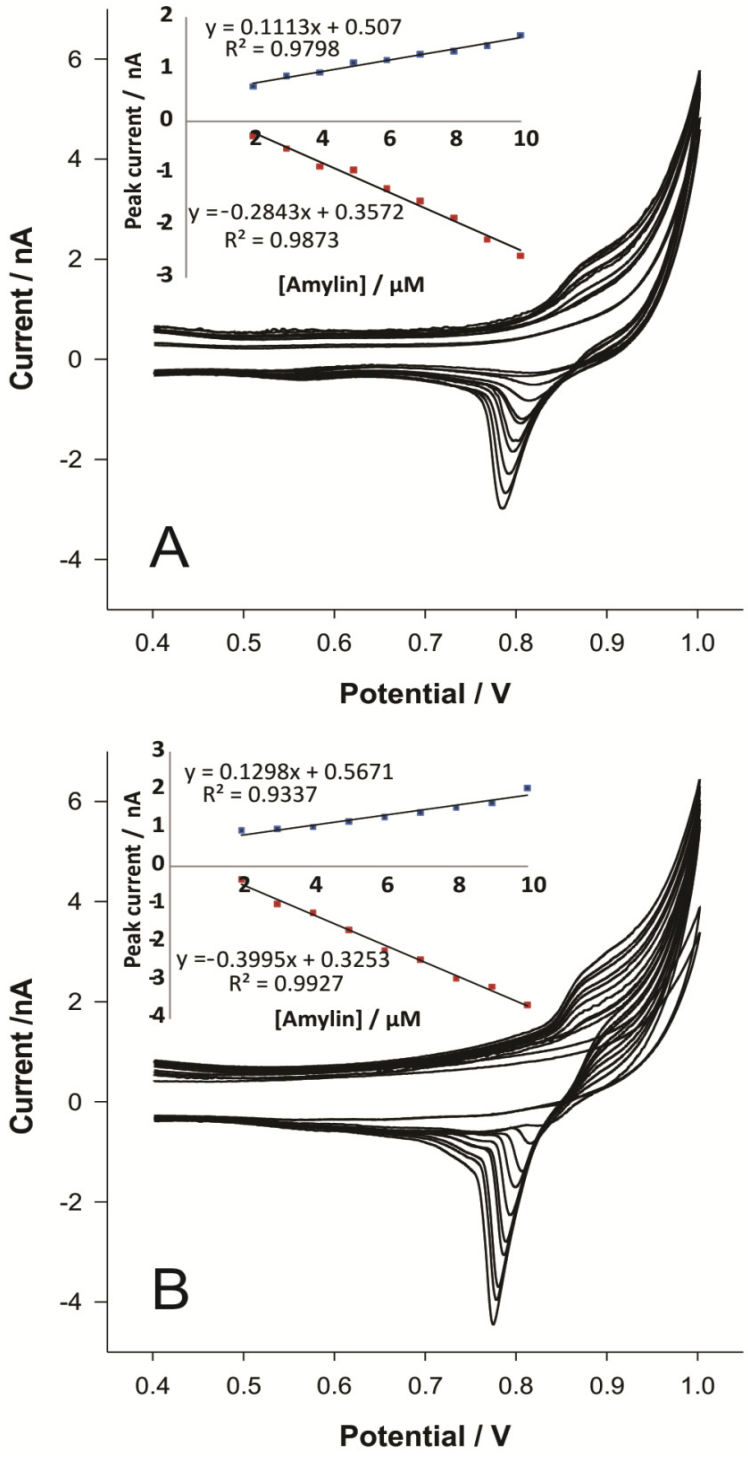

Figure 4.1.3.1: CV of rA at different concentrations (1 – 10 µM, inner to outer curves) in an aqueous phase of (A) 1 mM PBS at pH 7.3 and (B) 10 mM HCl. CV with 0 µM rA is included. Insets show the plots of forward steady-state current or reverse peak current as a function of rA concentration over the range of 2-10 µM. Scan rate 5 mV s^{-1}.

The observation that transfer currents are in agreement with molecular charge is consistent with the larger peak currents obtained from more highly charged species,[144, 147] although this usually necessitates going to lower (more acidic) pH in the aqueous phase. As a result the improvements in observed currents when using acidic media are likely to be outweighed by the disadvantages arising from performing measurements under non-physiological conditions. The insets in Figure 4.1.3.1 show linear correlations between the steady-state current (forward sweep) or peak current (reverse sweep) and the rA concentration in the aqueous phase. Clearly, sensitivity is higher under acidic conditions than physiological conditions, as expected based on differences in molecular charge, and also the calibration plots based on reverse peak currents are more sensitive than the forward steady-state currents, which is a result of rA accumulation in the organogel during the forward scan. Note that the reverse peaks in Figure 4.1.3.1 (B) are sharper than those in Figure 4.1.3.1 (A), which may be indicative of different detection mechansims. Moreover, concentrations down to 2 μM (7.8 μg mL^{-1}) of rA were easily detected by CV (a reverse peak was observed for 1 μM rA in 10 mM HCl, but the current was below the linear range of the calibration graph), showing the potentiality of this electrochemical approach at the ITIES for detection of the polypeptide.

4.1.3.2 Sensing in a protein mixture

Figure 4.1.3.2 shows the voltammetric response to 10 μM rA in the presence of a mixture of 10 μM haemoglobin (Hb), 10 μM myoglobin (Mb) in 1 mM PBS solution. The peak currents for rA are 5.8 nA on the forward sweep and -1.2 nA on the reverse sweep. The voltammogram in the presence of only Hb and Mb (i.e. without rA) shows no transfer wave on the forward or reverse sweeps, although there is an increase in current at more positive potentials. This is attributed to adsorbed protein,[87] but as the pH is above or equal to the iso-electric point of Hb and Mb, no associated peaks are observed.[78, 79] This is typical behaviour for proteins at the polarised liquid – liquid interface. The

accepted mechanism for detection of the protein is through complexation of the cationic protein with the organic phase anion.[119] There has been no evidence to date of an anionic protein complexing with the organic phase cation. Hence at physiological pH, no ion transfer processes are observed for haemoglobin or myoglobin, due to their respective iso-electric points. However the iso-electric point of rA is 9, so at physiological pH it has a charge of 2+. This feature of its physiochemical properties is what allows rA to be detected in the presence of haemoglobin and myoglobin. Although the charge on the rA is not optimal, as the larger the positive charge the better the electrochemical signal will be. This disadvantage is outweighed by the ability to detect rA in the presence of other proteins.

It can be seen that the CV in the presence of rA no longer resembles that of the corresponding CV in Fig. 4.1.3.1 A. This disruption of the steady-state behaviour is expected, as it has been shown in previous work that adsorbed proteins affect ion transfer at the ITIES.[144, 148, 149] In such a situation, the rA must penetrate an adsorbed layer of protein on both the forward and reverse sweep, hindering its transport and resulting in a distortion of the rA transfer signal, leading to much broader responses.

There have been many reports of the detection of biomolecules at the ITIES,[5] but to-date there has been little work done in real biological samples or complex matrices due to difficulties with selectivity and background interference. Amemiya et al. used voltammetry at the ITIES to detect heparin in blood plasma[70] and more recently Osakai et al. developed a method for monitoring protein concentration in urine samples by employing an ITIES hydrodynamic flow cell[89]. Presented here is the label free detection of a polypeptide, rA, in the presence of a mixture of proteins at physiological pH. Coupled with recently developed adsorptive stripping techniques[149], these results could provide the basis for use of the ITIES in more realistic biological samples.

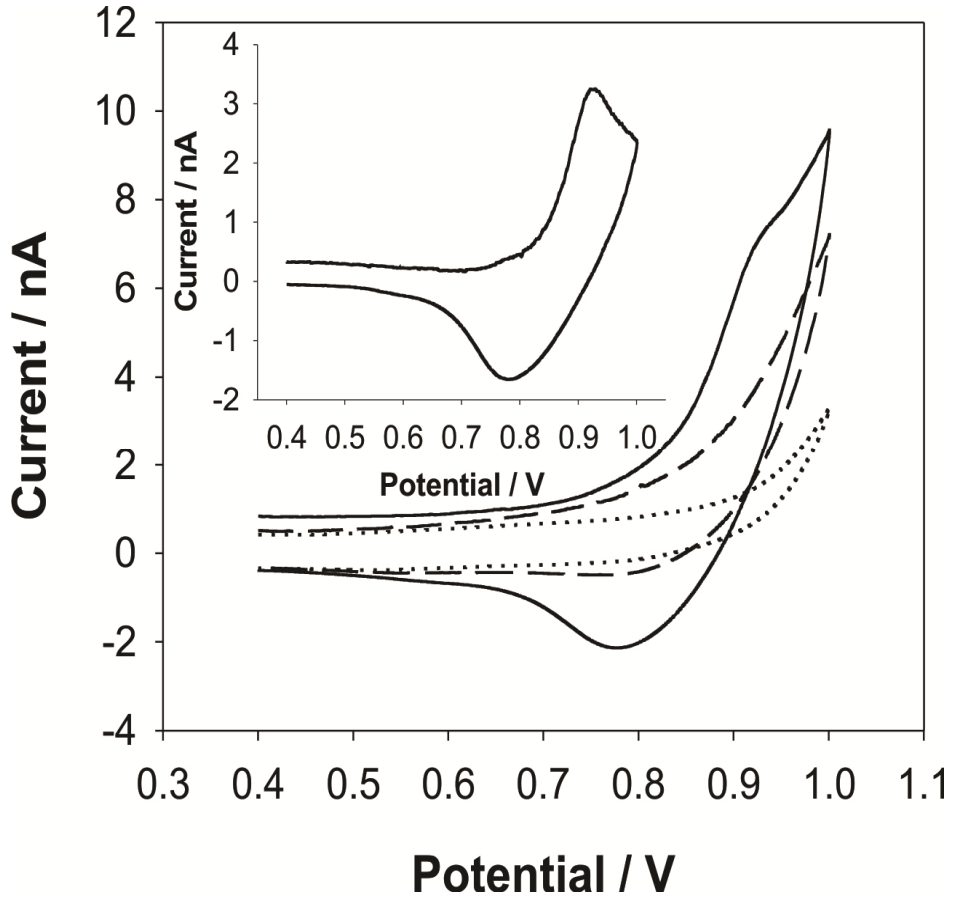

Figure 4.1.3.2: CV of aqueous phase 1 mM PBS (dotted line), 10 μM Haemoglobin + 10 μM Myoglobin in 1 mM PBS (dashed line) and 10 μM rA + 10 μM Haemoglobin + 10 μM Myoglobin in 1 mM PBS (solid line), pH 7.3. The inset voltammogram shows the result for subtraction of the CV in the presence of Haemoglobin + Myoglobin (dashed line) from that in the presence of rA + Haemoglobin + Myoglobin (solid line). Scan rate 5mV s^{-1}.

4.1.4 Conclusion

The 37-amino acid peptide rA has been subjected to study of its selective detection at an array of microinterfaces formed between liquid aqueous and gelled organic electrolyte phases. Importantly, the electroactivity of rA was maintained at physiological pH and not just at acidic pH, enabling detection under physiological conditions. As a result, electrochemistry at the gelled

ITIES opens up the possibility for rA detection in physiological matrices, as demonstrated here for its detection in the presence of a protein mixture. Coupling this observation with recently developed adsorptive stripping techniques,[16] to achieve a lower detection limit, may provide a competitive strategy for label-free biomolecular detection.

Chapter 4

Methods for selective detection of proteins at the ITIES (II)

Stripping voltammetric detection of insulin at liquid–liquid microinterfaces in the presence of bovine albumin

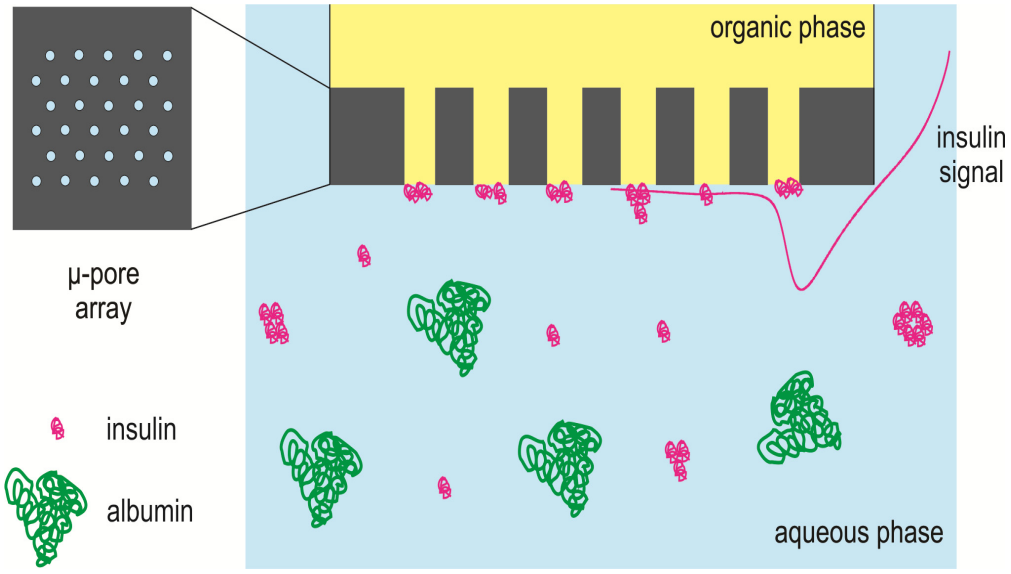

4.2.1 Introduction

The ability to detect proteins and peptides using simple methods with miniaturised devices offers many benefits including the possibility for point-of-care measurements that may revolutionise diagnostic medicine and a wide range of industrial and environmental applications.[150-152] Advances in areas such as biomicroelectromechanical system (BioMEMS) and lab-on-a-chip technologies open up opportunities for the detection of important biological molecules such as disease indicators. Consequently, new strategies are constantly emerging that have the potential to contribute to a new generation of portable analytical and bioanalytical devices. Electrochemical methods have been greatly successful in the detection of biomolecules such as glucose in whole blood.[153, 154] Electrochemical measurement at interfaces between two immiscible electrolyte solutions (ITIES) is one such emerging area that may contribute to this revolution.[23, 50] Electrochemistry at the ITIES provides scope for the detection of analyte species based on ion transfer reactions, rather than oxidation or reduction processes, and offers a label-free strategy for detection of proteins, amongst other target analytes.[115]

Diabetes mellitus is a metabolic disease associated with either a deficiency in insulin production (type 1 diabetes) or an ineffective use of insulin by the cells (type 2 diabetes).[155] Thus, the determination of insulin is clinically important and an assortment of techniques have been employed for its detection, such as enzyme-linked immunosorbent assays,[156] electrochemical impedance spectroscopy,[157] mass spectrometry,[158] microcantilever biosensors,[159] capillary electrophoresis,[160] and direct oxidative electrochemistry.[161] The large variety of methods investigated for insulin detection is indicative of the on-going need for alternative methods for the detection of insulin which might be amenable to point of care testing.

Presented here is the electrochemical behaviour and detection of insulin at an array of microscale ITIES. In this study, intentional adsorption of insulin at the electrified interface prior to the voltammetric measurement is employed. Furthermore, the challenge of insulin detection in the presence of another protein, albumin, which is abundant in serum, has been explored. The ability to detect a target protein in the presence of a protein mixture is a fundamental challenge which needs to be addressed, for electrochemistry at the ITIES to become a viable option in bioanalytical science. This work explores the selective detection of insulin through the use of electrochemical adsorption. Proteins may have different maximum adsorption potentials. Once the adsorption potential profile has been defined for a given set of protein, the difference in these adsorption potentials may be used to selectively detect a protein in a mixture. The results indicate that, although the voltammetric desorption peaks cannot be separated, the use of tuned adsorption potentials enables the detection of insulin in the presence of albumin.

4.2.2 Experimental details

4.2.2.1 Reagents

All the reagents were purchased from Sigma-Aldrich Australia Ltd. and used as received, unless indicated otherwise. Mono-component zinc insulin (porcine) was purchased from CSL Laboratories, Australia. The gellified organic phase was prepared using bis(triphenylphosphoranylidene) tetrakis(4-chlorophenyl)borate ($BTPPA^+TPBCl^-$, 10 mM) in 1,6-dichlorohexane (1,6-DCH) and low molecular weight poly(vinyl chloride) (PVC).[120] The organic phase electrolyte salt $BTPPA^+TPBCl^-$ was prepared by metathesis of bis(triphenylphosphoranylidene)ammonium chloride ($BTPPA^+Cl^-$) and

potassium tetrakis(4-chlorophenyl) borate (K^+TPBCl^-).[121] Aqueous stock solutions of albumin (from bovine serum, 98 %) and insulin (porcine) were prepared in 10 mM HCl (pH 2) on a daily basis and stored at +4 ºC. All the aqueous solutions were prepared in purified water (resistivity: 18 MΩ cm) from a USF Purelab Plus UV.

4.2.2.2 Experimental set-up

Once prepared as described in section 2.1.3 the silicon micropore membrane was then inserted into the aqueous phase (10 mM HCl, without or with albumin and/or insulin). Voltammetric experiments were then performed. The electrochemical cell arrangement used for the experiments was a two-electrode cell,[122] with one Ag|AgCl electrode in the organic phase and one in the aqueous phase. The organic phase reference electrode was immersed in an aqueous reference solution of 10 mM $BTPPA^+Cl^-$ in 10 mM LiCl. All potentials are reported with respect to the experimentally-used reference electrodes. All voltammetric experiments were run at a sweep rate of 5 mV s^{-1}. A thirty micropore array was employed for all experiments (described in section 2.1.3)

4.2.3 Results and discussion

4.2.3.1 Adsorptive stripping voltammetry of insulin and albumin

As shown previously for lysozyme[88] and haemoglobin,[162] the potential-controlled adsorption of the protein/polypeptide can be employed for efficient preconcentration and lead to improvements in detection limits. However, the issue of selectivity is still open to question. With an AdSV approach, two opportunities for selectivity are presented: the adsorption process and the detection process. Presented here is an analysis of the prospects for selectivity for one protein in the presence of another by examining insulin and albumin adsorption and detection. After characterization of the adsorption behaviour of insulin, the influence of bovine serum albumin on the electro-activity of insulin was investigated.

The optimum adsorption potentials of insulin and albumin were investigated using AdSV, where the adsorption time was held constant at 60 s, with a fixed concentration of protein. The adsorption potential was varied from 0.6 V to 1.0 V, after which linear sweep voltammetry from the adsorption potential to 0.4 V was implemented. Figure 4.2.3.1(A and B) shows the resulting voltammograms for 1 μM insulin and 1 μM albumin, respectively. A plot of the resulting peak currents against the adsorption potential is shown in Figure 4.2.3.1(D). Insulin (○) has its first observable voltammetric response following adsorption at 0.775V, and its response peaks at an adsorption potential of 0.9 V, beyond which the response diminishes. Albumin (●) has its first observable voltammetric response following adsorption at 0.825 V, and its response peaks at an adsorption potential of 0.975 V, beyond which the current response also diminishes. Since the optimal adsorption potentials for

the two proteins are different, it was postulated that selective adsorption of insulin in the presence of albumin could be achieved by careful selection of the adsorption potential. AdSV of a mixture of 1 μM insulin and 1 μM albumin (Figure 4.2.3.1(C)) was performed to characterise the adsorption behaviour of the mixture relative to the behaviour of the individual protein solutions. The resulting plot of peak current versus adsorption potential (Figure 4.2.3.1(D) – symbol ▼) showed a voltammetric response at 0.825 V that peaked with a maximum current response at 0.975 V. Unfortunately, the adsorption of the two proteins could not be resolved from one another in such an experiment. The adsorption behaviour of the mixture was expected to result in two adsorption maxima, corresponding to the adsorption of insulin at ~0.9 V and albumin at ~0.975 V. From Figure 4.2.3.1(D) it can be seen that the mixture of insulin and albumin showed no independent behaviour, and it would appear that the presence of albumin affects the adsorption of insulin, possibly through protein – protein interactions or inhibition of the adsorption process.

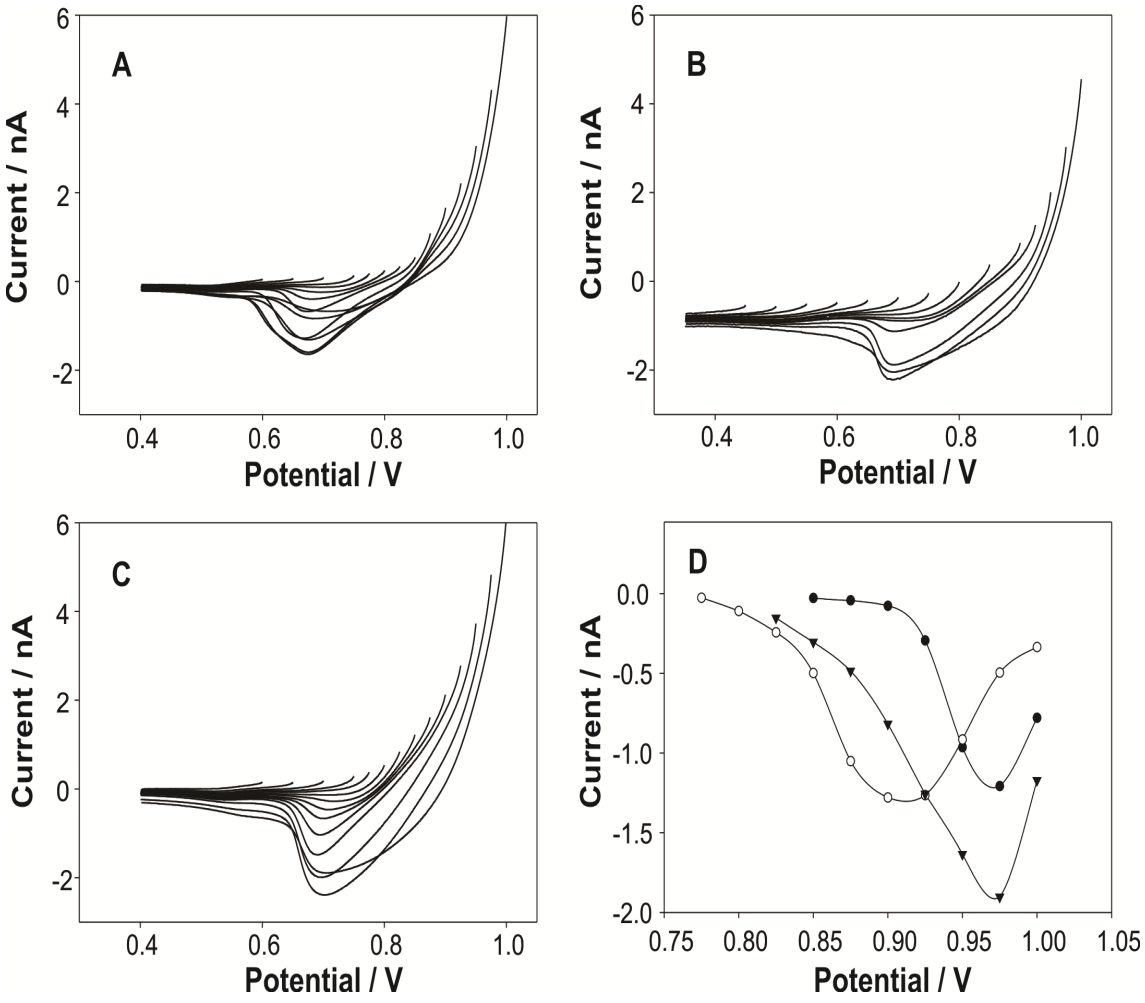

Figure 4.2.3.1: Adsorptive stripping voltammetry of insulin, albumin and their mixtures at the μITIES array. AdSV of (A) 1 μM insulin, (B) 1 μM BSA and (C) a mixture of 1 μM insulin + 1 μM BSA in aqueous phase of 10 mM HCl, 60 s pre-concentration time at different applied potentials, from 0.6 V up to 1.0 V. Plot (D) shows the peak currents resulting from the varying applied adsorption potentials for (○) insulin (●) BSA and (▼) the mixture. Peak currents were estimated from a baseline extrapolated from the current at potentials lower than the peak maximum. Scan rate 5 mV s^{-1}.

4.2.3.2 Detection of insulin in the presence of albumin

Although the selective adsorption approach did not provide clear-cut evidence that one protein could be selectively adsorbed in the presence of another, the detection of insulin in the presence and absence of BSA was investigated using the AdSV approach. Albumin was used as a model interferent since it is an abundant protein present in serum that could potentially interfere in any detection method. Here, insulin detection was investigated with preconcentration at 0.9 V (the optimum adsorption potential for insulin, see section 4.2.3.1) for 60 s in the presence of 1 μM BSA. At this adsorption potential, albumin is not expected to produce a significant voltammetric response (Figure 4.2.3.1(D)). In Figure 4.2.3.1(A) the AdSV of 1 – 6 μM insulin in the presence of 1 μM BSA is shown, demonstrating an insulin dependent response. This demonstrates that by optimally tuning the adsorption potential, some degree of selectivity can be achieved, although with a cost to sensitivity, as shown in Figure 4.2.3.1(B). Although there is no concentration-dependent response linearity in the concentration range studied for both cases (absence and presence of albumin), insulin peaks were resolved in the presence of BSA in the aqueous solution. The exact mechanism of disruption of linearity remains unclear at present, but this process could involve protein – protein interactions and/or inhibition of insulin adsorption by interfacially-adsorbed albumin. It is also possible that insulin self-association, which is concentration dependent at micromolar concentrations, might also contribute to the disruption of linearity.[163] These putative phenomena result in a decrease in the sensitivity of the detection system. Nevertheless, this demonstrates that even though bovine serum albumin interferes with the electroactivity of insulin, detection of insulin is still achievable in the presence of another protein.

The challenge ahead is to improve the selectivity and sensitivity of this detection strategy. It is possible to make the measurement more selective by implementing a sample pre-treatment or separation step. For example, this could be a capillary electrophoretic separation combined with detection by electrochemistry at the ITIES.[36] Alternatively, passage through a size-exclusion[89] or other suitable filter membrane might be more practical to rapidly and conveniently separate the protein of interest from other proteins. Optimisation of these separation strategies will be important to ensure rapidity and accuracy.

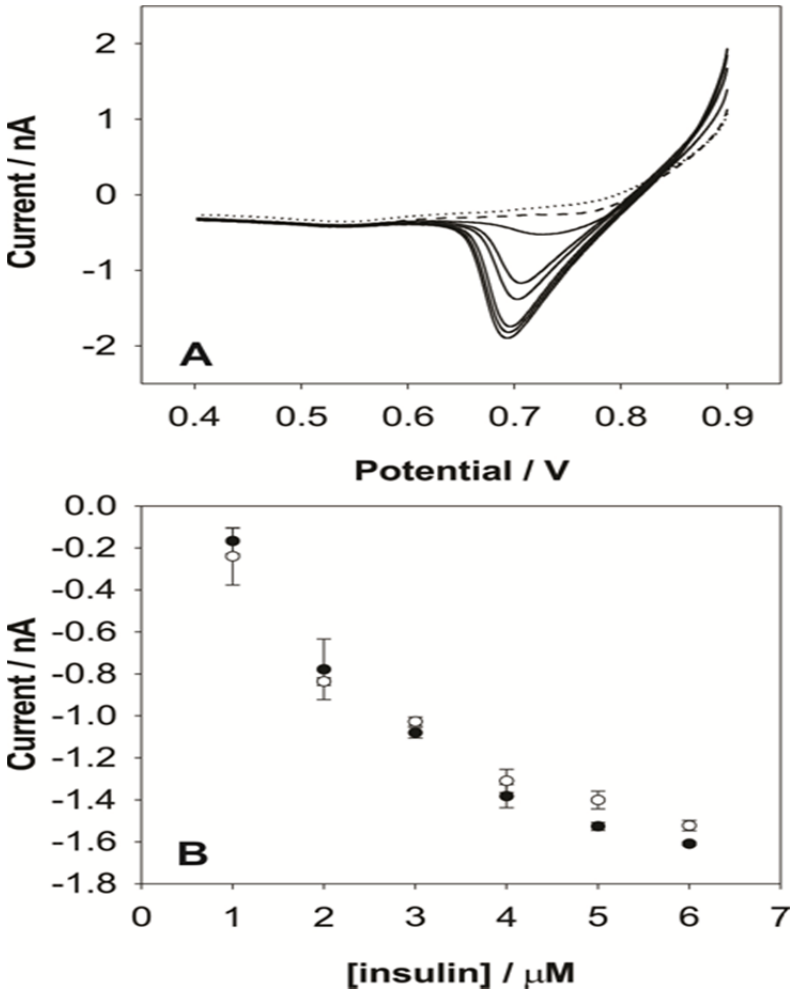

Figure 4.2.3.2: Adsorptive stripping voltammetry of insulin in the presence of albumin. AdSV of insulin (1, 2, 3, 4 5 and 6 μM) in the presence of 1 μM BSA (A) for an adsorption time of 60 s. (A) The dotted line is the response to the background electrolyte only and the dashed line is the response to 1 μM of albumin after 60 s preconcentration time at +0.9 V. Error bars are calculated from the standard deviations of peak currents from three separate calibration curves *(for both Insulin and the mixture of insulin and albumin)* performed on a single microinterface array. The array was washed between runs and background CV and LSV was performed to insure no carryover between experiments. (B) Plots of the current height of the insulin desorption peak in the absence (●) and the presence of albumin (○). Scan rate 5 mV s^{-1}.

4.2.4 Conclusions

The detection of insulin has been achieved by use of AdSV at the ITIES. Investigation of the potential-dependent adsorption of both insulin and albumin revealed a 75 mV difference in optimal adsorption potential. By selecting an adsorption potential of 0.9 V, where no electrochemical response from albumin was expected, AdSV was able to successfully detect insulin in the presence of albumin. This work provides the basis for the use of electrochemistry at the ITIES as a bioanalytical tool and demonstrates for the first time that potential-dependent selective adsorption may offer a route to selective detection based on this strategy. However, improvements in sensitivity and selectivity remain as the immediate challenges.

Chapter 4

Methods for selective detection of proteins at the ITIES (III)

Protein – antibody interactions at the polarised liquid – liquid interface

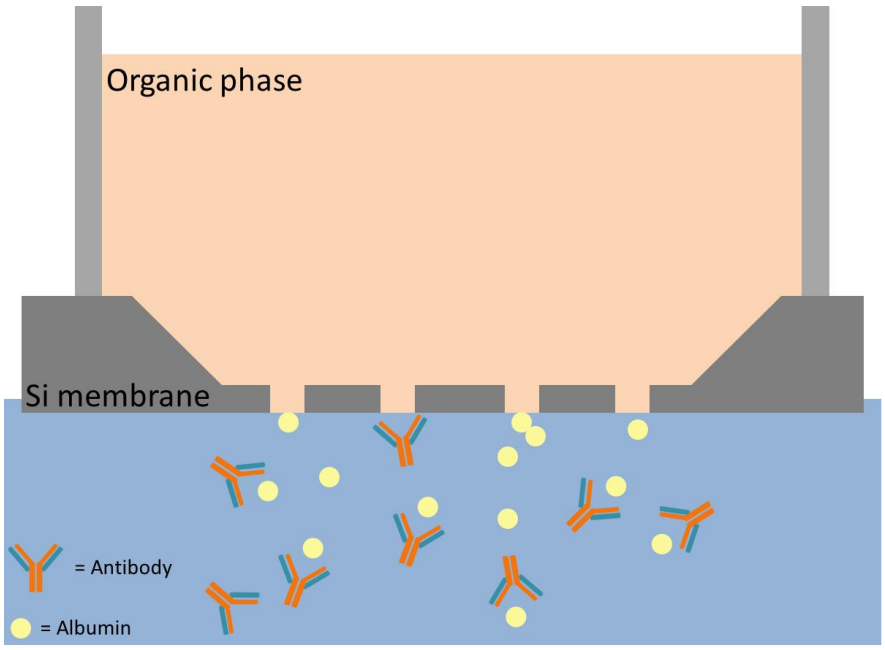

4.3.1 Introduction

One of the major analytical challenges faced in the field of biosensors is selectivity, and this is certainly true of electrochemistry at the ITIES. While a wide range of different analytes have been studied successfully, cases of selective detection of a biomolecule in a complex mixture are relatively rare using electrochemistry at the ITIES. The most successful cases being the selective detection of protamine in the presence of NaCl[67] and the detection of heparin in blood plasma using quaternary ammonium cations as an ionophore[70].

Antibodies are well known for exhibiting binding specificity toward the target antigen, in this case a protein antigen.[164-166] Due to this there may be scope for their use to achieve protein selectivity, but also the fundamental electrochemistry of antibodies, at the polarised liquid – liquid interface, is to date unknown. In this study polyclonal antibodies were selected for use as they will have varying binding sites for the antigen as opposed to monoclonal antibodies which have a single binding site on the antigen. [165] This would generally result in lower association constants, but in this case where non ideal conditions are used it would provide the best opportunity for interactions by having more than one possible binding site. Antibodies are known to interact with antigens through a variety of ways such as hydrogen bonds, electrostatic forces, Van der Waal forces, hydrophobic/hydrophilic interactions and such interactions are influenced by the environment, for example factors such as ionic strength, pH and temperature all contribute to the interactions.[164-167] Although it is commonly thought that at low pH dissociation of any antigen - antibody complex will occur, it is still possible for non-specific interactions to occur. It has been observed by Morgan et al.[168] that at low pH (2.5), where the dissociation of the Aβ peptide from its antibody was expected, the ELISA (enzyme linked immunosorbent assay) showed binding between the two

molecules. This was attributed to non-specific binding, possibly inducted by some denaturation of the molecules at low pH. This feature can be removed by adjusting the pH to 3.5 where dissociation occurs without non-specific binding and false positives are not produced.[168] On this basis it would be possible to observe some interactions between a protein and its antibody at low pH. The interactions between protein antigens and antibodies have yet to be reported in the literature in terms of their electrochemical behaviour at the liquid – liquid interface. The effect of antibodies immobilised on the surface of a microporous silicon membrane on the transfer of TEA^{+}[169] has been reported, however as the antibodies were immobilised their direct electrochemistry was not established and also there was no antigen present to interact with the antibody. Although there is little work reported for the use of antibodies in liquid – liquid electrochemical experiments, there have been numerous examples for that of solid – liquid electrochemistry. The electrochemistry of immunoglobulin G (IgG) has been investigated in terms of its effects on faradaic processes where it was found to adsorb at electrode surfaces.[170, 171] Antibodies have also been employed in conducting polymer membranes in attempts to develop an electrochemical immunosensor[172] and the interactions between rabbit IgG antigen and antibody were observed by amperometry in a flow injection system.[173] The work presented here aims to provide a preliminary investigation into the behaviour of an antibody, anti – bovine serum albumin (anti – BSA), and its antigen, bovine serum albumin (BSA), at the interface between two immiscible electrolyte solutions.

4.3.2 Experimental section

4.3.2.1 Reagents

All the reagents were purchased from Sigma-Aldrich Australia Ltd. and used as received, unless indicated otherwise. The liquid organic phase was prepared

using bis(triphenylphosphoranylidene) tetrakis(4-chlorophenyl)borate ($BTPPA^+TPBCl^-$, 10 mM) in 1,6-dichlorohexane (1,6-DCH). The organic phase electrolyte salt $BTPPA^+TPBCl^-$ was prepared by metathesis of bis(triphenylphosphoranylidene)ammonium chloride ($BTPPA^+Cl^-$) and potassium tetrakis(4-chlorophenyl) borate (K^+TPBCl^-).[121] Aqueous stock solutions of albumin (from bovine serum, 98 %) were prepared in 10 mM HCl (pH 2) or 1 mM PBS (pH7.4) on a daily basis and stored at +4 ºC. All the aqueous solutions were prepared in purified water (resistivity: 18 MΩ cm) from a USF Purelab Plus UV.

4.3.2.2 Experimental set-up

For this work the organic phase was not gellified. The liquid organic phase solution was introduced into the silicon micropore arrays via the glass cylinder, and the organic reference solution was placed on top of the organic phase. The silicon membrane was then inserted into the aqueous phase (10 mM HCl or 1 mM PBS, without or with albumin and/or anti-albumin). Voltammetric experiments were then performed. The electrochemical cell arrangement used for the experiments was a two-electrode cell,[122] with one Ag|AgCl electrode in the organic phase and one in the aqueous phase. The organic phase reference electrode was immersed in an aqueous reference solution of 10 mM $BTPPA^+Cl^-$ in 10 mM LiCl. All potentials are reported with respect to the experimentally-used reference electrodes. All voltammetric experiments were run at a sweep rate of 5 mV s^{-1}. An eight micropore array was employed for all experiments (described in section 2.1.3)

4.3.2.3 Preparation of antibody solution

The antibody solution was prepared from whole serum IgG anti – bovine albumin produced in rabbit (Sigma) which was stored at -18 °C. The polyclonal antibody contained 15 mM sodium azide as a preservative. To ensure that the sodium azide caused no interference with the electrochemistry, a dialysis was performed. To do this the antibody serum was thawed and added into a 1 mL dialysis tube (Float-A-Lyzer G2, Spectrum Labs). The dialysis tube has a molecular weight cut off range of 100 – 500 daltons (Da), as sodium azide has a molecular weight of 65 g mol^{-1} it is allowed pass through the membrane while the antibody cannot. The antibody was allowed to dialyse for 24hrs in 2 L of deionised water. The water was changed four times through the dialysis. Once the dialysis was complete the antibody serum was used by direct addition to the aqueous solution in the electrochemical cell. The antibody was only used directly after the dialysis and was not refrozen.

4.3.3 Results and discussion

4.3.3.1 Voltammetry of anti – albumin

Figure 4.3.3.1 shows the CV of 0.3 μM anti-BSA (prepared as described in 4.3.2.3) in an aqueous phase of 10 mM HCl. When compared to the background scan it can be seen that there are no significant charge transfer processes which occur in the potential window studied. This would indicate that the antibody is not electroactive in this region, possible due to not having enough ionisable side chains which would leave the molecule with insufficient charge.[79, 148] As the iso-electric point of the antibody is ~6.5[174], some portion of its amino acid chain should be ionised. It may be possible that the antibody has enough ionisable amino acid side chains, but does not undergo facilitated

ion transfer of the organic electrolyte within the available potential range used for the experiment. This would require further investigation to clarify, although it does not have any negative implications for using this antibody to achieve selectivity in a protein detection experiment, as it can be seen that the antibody will not produce any significant background interference in the regions where protein voltammetry is typically observed. Also the concentration of antibody is at the lower end of what would be typically used for CV experiments involving protein detection at the ITIES so the lack of a voltammetric response could be concentration dependant. This is due to practical limitations on the amount of antibody available for use with each experiment, such as cost and the difficulty in preparing a more concentrated solution of anti-BSA due to the fixed concentration of the serum, at 3 mg/mL of anti-BSA. A scaled down version of the experiment involving a much smaller volume of aqueous phase would allow for higher concentrations of the antibody to be used in a more practical manner.

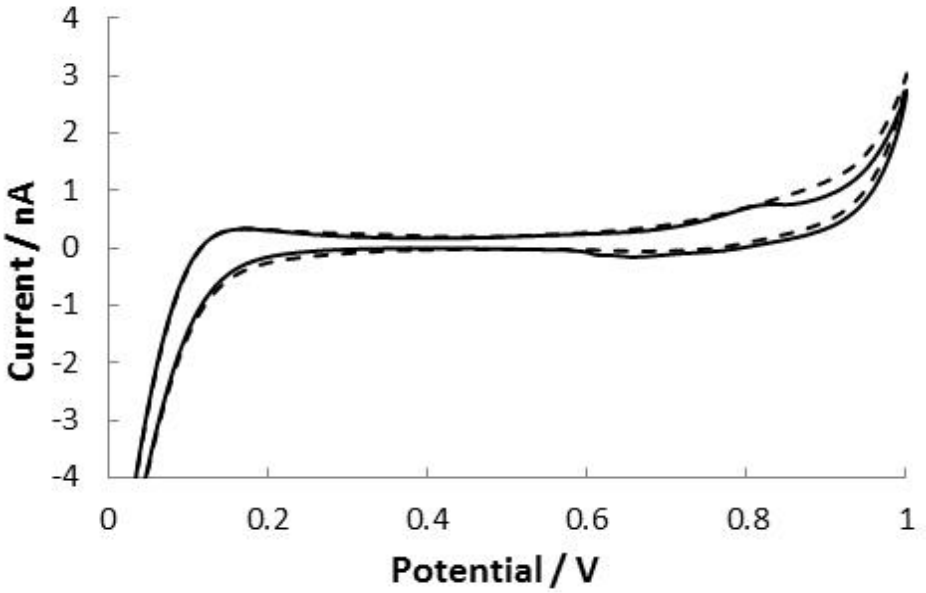

Figure 4.3.3.1: CV of the μ-ITIES array containing 10 mM HCl in the absence (dashed line) and presence of 0.3 μM anti-BSA (solid line). Scan rate 5 mV s^{-1}

4.3.3.2 Electrochemistry of BSA and anti-BSA mixture

The anti-BSA and BSA voltammetric responses were characterised so they could provide as a suitable reference for comparison of the mixture of the antibody and protein, as seen in figures 4.3.3.1 and 4.3.3.4 respectively. Figure 4.3.3.2 shows the voltammetry of 10 μM BSA + 0.3 μM anti-BSA in 10 mM HCl. The background scan of 0.3 μM antibody was taken before the addition of protein and used as a reference against peak currents produced. Once the protein was added to the antibody solution it was given 20 mins to interact before the first scan. After this scans were run periodically up to 120 min. It was observed that although the reverse peak current remained more or less unchanged with only minor deviations, the forward peak current grew in magnitude over time, as can be seen from Figure 4.3.3.3, which plots peak current at 0.9 V against time after addition of the protein to the antibody solution. This response is indicative of some new charge transfer process which is characteristic of the protein – antibody mixture, or possible just the protein, and is time dependant. Figure 4.3.3.4 shows the voltammetry of BSA in 10 mM HCl. The BSA shows little response, but a small increase in peak current on the forward scan is seen at around 0.9 V. Three consecutive scans of 10 μM BSA were run and it can be seen that they overlay almost perfectly showing that the system is stable and cycling has no effect of the peak currents. This would imply that there is some form of interaction between the protein and antibody which in turn produces an increase in forward peak currents but does not seem to affect the reverse scan. Forward peak currents are associated with either positive ions transferring from the aqueous phase to the organic phase or negative ions transferring from the organic. Although the conditions for BSA – anti BSA binding were certainly not at an optimum, the use of polyclonal antibodies provides the best opportunity for interactions in unfavourable conditions.[167] At this point there is not enough evidence to establish a detailed mechanism for the interactions taking place. More

investigation is needed to elucidate the mechanistic information of the protein – antibody interactions, although the preliminary results indicate that protein – antibody interactions may be of use for biomolecular detection at the ITIES, or at least produce some unique electrochemical response.

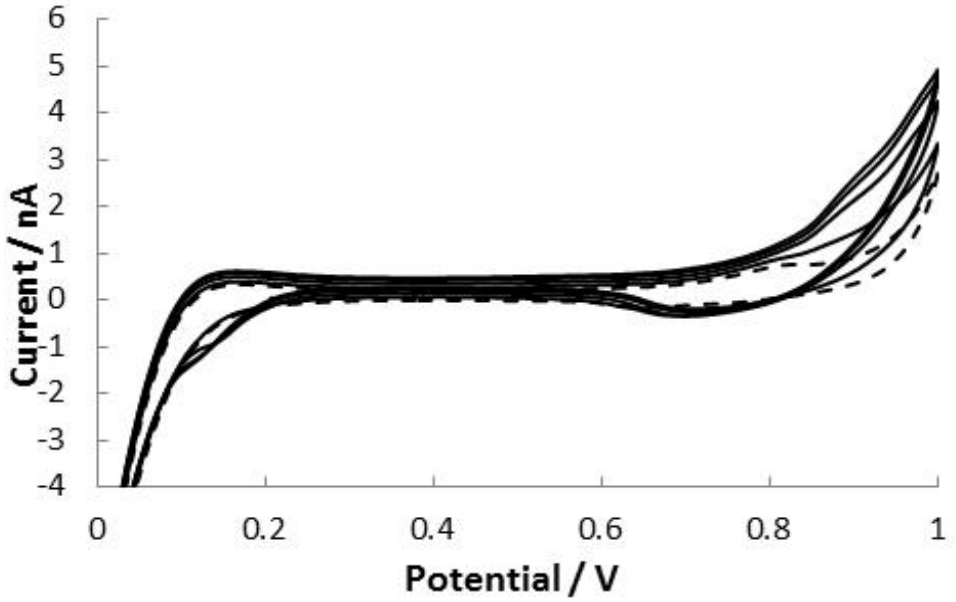

Figure 4.3.3.2: CV of "blank" 0.3 μM anti-BSA in 10mM HCl (dashed line) and 0.3 μM anti-BSA + 10 μM BSA (solid lines) Scans of mixture are taken over time from 20 minutes after addition of BSA to the anti BSA, up to 120 minutes after addition. Scan rate of 5 mV s^{-1}.

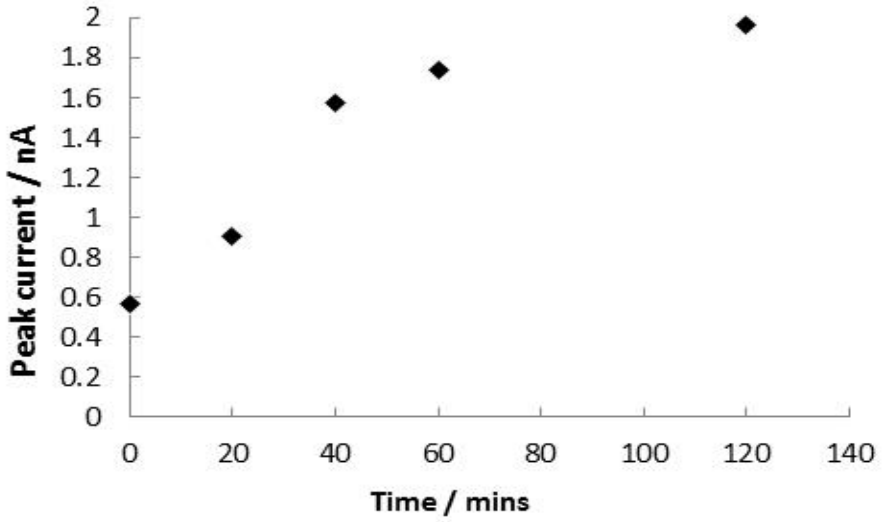

Figure 4.3.3.3: Plot of peak current at 0.9 V against time after addition of BSA to the anti-BSA solution. Data relating to the CV's in Figure 4.3.3.2. Peak current at 0 mins corresponds to current at 0.9 V for the background CV produced from the 0.3 μM anti-BSA solution.

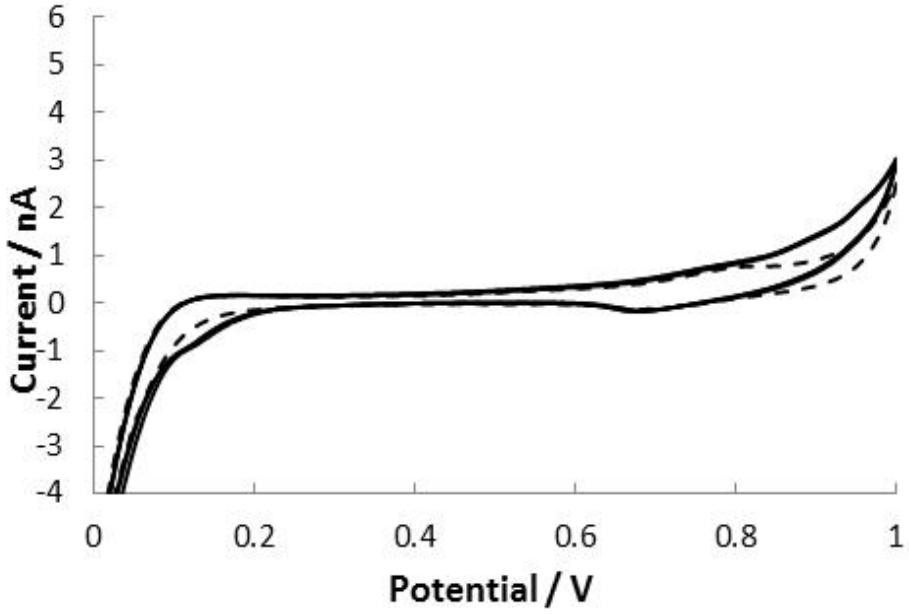

Figure 4.3.3.4: CV of blank 10 mM HCl (dashed line) and 10 μM BSA (solid line). Shown is three CVs of the BSA scan which overlap. Scan rate 5 mV s^{-1}.

4.3.3.3 Antibody – antigen electrochemistry at physiological pH

The electrochemistry of BSA and an anti-BSA and BSA mixture was investigated at physiological pH as these conditions are most likely to favour protein – antibody interactions. Unfortunately these are also the conditions least favourable for protein detection at the ITIES as proteins are generally not positively charged at this pH, and thus do not undergo charge transfer processes. Figure 4.3.3.5 shows the voltammetry of 10 μM BSA and 10 μM BSA + 0.3 μM antibody at pH 7.3 in 1 mM PBS solution. It was observed that the voltammogram shifted slightly towards more positive potentials, this shifting is most likely due to protein and antibody adsorbing at the interface and at the electrode surface.[170, 171] As neither the BSA nor mixture of protein and antibody exhibits any distinctive electrochemical features under these conditions it can be concluded that using voltammetry at physiological pH is not a viable option. It is worth noting that although this particular experiment produced no positive results for selective detection, a change in protein – antibody combination could warrant investigation. A protein or peptide that is positively charged at physiological pH with its corresponding antibody may produce different results. Amylin is one possible example of a peptide which could be viable for such studies as it is a cation at pH 7.3[175].

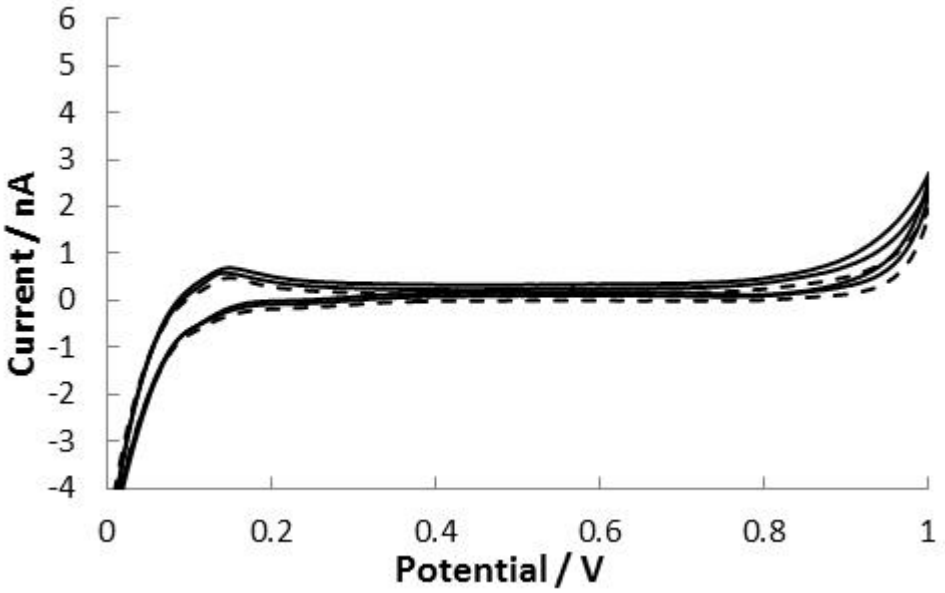

Figure 4.3.3.5: CV of blank 1 mM PBS (dashed line) 10 μM BSA and a mixture of 10 μM BSA + 0.3 μM anti-BSA (solid lines). The mixture is the solid line with larger positive currents. Scan rate 5 mV s^{-1}.

4.3.4 Conclusions

The electrochemistry of the antibody, anti-bovine serum albumin IgG, was investigated at the electrified liquid – interface. It was shown that at pH 7.3 there was no electrochemical response observed for the BSA and anti-BSA mixture, which is expected, as all previous studies showed that when a protein is neutral or anionic there is no ion transfer visible. The albumin control at pH 7.3 also showed no response, although on addition of the albumin and the albumin – antibody mixture there was a shift in the background voltammogram, this is in line with reports of protein and antibody adsorption to interfaces, but it is of little analytical use for cyclic voltammetric methods at the ITIES. At pH 2 BSA produces a stable and reproducible voltammogram and the anti-albumin produces little deviations from the background currents. The mixture of BSA and anti-BSA shows an increase in current on the

forward sweep at ~0.9 V which is time dependant. This is indicative of some protein – antibody interaction, which as of yet is undefined. It is possible some non-specific interactions are occurring between the antigen and antibody. Although there are many unknowns in regards to the mechanisms of interactions and the cause of the increase currents it would appear there would be scope for further research into this area.

As this is a preliminary study it has if anything raised more questions than provided answers and there are many avenues of future work which could be considered. As stated previously in the discussion, the miniaturisation of the aqueous phase to accommodate more practical and cost effective dilutions of the antibody should be considered for any future work. The effects of higher concentrations of antibody are still unknown and having the antibody in excess of the protein concentration may give alternative results. Also as mentioned in the discussion, the choice of the antigen – antibody combination needs to be given some thought, perhaps a peptide such as amylin which is electroactive at physiological pH, would allow for the observation of protein – antibody interactions under more favourable conditions. In this work the electrochemistry was probed using only cyclic voltammetry, perhaps using alternative techniques such as AC voltammetry or electrochemical impedance spectroscopy might give further information. It would also be worth considering the use of non-electrochemical techniques to probe the antibody – protein interactions, for example, the non-specific binding may be possible to evaluate by using ELISA with the anti-albumin and albumin using the conditions employed for the electrochemistry.

Chapter 5

Impact of surfactant on the electroactivity of proteins at an aqueous-organogel microinterface array

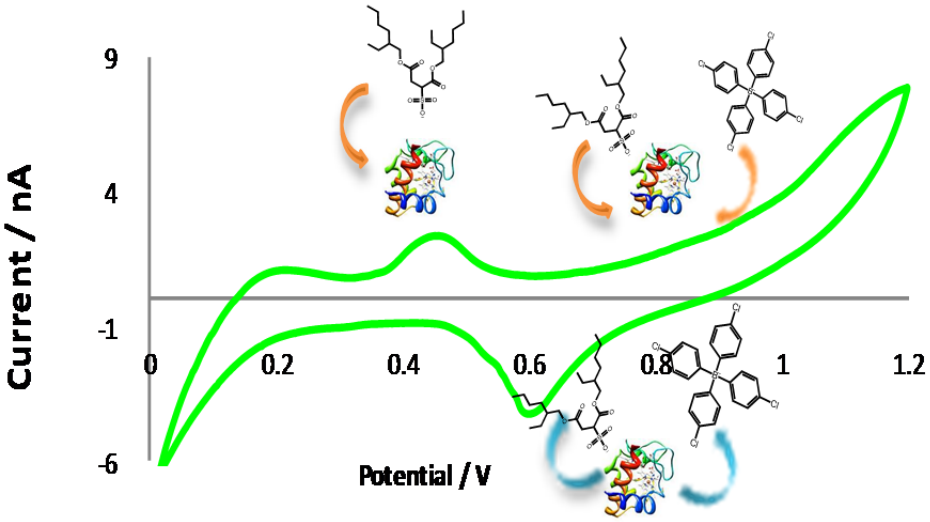

5.1 Introduction

The effect of surfactant on the voltammetric behaviour of hemoglobin (Hb), myoglobin (Mb), and cytochrome *c* (Cyt c) at a liquid-liquid interface was investigated. Hb, Mb and Cyt c are all haem-containing proteins. Haemoglobin, molecular mass 64 kDa,[176] is responsible for oxygen transport in red blood cells.[177, 178] Myoglobin, comprised of a single chain of 153 amino acids with a molecular mass of 16.7 kDa,[104] is an oxygen-binding protein responsible for the transportation and storage of 0_2 in muscle cells.[106] Elevated levels of Mb can be associated with acute myocardial infarction (AMI).[107, 110] Cytochrome *c*, molecular mass 13 kDa[179], is found in the mitochondria and is mainly associated with adenosine triphosphate (ATP) synthesis.[179]

The work presented in this chapter is concerned with the impact on protein electroanalytical behaviour of the modification of the gelled ITIES with a surfactant, Sodium 1,4-bis(2-ethylhexoxy)-1,4-dioxobutane-2-sulfonate (AOT). Surfactants have received much attention in the field of biotechnology as reagents for protein extraction, separation, pre-concentration and purification,[180, 181] including study of the effects of water composition[182], pH[183] and other factors on the extractions. Reverse micelles are of particular interest as they provide a unique environment within the organic solvent phase which allows the retention of a protein's 3-dimensional structure and function.[184]

From an electrochemical perspective, surfactants have been used to modify electrode surfaces and to enhance the electrochemical response to proteins.[185-187] The direct electrochemistry of Hb[188] and cytochrome *c* oxidase[189] was reported at surfactant-modified glassy carbon electrodes. Similarly the electrochemistry of cytochrome P450 was reported on a surfactant-modified pyrolytic graphite electrode, where the surfactants were used to mimic the

biological cell membrane in order to achieve optimal electron transfer.[190] Vagin *et.al* have reported spontaneous micelle formation at the ITIES when the sodium salt of bis(2-ethylhexyl)sulfosuccinate (NaAOT) was added to the liquid organic phase.[65] Osakai and co-workers have reported the adsorption/desorption of proteins in the presence of surfactants[80] and have demonstrated the transfer of proteins from the aqueous to the organic phase via electrochemically-controlled reverse micelle formation.[72] The group also investigated the mechanism of solvent extraction of proteins from the aqueous to organic phases in terms of interfacial potential and surface tension.[75] However, these reports discussed extraction and mechanistic issues without addressing analytical impacts such as sensitivity enhancement.

The aim of the work reported herein was to investigate the influence of the surfactant AOT on the electroanalytical behavior of Hb, Mb and Cyt *c* at the μITIES array. In particular, the mechanism of protein-surfactant interaction at an array of micro-sized interfaces between aqueous and gelled organic phases was of interest, because these miniaturised and stabilised interfaces provide a platform for sensing and detection applications. However their behaviour is different from liquid-liquid ITIES, in that radial diffusion from the aqueous phase is coupled with slower diffusion in the gelled organic phase.[119, 191] Addition of the surfactant to the organic phase may result in modified behaviour in comparison to that at regular liquid-liquid ITIES.[72, 80] As reported recently by Jensen and co-workers, the formation of dielectric layers and charge regulation on either side of the ITIES will affect the interfacial properties[87], thus the addition of an anionic surfactant to the organic phase in the presence of a cationic protein in the aqueous phase is expected to affect protein behaviour at the interface and hence influence the electroanalytical response.

5.2 Experimental details

5.2.1 Reagents

All the reagents were purchased from Sigma-Aldrich Australia Ltd. and used as received unless indicated otherwise. The gelled organic phase was prepared using bis(triphenylphosphoranylidene)ammonium tetrakis(4-chlorophenyl)borate (BTPPATPBCl, 10 mM) in 1,6-dichlorohexane (1,6-DCH) and low molecular weight poly(vinyl chloride) (PVC).[120] The surfactant AOT was added to the organic phase, as the sodium salt dissolved in 1,6-DCH, during gel preparation. The BTPPATPBCl salt was prepared by metathesis of bis(triphenylphosphoranylidene)ammonium chloride (BTPPACl) and potassium tetrakis(4-chlorophenyl)borate (KTPBCl) as previously described.[192] The bis(triphenylphosphoranylidene) bis(2-ethylhexyl)sulfosuccinate salt, (BTPPAAOT) was prepared by metathesis of BTPPACl and bis(2-ethylhexyl)sulfosuccinate sodium salt NaAOT. The reactants were added in a 1:1 molar ratio, and dissolved in a 1:1 (volume:volume) mixture of acetone and methanol. The white precipitate reaction product was separated and washed with cold de-ionized water and dried on a vacuum pump. The product was dried in a desiccator overnight and stored at +4 ºC. Stock solutions of Mb, Hb and Cyt c were prepared in aqueous 10 mM HCl on a daily basis and stored at +4º C. Tetraethyl ammonium (TEA^+) chloride solutions were prepared in aqueous 10 mM HCl. All aqueous solutions were prepared with purified water of resistivity 18 MΩ cm, from a USF Purelab plus UV system (Millipore Pty Ltd, North Ryde, NSW, Australia).

5.2.2 Experimental set-up

Once prepared as described in section 2.1.3 the gelled organic phase solution was introduced into the silicon micropore arrays via the glass cylinder, and the organic reference solution was placed on top of the gelled organic phase. The silicon membrane was then immersed into the aqueous phase (10 mM HCl, Mb, Hb or Cyt c in 10 mM HCl, and/or TEA^+ in 10 mM HCl).

The electrochemical cell employed two electrodes,[122] with one Ag|AgCl electrode in the organic phase, via an reference phase composed of aqueous 10 mM BTPPACl in 10 mM LiCl, and one directly in the aqueous phase. Up to three voltammetric cycles were run in succession and typically the third CV cycle was used for measurement, unless indicated otherwise. For Mb, stable CVs over these three cycles were obtained but for Hb and Cyt c, currents increased on repeated cycling. An eight micropore array was employed for all experiments (described in section 2.1.3)

5.3 Results and discussion

5.3.1 Effect of surfactant concentration on myoglobin electrochemistry

The effect of surfactant concentration on protein detection at the ITIES was investigated using cyclic voltammetry (CV) (Figure 5.3.1). The surfactant was added to the gelled organic phase, during gel preparation, as the sodium salt of AOT. A range of surfactant concentrations were studied. The main change on the forward sweep of these CVs is appearance of a new peak at ca. 0.4 V (Figure 5.3.1(b,c,d)) and a small shoulder at ca. 0.95 V (Figures 5.3.1(b,c)). The large forward peak at the positive limit of the potential window (Figure

5.3.1(a-d)) is the potential window-limiting background electrolyte transfer. These features do not appear without the presence of both protein (aqueous phase) and NaAOT (organogel phase). The peak at ~0.45 V is much more pronounced at the highest concentration of surfactant used (10 mM) and suggests a protein-surfactant interaction as this feature is not visible in the absence of surfactant. The main impact of surfactant on the reverse scan was the increase in the peak at ca. 0.65 V with surfactant concentration. In the absence of surfactant, this peak Figure 5.3.1(a) is attributed to dissociation of the protein-organic anion complex and desorption of the protein from the interface.[84] This peak increases significantly with surfactant concentration. A comparison of the reverse peak currents for 6 μM Mb in the absence (Figure5.3.1(a)) and presence of a high concentration of surfactant (Figure 5.3.1(d)) shows a six-fold increase, from approximately 0.5 nA to 3 nA. The peak shape is also seen to change, with the appearance of a slight shoulder in the presence of surfactant. The overall shape of the voltammogram is shown to change considerably in the presence of 10 mM NaAOT in the organogel. A marked increase in background charging current is also evident, which is attributed to the formation of a surfactant-protein assembly at the interface, which alters its capacitance.[193] The background current at 0.3 V, where no interfacial charge transfer occurs, is seen to increase by an order of magnitude in the presence of 10 mM surfactant (Figure 5.3.1(d)) relative to the voltammogram where no surfactant is present (Figure 1(a)).

The interfacial coverage of Mb at the μITIES array was determined from the charge under the reverse scan peak (0. 65 V) using equation 5.3.1.[125]

$$|Q| = z_i F A \Gamma \quad \text{Eqn 5.3.1}$$

Here, $|Q|$ is the charge under the desorption peak (C), z_i is the charge on the protein, F is Faraday's constant (C mol^{-1}), A is the total geometric area of the

microinterfaces (cm^2) in the array, and Γ is the surface coverage. The interfacial coverage at surfactant concentrations of 0, 0.1, 1 and 10 mM were determined to be ~ 50, 60, 248 and 850 pmol cm^{-2}, respectively. Given that the concentration of Mb was fixed at 6 μM, this indicates that the surfactant facilitated a 17-fold increase in the interfacial coverage of adsorbed protein at the interface. An adsorbed monolayer of Mb has an interfacial coverage of 1.02 x 10^{-11} mol cm^{-2}, taking into consideration the assumptions that the molecule is spherical, occupies a close-packed hexagonal arrangement and is not distorted by the adsorption process. The monolayer coverage data was calculated from equation 5.3.2 below, where Γ_{mon} is the interfacial coverage of a monolayer, r_h is the hydrodynamic radius of Mb (2.12 nm)[194], N_A is Avogadro's number, and 0.87 is a factor to include the maximum occupied area when hexagonal close packing is assumed.[147] The interfacial coverages of 50, 60, 248 and 850 pmol cm^{-2} can therefore be expressed as a function of monolayer coverage, and correspond to 4.6, 6.1, 24 and 83 monolayers, respectively.

$$\Gamma_{mon} = \frac{0.87}{\pi r_h N_A} \quad \text{Eqn 5.3.2}$$

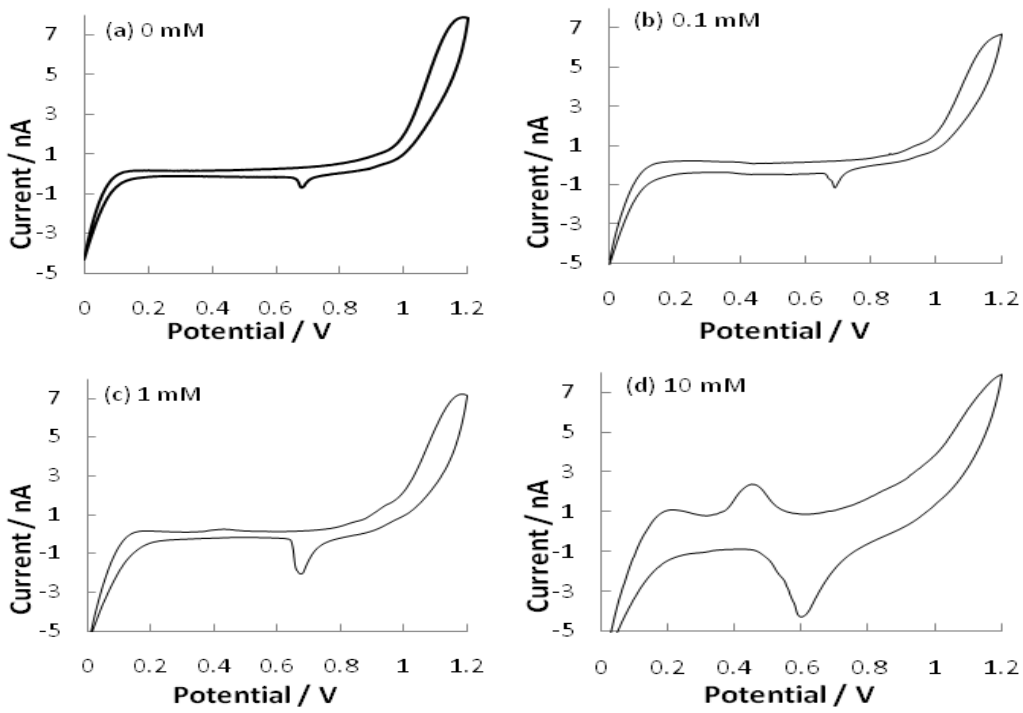

Figure 5.3.1: CV of 6 µM Mb in the presence of (a) 0 mM, (b) 0.1 mM, (c) 1 mM and (d) 10 mM organic-phase surfactant, NaAOT. Scan rate 5 mV s^{-1}. All CVs are the third scan of three.

5.3.2 Surfactant behaviour at the µITIES array

To probe the interaction of the surfactant with the protein, the BTPPAAOT salt was employed as the only electrolyte in the organogel phase. The protein-TPBCl interfacial interaction is the basis for protein detection by voltammetry at the ITIES in the absence of surfactants.[77-79, 82, 84, 85, 88, 118, 120, 148] By addition of a hydrophobic salt of the surfactant as the electrolyte in the organic phase, the interactions of TPBCl anions with cationic protein are removed, and consequently the protein-surfactant interactions can be monitored more easily. As a result, any electrochemistry seen in the presence of the protein can be

attributed to interactions between the cationic protein and the AOT anion in the organic phase.

The electrochemical window for the BTPPAAOT electrolyte (Figure 5.3.2(a)), was significantly narrower (ca. 200 mV wide) than that for NaAOT added to the BTTPATPBCl electrolyte (Figure 5.3.2(b)) (ca. 700 mV wide). Evidently, the removal of the usually-used organic phase electrolyte anion TPBCl has an impact. In its presence, the available potential window is limited at the positive side by transfer of this anion from the organic phase into the aqueous phase; in its absence, the anion present, AOT, transfers at a lower potential and hence the positive limit is lower resulting in the narrower available potential window. However, the fact that the potential window is wide in the presence of both TPBCl and AOT organic phase anions indicates that some additional process occurs to prevent, or at least diminish the impact of, AOT transfer into the aqueous phase. An AOT-associated process occurs at ca. 0.4 V in the presence and absence of both TPBCl and protein (Figures 5.3.1 and5.3. 2). The current for this process is larger in the absence of TPBCl than in its presence. Notably, in the presence of TPBCl, AOT is added as a sodium salt, which may have a lower solubility in the organic phase than BTPPAAOT. Hence the charge transfer process at ca. 0.4 V may simply be a concentration-dependent transfer (or adsorption) of AOT.

On addition of 6 μM Mb to the cell containing organic phase BTTPAAOT (Figure 5.3.2(a)), a new adsorption/desorption feature appeared, at ~0.32 V on the forward sweep and at ~0.25 V on the reverse sweep.[72] This feature is attributed to interactions between the cationic protein and the anionic surfactant. For each blank CV an increase in current is observed towards the positive end of the potential window, due to background electrolyte transfer.[75] This process is due to the anionic AOT transfer in the absence of TPBCl (Figure 5.3.2(a)), and the larger current relative to that in Figure 5.3.2(b) may

be a result of solubility when present as the organic cation salt. The CV without protein and with organogel containing 10 mM NaAOT and 10 mM BTTPATPBCl (Figure 5.3.2(b)) shows a small peak at *ca*. 0.4 V on the forward scan and a reverse peak at *ca*. 0.3 V. This feature is concentration-dependent and attributed to surfactant transfer/adsorption, as seen in Figure 2(a). The fact that this AOT-associated peak increased in magnitude with concentration in the presence of protein (Figure 5.3.1 (a)) indicates the formation of a protein-surfactant complex; this peak is seen in all voltammograms containing high surfactant concentrations.

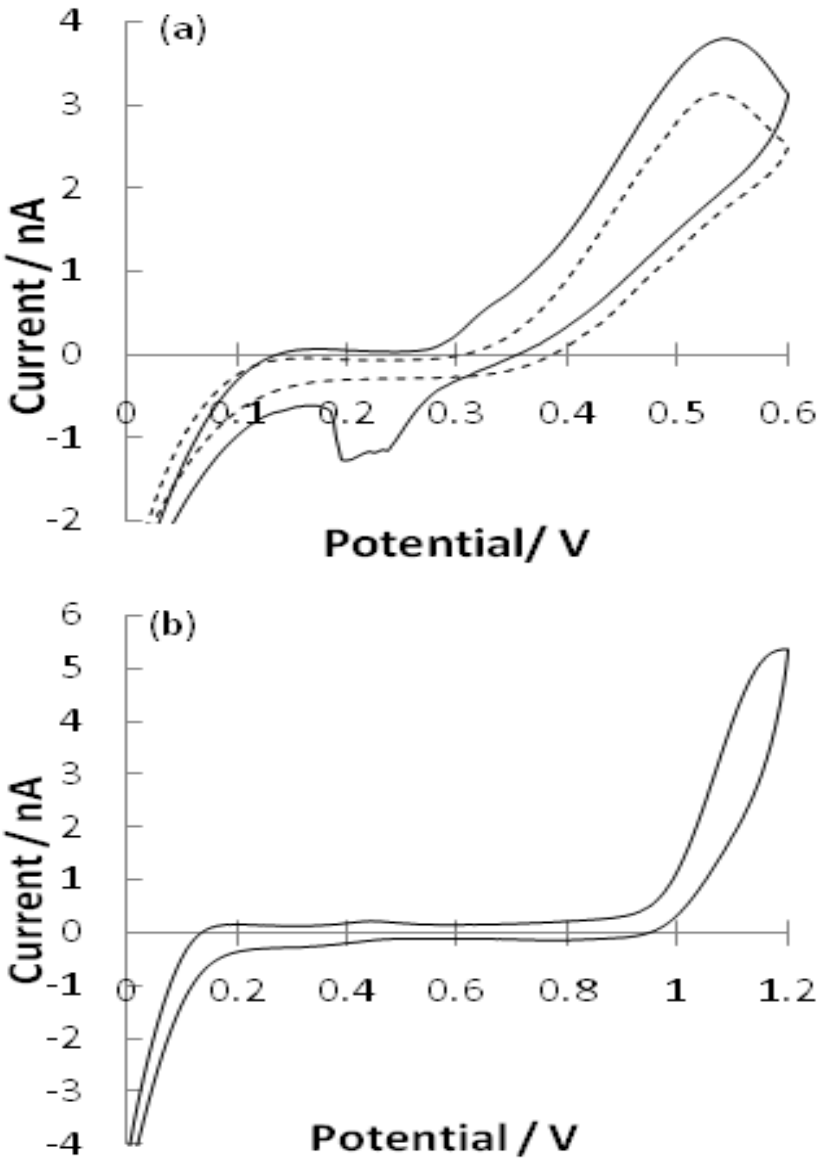

Figure 5.3.2: (a) CV in the absence (dashed line) and presence (solid line) of 6 μM Mb. Scan rate 5mVs^{-1}. The organic phase contains 10 mM BTTPAAOT. (b) CV with the organogel phase containing 10 mM BTTPATPBCl plus 10 mM NaAOT. Scan rate 5 mV s^{-1}. All CVs are the third scan of three.

5.3.3 Influence of aqueous phase cation on electrochemical response

To further investigate the role of AOT on the system, NaCl was added to the aqueous phase as 1 mM NaCl in 9 mM HCl, keeping the concentration of chloride constant as with previous experiments. 10 mM NaAOT was used in the organic phase containing 10 mM BTTPA TPBCl. The aim of this experiment being to compare the result to Figure 5.3.2(b), where the only aqueous cation was H^+. The results shown in Figure 5.3.3 show that upon addition of the NaCl to the aqueous phase a linear response between current and voltage is observed. This type of response has been previously reported in the literature by Vagin et al. and is attributed to spontaneous micelle formation between the aqueous cation and the surfactant molecules.[65] Although it is perhaps more likely that the interface is no longer polarisable due to the fact that Na^+ ions are present on both sides of the interface and are free to transfer under applied potentials. If that was the case, the interface should behave like an ideally non – polarisable electrode, producing a vertical line for the plot of current vs potential. Given that a sloped line was obtained, as seen in Figure 5.3.3, this may be indicative of the high resistance of the cell under the conditions employed.

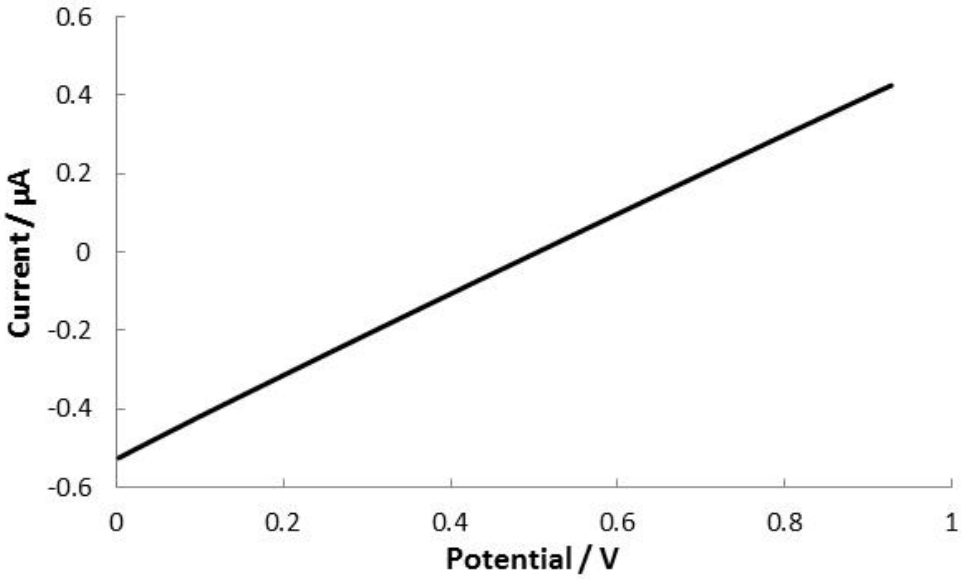

Figure 5.3.3: LSV of 1 mM NaCl in 9 mM HCl aqueous phase with 10 mM NaAOT present in the organic phase. 10 mM BTPPA TPBCl present as normal, scan rate 5 mV s^{-1}.

5.3.4 Effects of surfactant on simple ion transfer

The effects of AOT on simple ion transfer were investigated. Shown in Figure 5.3.4 is the CV of 10 µM TEA^+ in the presence of varying concentrations of AOT in the organic phase as its sodium salt. It would appear that the presence of AOT has an effect on TEA^+ transfer, although there is no obvious trend visible. This may provide an insight to a more complicated mechanism which underlies the process. The structure of the surfactant at the interface is likely to be concentration dependent, as seen by the appearance of a peak at 0.4 V on the forward sweep which is only observed at the highest concentration of surfactant, 10 mM. This could produce differences in the structure and potential of the electric double layer and in turn affect the ion transfer process. Previous results have indicated that the presence of surfactants or lipid layers at the interface can both increase and decrease ion transfer at the ITIES.[195-198] In the case where surfactant decreased the rate of ion transfer, it was proposed

that the presence of surfactant formed close packed layers at the interface. This packed layer formation was thought to inhibit ion transfer across the interface. Where the presence of surfactant was found to increase ion transfer across the interface, it was proposed that a change in double layer structure was responsible for the observed effects, which is backed up by the theoretical work of Strutwolf et al. [195] It may be the case, as seen in Figure 5.3.4, that the varying concentrations of surfactant, result in differing double layer properties, affecting the ion transfer of TEA^+.

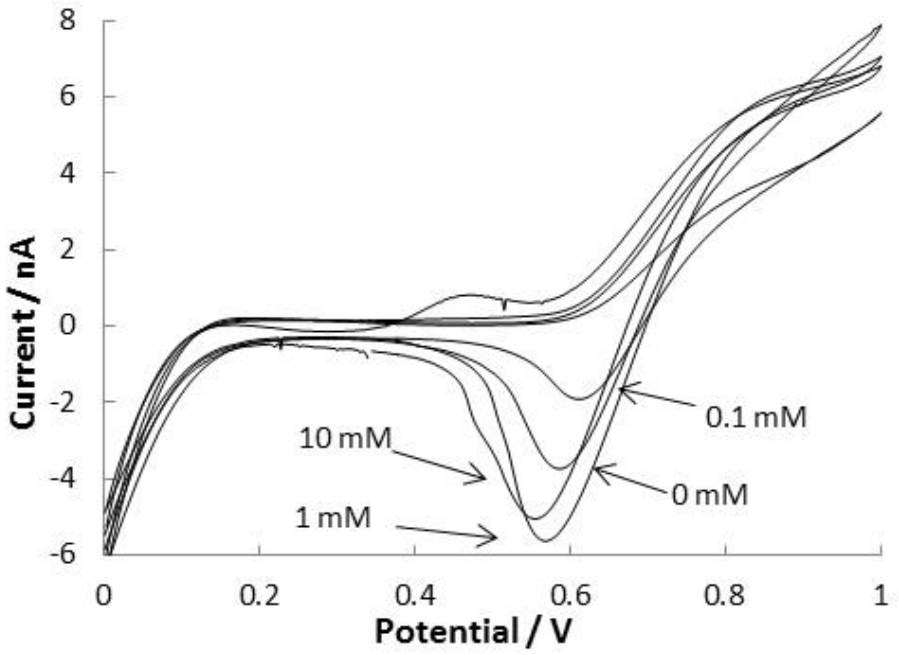

Figure 5.3.4: CV of 10 μM TEA^+ in the presence of 0 – 10 mM AOT in the organic phase. Aqueous phase electrolyte is 10 mM HCl, organic phase electrolyte is 10 mM BTPPA TPBCl. Scan rate 5 mV s^{-1}.

5.3.5 Comparison of electrochemical sensitivity in the presence and absence of surfactant

CV was employed to construct a calibration curve for Mb over the concentration range of 1 – 6 μM (aqueous phase) in the presence of 10 mM NaAOT in the gelled organic phase (Figure 5.3.5). These data were then compared to those obtained in the absence of surfactant.[148] The most prominent peak in these voltammograms, in the presence or absence of surfactant, is the protein desorption peak (+0.65 V) on the reverse scan and so this was used to compare the electrochemical sensitivities. The peak currents observed at the lowest concentration, 1 μM Mb, in the absence and presence of surfactant were -0.07 nA and -0.40 nA, respectively; in the case of the maximum concentration, 6 μM Mb, the peak currents observed were -0.5 nA and -3.0 nA, respectively. The addition of surfactant induced a *ca*. six-fold increase in peak currents. The plots of reverse peak current versus concentration of Mb were linear, with R^2 values of 0.99 in both the presence (Figure 5.3.5(b)) and absence[148] of surfactant. However the slopes were -0.08 nA μM^{-1} and -0.50 nA μM^{-1} in the absence and presence of surfactant, respectively, indicating an increase in sensitivity in the presence of surfactant. The forward sweep in the presence of 10 mM NaAOT shows a peak at ~0.4 V (Figure 5.3.5(a)). This peak increased in magnitude with increasing concentration of protein, with a slope of 0.28 nA μM^{-1}, but does not appear in the absence of surfactant.[148] It is likely that the presence of AOT at the interface facilitates the adsorption of Mb, resulting in larger currents than in the absence of surfactant.[148] This is reflected by the large increase in calculated surface coverage discussed above. It appears that a protein-surfactant-electrolyte anion complex is formed and accumulates at the interface during the course of the potentiodynamic cycle. The mechanism by which the protein, surfactant and organic anion interact to produce the

voltammetry shown is more complex than the protein – surfactant interfacial reaction proposed by Osakai and co-workers[80], which considered the interaction of anionic surfactants with cationic proteins. The additional interaction of organic phase electrolyte anion in the present study has been reported to be the basis of the interfacial charge transfer process.[77,78, 79, 84, 85, 118, 119] The mechanism may simply be a competition for cationic sites within the protein by both AOT and TPBCl.

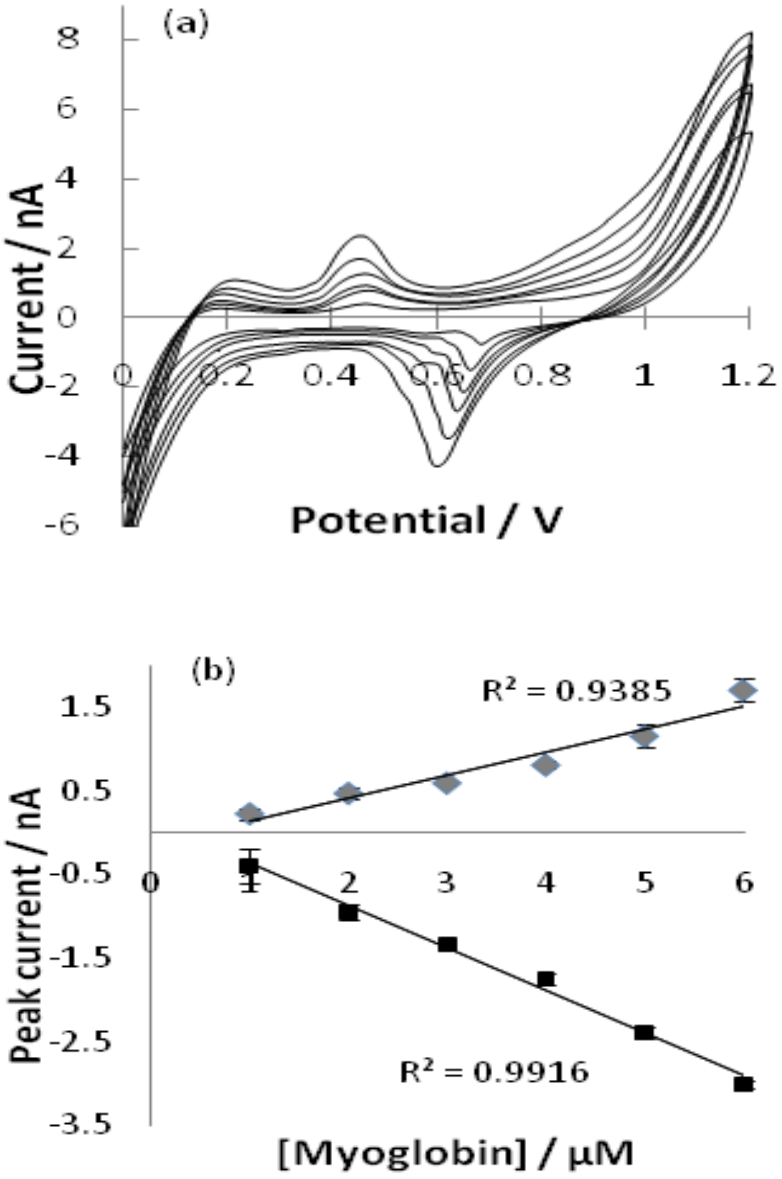

Figure 5.3.5: (a) CV of 1, 2, 3, 4, 5 and 6 µM Mb, scan rate 5 mVs^{-1}. Organic phase contains 10 mM NaAOT. (b) Plot of peak at current ~0.4 V versus myoglobin concentration on the forward sweep (positive current values), and plot of peak at current at ~0.65 V versus myoglobin concentration on the reverse sweep (negative current values), showing linear dependence of peak current with concentration for the reverse peak. All CVs are the third scan of three. Data in part (b) are the means of three scans, with the error bars representing +/- one standard deviation.

5.3.6 Comparative voltammetry of haemoglobin, myoglobin and cytochrome c

In order to assess whether the impact of surfactant on protein voltammetry was general, CV was carried out on three haem-containing proteins, haemoglobin, myoglobin and cytochrome *c*. The aim here was to determine if the effects of the surfactant were consistent across a range of proteins or if the effects were varied depending on the protein characteristics (structure, size, charge). The CVs with and without surfactant are shown in Figure 5.3.6. It can be clearly seen that the surfactant effects are similar in the presence of all proteins. The background charging current increases dramatically in the presence of 10 mM NaAOT in the organic phase, and the peak currents for the protein desorption show marked increases (Figure 5.3.7). The surfactant – protein peak is present on the forward scan at ~ 0.4 V for all three proteins and in the case of Cyt *c* the reverse peak corresponding to the surfactant-related desorption can be more clearly seen, at ~0.3 V, than for Mb and Hb. This indicates that although the approach is not inherently selective for one protein over another, it can still identify individual proteins as each yield a characteristic voltammetric response, i.e. distinctive shapes and potentials are recorded for each protein. These results are consistent with the concept of facilitated adsorption of the protein by the surfactant,[80] as the proteins are present in a cationic state and the surfactant is anionic and surface active. The pre-peaks seen on the forward scan, at ca. 0.85 – 0.9 V, are visible in the presence and absence of surfactant and their potentials are unaffected by the surfactant. This is further evidence that the surfactant serves to enhance adsorption at the interface and that the proposed mechanism of FIT-based protein detection[84] is operating in both systems. The data listed in Figure 5.3.7 also show that the peak current to protein charge ratio is constant across the three proteins studied and varies only with the absence/presence of surfactant.

This indicates again the beneficial role of the surfactant, as the greater ratio is indicative of greater levels of protein adsorption in the presence of surfactant.

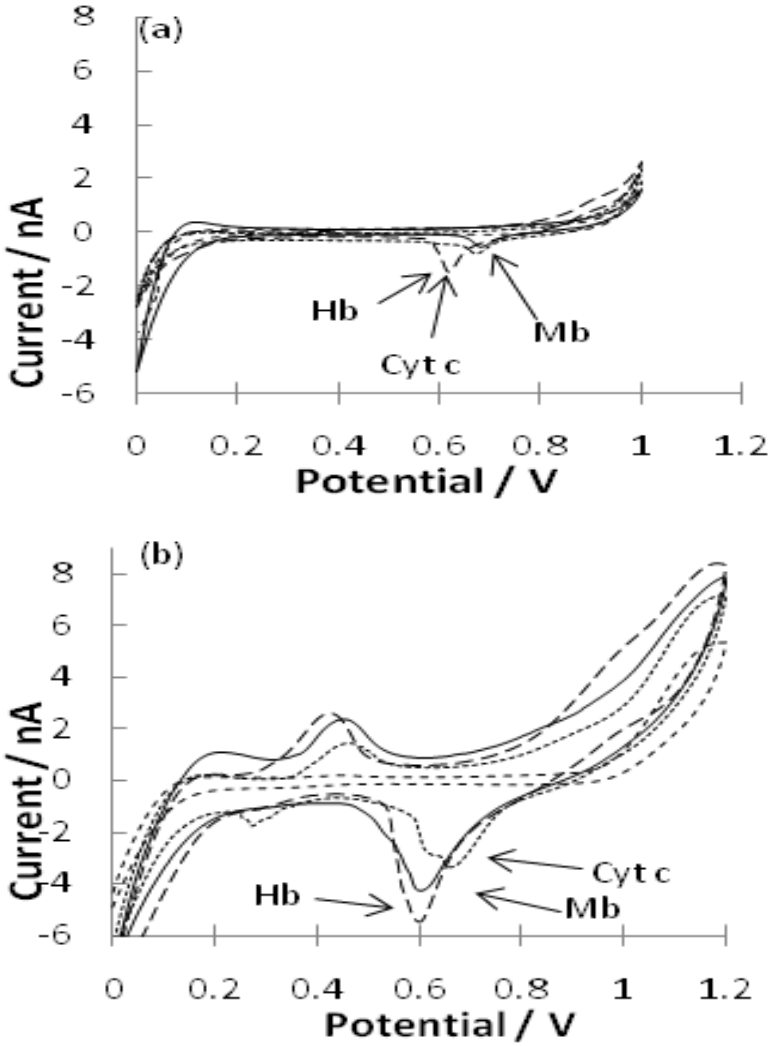

Figure 5.3.6: (a) CV of 6 μM Mb (solid line), Hb (long dash) and Cyt c (dots), scan rate 5 mV s^{-1}. The short dashed line represents the blank CV. No surfactant is present in the organic phase. (b) CV of 6 μM Mb (solid line), Hb (long dash) and Cyt c (dots), scan rate 5 mV s^{-1}. The short dashed line represents the blank CV. The organic phase contained 10 mM NaAOT. All CVs are the third scan of three.

Protein	**|Peak current| (i_P)** (without surfactant) **nA**	**|Peak current| (i_P)** (with surfactant) **nA**	**Protein Charge (z_i) at pH 2**	**i_P/ z_i ratio** (without surfactant)	**i_P/ z_i ratio** (with surfactant)
Hb	*1.27*	*4.66*	*+62*	*0.02*	*0.08*
Mb	*0.71*	*2.95*	*+32*	*0.02*	*0.09*
Cyt *c*	*0.54*	*2.47*	*+27*	*0.02*	*0.09*

Figure 5.3.7: Summary of current data and current-charge ratios obtained from Figure 4.Data obtained for the CVs shown in Figure 4. Hb = haemoglobin, Mb = myoglobin, Cyt c = cytochrome c. Peak currents taken from the desorption peak at ca. +0.6 V.

5.3.7 Multi-sweep CVs in the presence of surfactant

The voltammograms presented in Figure 5.3.8 (a,b and c) show repeated CVs for Mb, Hb and Cyt c respectively. The Mb CV is quite stable, while that for Hb is more variable. However, for Cyt *c*, there is a substantial variation over the course of the repeated CVs: all peaks present on the forward and reverse sweeps increase in magnitude with increasing cycle (Figure 5.3.8(a)). It was found that the desorption peak current, at ~0.65 - 0.7 V, is ~ -1.55 nA on the first scan and by the seventh scan has increased to ~ -3.7 nA. This indicates that an increased amount of protein is adsorbed at the interface with each

cycle, resulting in larger peak currents. This effect of increasing peak currents with scan number is not present in the corresponding experiments without surfactant (Figure 5.3.6(a)) where the voltammograms for a given concentration of protein show a high degree of reproducibility. The multi-peak character of the protein desorption peak becomes more pronounced with increasing cycle number. This may indicate a more complex structural relationship between the surfactant and protein, which merits further investigation.

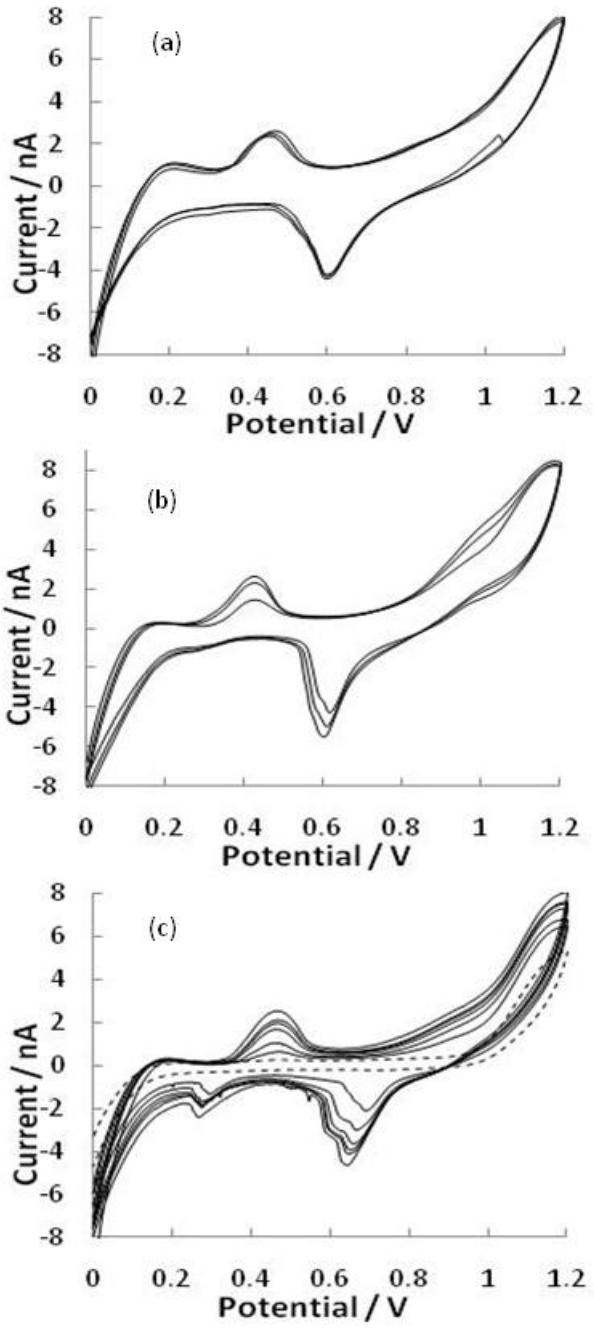

Figure 5.3.8: CVs of 6 μM Mb (a), Hb (b) and Cyt *c* (c) in the presence of 10 mM organic-phase surfactant, NaAOT. Scan rate 5 mV s^{-1}.Overlay of three consecutive CV's shown.

5.3.8 LSV and AdSV in the presence of surfactant

Linear sweep voltammetry was carried out in the presence of 10 mM AOT as shown in Figure 5.3.9. The potential was swept from 1.2 V to 0 V with 6 μM Mb present in the aqueous phase. Two distinct processes are observed at ~ 0.75 V and ~ 0.3 V. These two processes are as observed previously in Figures 5.3.2, 5.3.5 and 5.3.6 where protein – surfactant interactions and protein – anion interactions are attributed to the processes at 0.3 V and 0.75 V respectively. The inset in Figure shows 5.3.9 shows that a shoulder peak is observed at the 0.3 V process. Again, using voltammetry alone it is difficult to deduce an exact mechanism of interaction between the protein and surfactant.

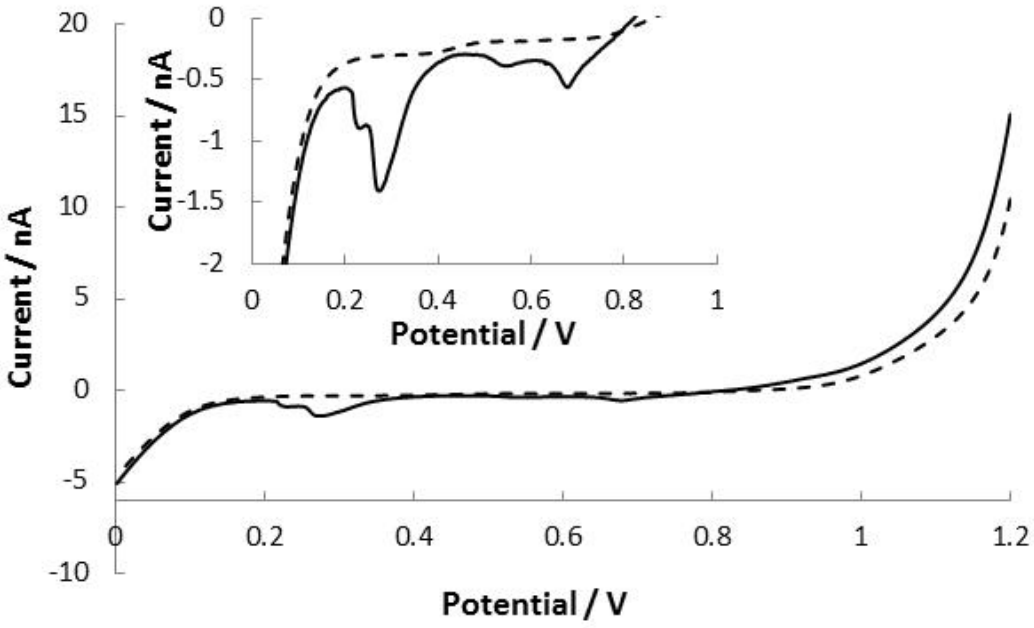

Figure 5.3.9: LSV of blank (dashed lines) and 6 μM Mb (solid line) in the presence of 10 mM NaAOT in the organic phase. Inset shows magnification of peaks obtained. Scan rate 5 mV s^{-1}.

That aside, the enhanced adsorption of proteins by the surfactant may be of use for achieving lower detection limits by using adsorptive stripping

voltammetry as a pre concentration step. The AdSV of 6 μM Mb was carried out as shown in Figure 5.3.10. The adsorption times used were 120 s and 400 s which produced peak currents at ~ 0.65 V of 2.2 nA and 3.4 nA respectively. This compares to a peak current of ~ 3 nA for cyclic voltammetry seen in Figure 5.3.5. Interestingly the process observed at 0.3 V is no longer visible in Figure 5.3.10, possibly its charge transfer has occurred during the adsorption time where no voltammetric data is observed. Another possibility is that the surfactant process is in competition with the normal protein – anion process which occurs at higher potentials. During CV where the potential is scanned from lower to higher voltages the surfactant – protein interactions occur first at ~ 0.4 V and the protein – anion interactions occur at ~ 0.9 V. In contrast to this when using AdSV the potential is held past 0.9 V from the beginning of the experiment allowing more time for protein anion interactions to occur. This may be a reasonable conclusion when looking at the data. Comparing Figure 5.3.10 to Figure 5.3.5 it can be seen that although the peak magnitudes are similar the shapes are noticeably different. The peaks are much more narrow and sharp when AdSV is used as compared to the wide peaks produced from CV. The sharp peaks are typical of what is observed in the absence of surfactant. Also when comparing Figures 5.3.9 and 5.3.10, it can be seen that when LSV is used with 0 s pre-concentration the processes involving the surfactant dominate. When considering the timescale the LSV allows half the time of a CV past 0.9 V, which again indicates that these two processes are competitive and time dependent.

If it is the case, where the surfactant – protein interactions do not take place at higher potentials, it would imply that the surfactants are not going to provide as large an increase, if any, in the sensitivity of the system using stripping voltammetric type methods. Although the appearance of a second set of peaks might provide some use in terms of protein detection.

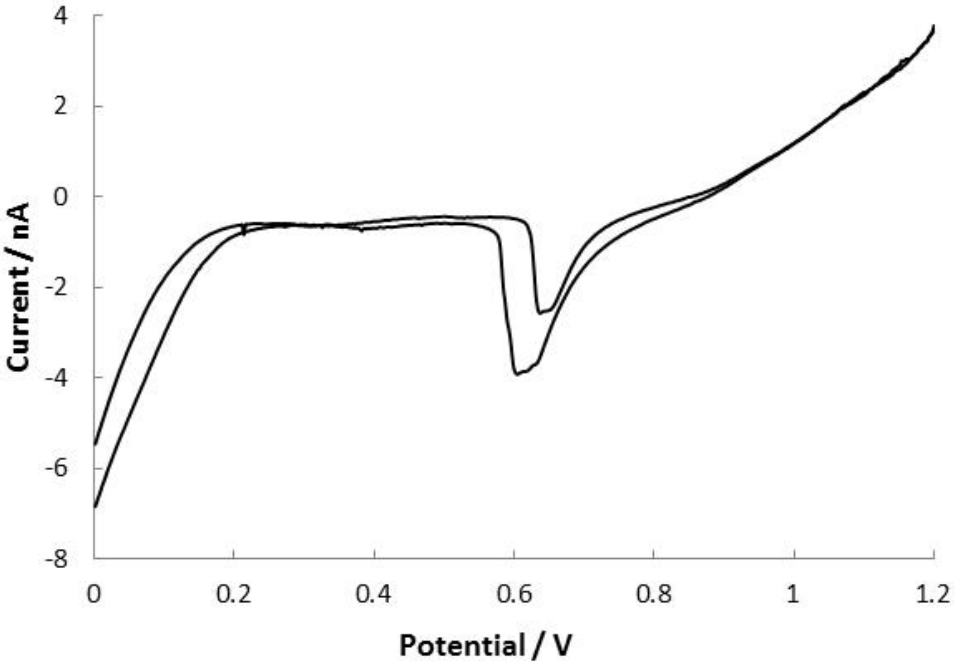

Figure 5.3.10: AdSV of 6 μM Mb in the presence of 10 mM NaAOT in the organic phase. Adsorptions time of 120s and 400s were used corresponding to the smaller and larger peak currents respectively. Scan rate is 5 mV s^{-1}.

5.4 Conclusions

The impact of added surfactant on the electrochemical behaviour of proteins at the water-organogel interface was examined. The addition of surfactant to the organogel phase was seen to enhance the current magnitude associated with protein detection. From interface coverage considerations, this surfactant enhancement was ca. 17-fold, while the current due to protein desorption from the interface was amplified by six-fold. The protein was shown to adsorb at the interface and interact with the surfactant resulting in a large capacitance change due to a protein-surfactant layer at the interface. The effects of the

surfactant were shown to be consistent across a range of haem-containing proteins, all showing large increases in peak currents in the presence of added surfactant. Repetitive cyclic voltammetry for a fixed concentration of cyt c showed increasing peak currents with each scan, attributed to a build-up of this protein at the ITIES. Linear sweep and stripping voltametry were investigated in the presence of surfactant, where it was found that the surfactant – protein and protein anion interactions may be competitive depending on the applied potential and timescale of the experiment. AdSV showed a slight improvement in peak current compared to the CV equivalent but not substantial gain in sensitivity was observed. These findings provide the basis for use of surfactant-modified interfaces in the development of enhanced electroanalytical detection of proteins. However, the approach would need to be coupled with either a method for sample clean-up or a separation step for use with biological samples or in an industrial process. Capillary electrophoresis coupled with liquid-liquid electrochemistry may be one way in which the enhancing effect of surfactants can be employed.[35]

Chapter 6

Voltammetric adsorption influenced protein aggregation at the ITIES

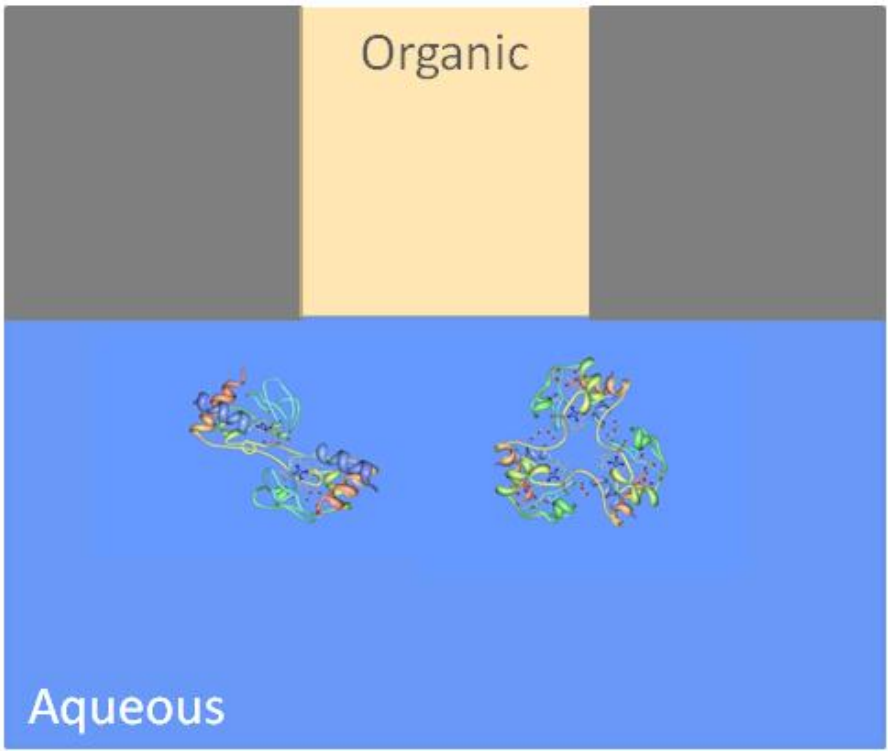

6.1 Introduction

Cytochrome c (cyt *c*) is a globular protein containing a covalently bound haem group[199]. It consists of 104 amino acids[200] and has a mass of 13 kDa[179]. The primary roles of cytochrome *c* are electron transport in the mitochondria relating to adenosine triphosphate (ATP) synthesis and apoptosis is vertebrates. Cytochrome *c* is known to form oligomers under certain conditions such as treatment with organic solvents and acids[201, 202]. The mechanism of cytochrome *c* polymerisation is still not fully understood. A recent study has determined the crystal structures of dimeric and trimeric cytochrome *c* complexes, which has shown that they polymerise through domain swapping of C-terminal helices from one cytochrome *c* molecule to another[203]. This study shows that the methionine 80 residue is dissociated from the haem group in order to facilitate the domain swapping.

Some proteins under certain conditions can convert from their native form, into highly ordered fibrillar aggregates[204]. The formation of fibrils has been associated with many diseases and neurodegenerative disorders, such as Alzheimer's, Spongiform encephalopathies, Huntington's disease, Parkinson's disease, spinocerebellar ataxia and type II diabetes just to name a few[199, 204-207]. Research has shown that many globular proteins can form amyloid fibrils under conditions which induce denaturation [208, 209]. It has also been proposed that the oligomeric intermediates of fibril formation are the species which are responsible for the associated neurodegenerative effects[210], which is why it is of great importance to understand the mechanistic process of the progression from native proteins to amyloid fibrils. Amyloids are known to form in extracellular space and have been shown to destabilise the cell membrane[206], this may make the liquid – liquid interface a suitable model for investigation in fibril formation and protein aggregation as it mimics one half of a phospholipid bilayer. Cytochrome *c* has shown to form amyloid fibrils when

its native fold is disrupted[199]. Kinetic effects of fibril formation have also been undertaken and studies of protein aggregation suggest that environments where protein crowding results in entropically favourable overlap of regions of the proteins giving rise to fibril formation[211].

The interface between two immiscible electrolytes provides a platform for the investigation into the behaviour of macromolecules based on ion transfer across the oil - water interface[5]. This label free method has been employed to investigate a range of biologically relevant molecules such as amino acids and peptides[115, 120] and various proteins such as haemoglobin, myoglobin and lysozyme[77, 79, 84, 148] . The proposed mechanism for detection of protein molecules at the ITIES is via facilitated ion transfer of the organic anion to the aqueous phase by complexation with the cationic protein[73, 79]. The primary objective of many investigations is to use the ITIES as the basis for detection, therefore the focus tends to lie in the area of achieving lower detection limits by miniaturising the interface[15, 19, 84] and improving problems associated with sensing in complex matrices and selectivity issues by employing ionophores[29, 32, 70] or developing more complex flow cell techniques[34, 89]. There has been less focus on understanding the complex behaviour of proteins at such interfaces. How protein structure, stability, size, charge, hydrophobicity effects the electrochemical behaviour are less well understood. It has been shown that denaturation of the haemoglobin leads to a reduced electrochemical response at the ITIES[82]. A recent study using spectroscopic methods showed that the structure and conformation of α – lactalbumin changed significantly when adsorbed at the oil-water interface[86]. Also its has been shown that proteins undergo a charge regulation process when adsorbed at such interfaces, indicating that the charge of the protein in bulk is not necessarily indicative of the charge of the molecules adsorbed at the interface[87]. Protein – protein interactions, which are likely to play a key role in the behaviour at the oil – water interface, and the effect of interfacial

concentration of adsorbed protein molecules has not been addressed. Recently the technique of adsorptive stripping voltametry (AdSV) was applied to achieve low limits of detection for lysozyme at the μITIES[88]. The technique effectively pre-concentrates the protein at the interface by holding a fixed adsorption potential for a given time, enhancing the current response from the facilitated ion transfer process.

Here we use AdSV as a method to investigate the effects of interfacial concentration on the electroactivity of cytochrome *c* at the polarised liquid-liquid interface. By adjusting the time held at a fixed adsorption potential the interfacial concentration can be controlled, and therefore the voltammetric response can be attributed to a known concentration of adsorbed protein rather that relating it to the bulk concentration. This provides the basis for use of AdSV at the ITIES as a tool for investigation of protein aggregation. This technique has the potential to probe protein – protein interactions, protein aggregation and polymerisation and protein fibril formation. The results shown in this work indicate that the polymerisation of cytochrome *c* can be induced under electrochemical control based on controlled aggregation of the denatured protein at the ITIES.

6.2 Experimental details

6.2.1 Reagents

All the reagents were purchased from Sigma-Aldrich Australia Ltd. and used as received, unless indicated otherwise. The gellified organic phase was prepared using bis(triphenylphosphoranylidene) tetrakis(4-chlorophenyl)borate ($BTPPA^+TPBCl^-$, 10 mM) in 1,6-dichlorohexane (1,6-

DCH) and low molecular weight poly(vinyl chloride) (PVC) [120]. The organic phase electrolyte salt $BTPPA^+TPBCl^-$ was prepared by metathesis of bis(triphenylphosphoranylidene)ammonium chloride ($BTPPA^+Cl^-$) and potassium tetrakis(4-chlorophenyl) borate (K^+TPBCl^-)[121]. Aqueous stock solutions of Cytochrome *c* (from equine heart) were prepared in 10 mM HCl (pH 2) on a daily basis and stored at +4 ºC. All the aqueous solutions were prepared in purified water (resistivity: 18 MΩ cm) from a USF Purelab Plus UV.

6.2.2 Experimental set-up

Once prepared as described in section 2.1.3 the gellified organic phase solution was introduced into the silicon micropore arrays via the glass cylinder, and the organic reference solution was placed on top of the gellified organic phase. The silicon membrane was then inserted into the aqueous phase (10 mM HCl or cytochrome *c* in 10 mM HCl. Voltammetric experiments were performed next, as previously described [79]. Ultraviolet/visible (UV/vis) absorbance spectroscopy was carried out using a Perkin-Elmer Lambda 35 instrument. The instrument was scanned in the range of 250 nm to 700 nm at the rate of 480 nm min^{-1}. The slit width was 1 nm with a resolution of 1 nm. The sample was run in a 1 x 1 cm quartz cuvette.

The setup used for the experiments comprised of a two electrode cell [122], with one Ag|AgCl electrode in the organic phase and one in the aqueous phase. The cell utilised in these experiments is shown in Figure 6.2.1, where x refers to the concentration of Cyt *c*. All potentials are reported with respect to the experimentally-used reference electrodes. The geometric area of the microinterfaces was 1.18×10^{-4} cm^2. Cyclic voltammetry (CV), linear sweep voltametry (LSV), and adsorptive stripping voltametry (AdSV) were carried out at a sweep rate of 5 mV s^{-1}, unless otherwise stated, and parameters such

as protein concentration, applied potential, and duration of the adsorption stage were varied. A thirty micropore array was employed for all experiments (described in section 2.1.3)

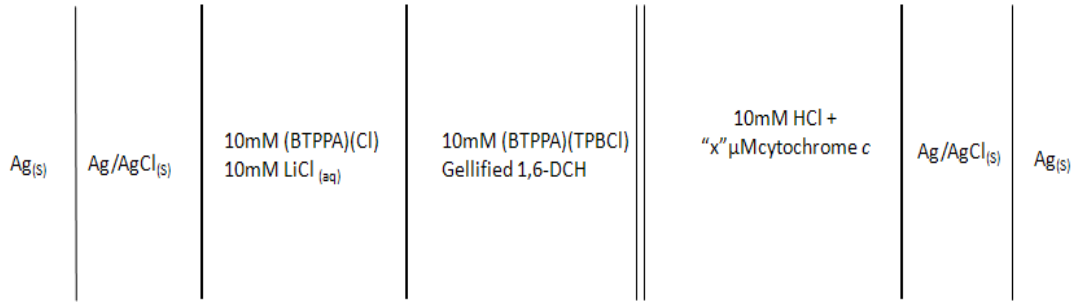

Figure 6.2.1: electrochemical cell employed in these experiments

6.3 Results and discussion

6.3.1 Optimisation of adsorption potential using LSV

Linear sweep voltammetry was performed with varying initial applied potentials in order to optimise the voltammetric signal obtained in the presence of cytochrome *c* (Figure 6.3.1(a)). This was done by measuring the peak current obtained in the presence of protein for corresponding initial applied potentials. The proteins adsorb under applied potentials, when $E_{applied} > E_{adsorbtion}$, where they undergo a facilitated ion transfer mechanism involving interactions with the organic phase anion, during the voltammetric scan, followed by desorption of the protein from the interface and back transfer of the organic anion[79]. The LSV was performed by scanning from a

positive to a more negative potential, where the initial applied potentials were varied from a minimum 0.6 V to a maximum of 1.0 V. As can be seen from Figure 6.3.1 (b), the peak current obtained is dependent on the initial applied potential. An optimal response was obtained at 0.975 V, which resulted in a peak current of – 4.8 nA. It can be seen from Figure 6.3.1 (b), that below 0.875 V no voltammetric response was obtained for cytochrome *c* due to insufficient amounts of adsorbed protein at the interface, and above 0.975 V the response is diminished as background processes dominate at this potential region and the organic anion can transfer without complexation to the protein.

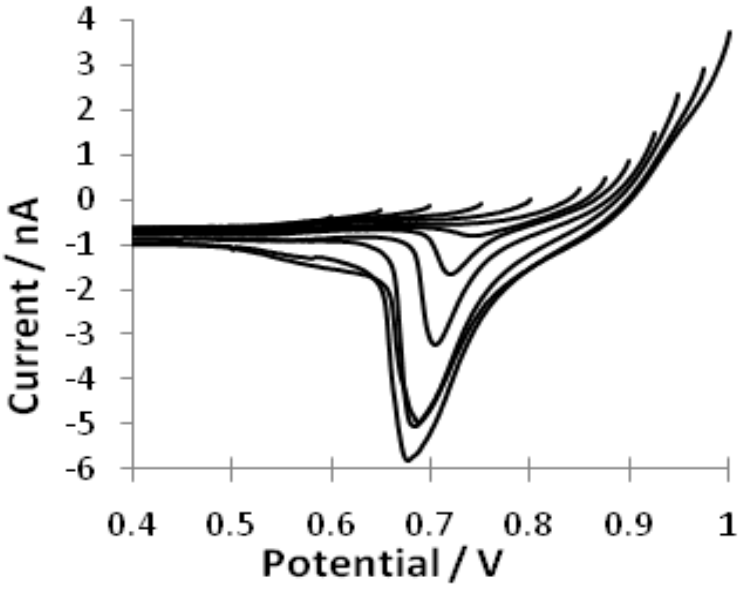

Figure 6.3.1 (a): LSV of 5 μM cyt c in 10 mM HCl, LSV potential initial potential from 0.6 V – 1.0 V, scan rate 5 mVs^{-1}. The electrochemical cell is as outlined in Figure 6.2.1.

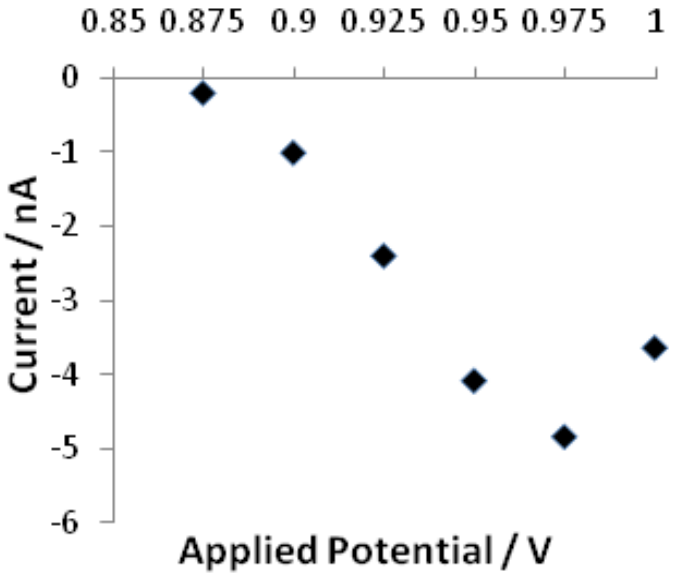

Figure 6.3.1 (b): Plot of applied potential vs peak current obtained from measurements of peak heights from the LSV data represented in Figure 6.3.1(a)

6.3.2 Adsorptive stripping voltammetry of cytochrome c

The influence of adsorption time on the electrochemical response of cytochrome *c* was investigated by using adsorptive stripping voltammetry. This involves applying a fixed adsorption potential, (0.975 V), for a set time (0 s – 1800 s) which effectively pre concentrates the protein at the interface, the protein is subsequently "stripped" back off the interface by it's desorption when the applied potential is swept back towards lower values[88]. Figure 6.3.2 (a) shows the resulting AdSVs obtained in the presence of 1 μM cytochrome *c* at various adsorption times. Figure 6.3.2 (b) shows a plot of peak current versus adsorption time and Figure 6.3.2 (c) shows a plot of current at 0.975 V versus adsorption time. The current at 0.975 V is representative of the charge transfer processes which occur under the applied potential, which are the adsorption of the protein and transfer of the organic anion to the aqueous phase, some current due to background electrolyte transfer is also likely as the adsorption potential is near the edge of the electrochemical window . As previously stated the peak current of the linear sweep *ca* ~ 0.67 V is due to the desorption of the protein and back transfer of the organic anion from the aqueous phase to the organic phase. Therefore Figure 6.3.2 (b) and 6.3.2 (c) should be related as the processes are co-dependent. On this basis the expected result would be that the current at 0.975 V, Figure 6.3.2 (c), would increase to more positive values with increasing adsorption time, but what is observed is a decrease in the current until it plateaus after which it increases slightly. The peak current values, Figure 6.3.2 (b), are shown to increase, (become more negative), with increasing adsorption time until again it reaches a plateau after which it decreases slightly. Figure 6.3.2 (a) provides some insight as to why these perhaps unexpected results occur. It can be clearly seen that the background current where no charge transfer processes occur (Figure 6.3.2 (a)), in the region from 0.6 V to 0.4 V, is changing dramatically with increasing adsorption time, from -0.75 nA at 0 s, to -5.57 nA at 1800 s

adsorption time. This is indicative of a change in the interfacial composition, likely due to non-desorbed protein. Also a small shoulder begins to emerge on the desorption peak at 0.65 V after times exceeding 600 s. This indicates a new process which is concentration dependant, as adsorption time is related directly to interfacial protein concentration. This process will be discussed further in following sections.

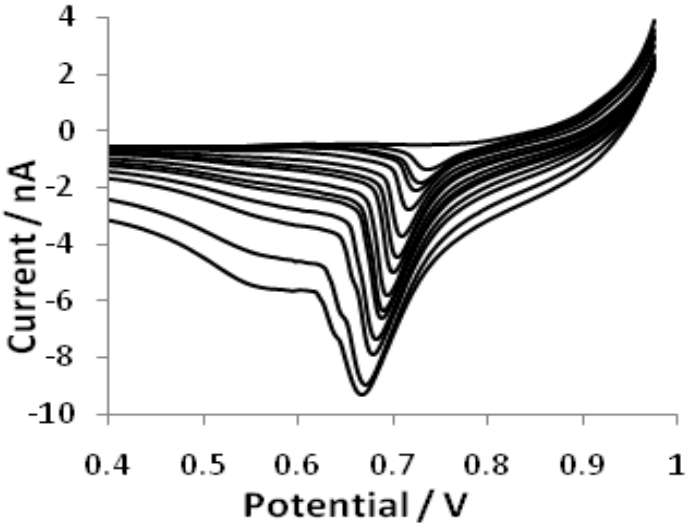

Figure 6.3.2 (a): AdSV of 1 µM cyt c in 10 mM HCl, adsorption potential of 0.975 V, adsorption times from 0 s – 1800 s, scan rate 5 mVs^{-1}. The electrochemical cell is as outlined in Figure 6.2.1.

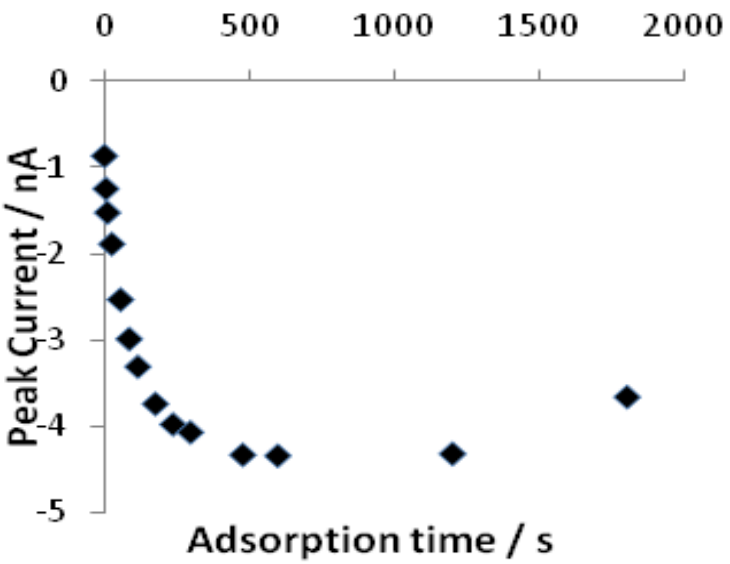

Figure 6.3.2 (b): Plot of peak current from the desorption peak vs adsorption time, data obtained from results shown in Figure 6.3.2 (a)

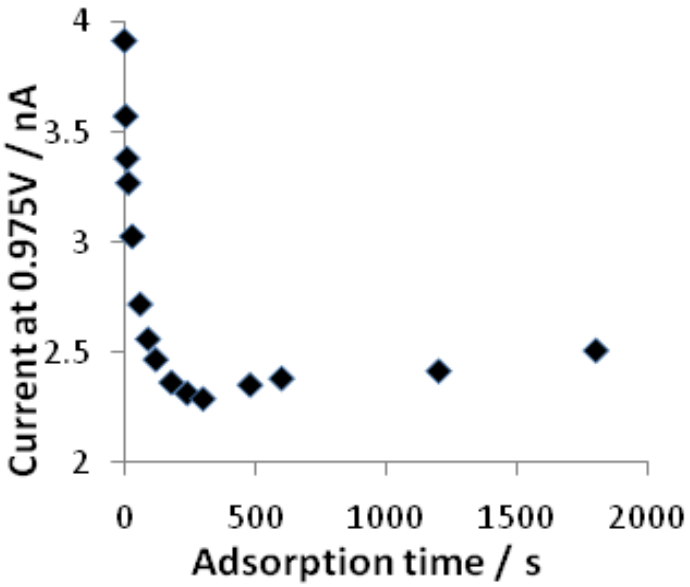

Figure 6.3.2 (c): Plot of current at 0.975 V vs adsorption time, data obtained from results shown in Figure 6.3.2 (a)

6.3.3 Influence of concentration on cytochrome c voltammetry

AdSV of cytochrome *c* was performed using fixed adsorption times (0, 60, 120, 300 s) while the concentration of the protein was varied (0.01 – 10.0 μM), the plots of peak current vs concentration and current at 0.975 V vs concentration are shown in Figures 6.3.3 (a) and 6.3.3 (b). The minimum measurable reverse peak is observed at 0.5 μM for 0, 60 and 120 s adsorption times, whereas at 300 s adsorption time a peak is measurable at 0.25 μM. The desorption peak current follows the general trend of increasing in magnitude before tending to plateau. This indicates that there is a maximum amount of adsorbed protein possible before the interface becomes saturated. The current at 0.975 V shows a general trend of increasing with concentration of cyt *c,* as more protein is adsorbed at the interface there is more organic anion transfer to the aqueous phase. It remains unclear however, why the currents in Figure 6.3.3 (b) are lower for increased adsorption time. It is possible that there is an effect of increased background ion transfer at higher adsorption times. As 0.975 V is at the far end of the available potential window in the potential region where background electrolyte will begin to transfer. This complicates the process as at this potential there will be protein adsorption and complexation of the organic phase anion, as well as aqueous cation transfer and some organic anion transfer.

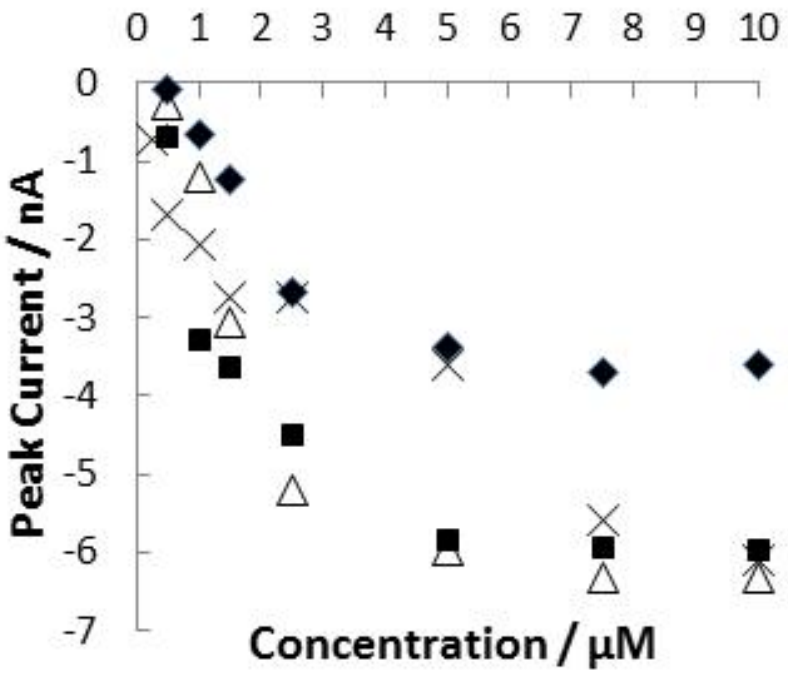

Figure 6.3.3 (a): Plot of peak current from the desorption peak vs adsorption time. Diamonds correspond to 0 s adsorption time, squares to 60 s, triangles to 120 s and crosses to 300 s. The concentration of cyt *c* is from 0.01 µM to 10.0 µM. The electrochemical cell is as outlined in Figure 6.2.1.

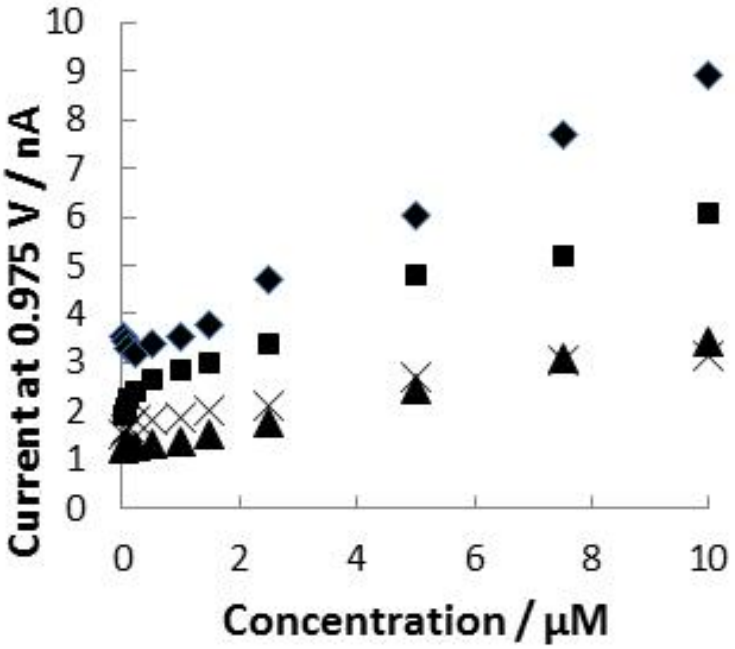

Figure 6.3.3 (b): Plot of current at 0.975 V vs adsorption time. Diamonds correspond to 0 s adsorption time, squares to 60 s, triangles to 120 s and crosses to 300 s. The concentration of cyt *c* is from 0.01 µM to 10.0 µM. The electrochemical cell is as outlined in Figure 6.2.1.

6.3.4 Voltammetry of cytochrome c aggregates

Figure 6.6.4 (a) shows the AdSV of 1 µM cyt *c* with an adsorption time of 300 s. It can be seen that as the concentration of cyt *c* is varied from 0.01 µM to 10.0 µM the desorption peak evolves from a single peak to a double and triple peak. The observation of up to three distinct desorption peaks points towards three different complexes undergoing facilitated ion transfer. Surface coverage calculations were carried out to relate the interfacial concentration of the proteins to the appearance of the single, double and triple peaks, which corresponds to 1.0 µM, 1.5µM and 7.5 µM bulk concentration of cytochrome *c* respectively. The calculations which are described in chapters 3 and 5, resulted in surface coverage's of 56 pmol cm^{-2}, 141 pmol cm^{-2} and 420 pmol

cm^{-2} for the 1.0 μM, 1.5 μM and 7.5 μM peaks. Since there is only cyt *c* present in the aqueous phase the only reasonable explanation for this unique behaviour is that protein – protein interactions are affecting the complexation of the organic anion. Cytochrome *c* is known to form dimmers, trimers, tetramers and other higher order oligomers under certain conditions such as treatment with ethanol or with trichloroacetic acid[201, 202, 212, 213]. It has been shown that polymerisation of cyt *c* occurs by domain swapping at the C-terminal helix but the mechanism of polymerisation remains unclear[200, 203]. The UV/Vis absorbance spectra (Figure 6.6. 4 (b)) shows that the Soret band is blue shifted from 411 nm in purified H_2O to 395 nm in 10 mM HCl (pH 2). This blue shift would suggest the possibility of a four co-ordinate Fe in the haem group[214],or certainly that the protein is denatured at this pH due to effects of the acidic environment[213]. This unfolded sate of cyt *c* into a highly expanded-denatured state is known as the D-conformer of the protein[213].Cyt *c* has also been shown to form amyloid fibrils under incubation at 75 °C in mild alkaline conditions which denatured the protein and promoted aggregation[199]. Therefore under the experimental conditions applied here cyt *c* polymerisation or aggregation should be possible. Since the multiple peaks are present only at higher interfacial concentrations of adsorbed protein, this would indicate that the adsorption process is inducing various forms of cyt *c* aggregates. Studies have shown that crowded environments strongly modify the association of macromolecules through attractive entropic interactions, which can cause protein aggregation and fibril formation[206].It has also been shown that there is a single free energy of aggregation barrier controlling the addition of protein molecules to amyloid fibrils[215]. It is proposed that the evolution of the second and third voltammetric peaks in Figure 6.6.4 (a) correlate to electrochemically induced aggregation of cytochrome *c* into a polymeric aggregate at the ITIES. This would indicate that electrochemistry at the ITIES has the ability to resolve between protein conformers based on adsorption and

ion transfer processes. This provides the possibility for a new avenue of research using the ITIES as a platform to investigate protein aggregation and fibril formation.

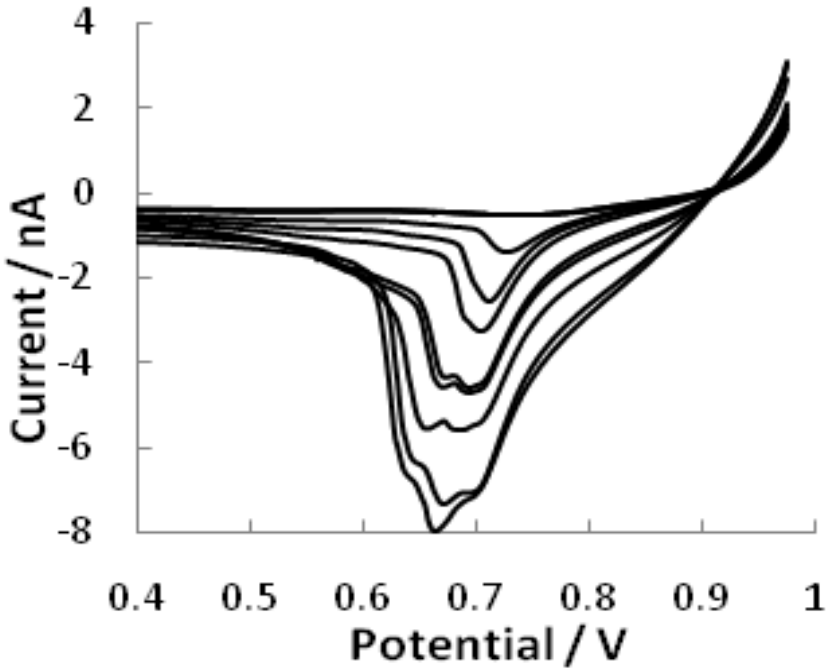

Figure 6.6.4 (a): AdSV of 1 μM cyt *c* in 10 mM HCl, adsorption potential of 0.975 V, adsorption times from 300 s. Concentrations of cyt *c* from 0.01 μM to 10.0 μM. Scan rate 5 mVs^{-1}. The electrochemical cell is as outlined in Figure 6.2.1.

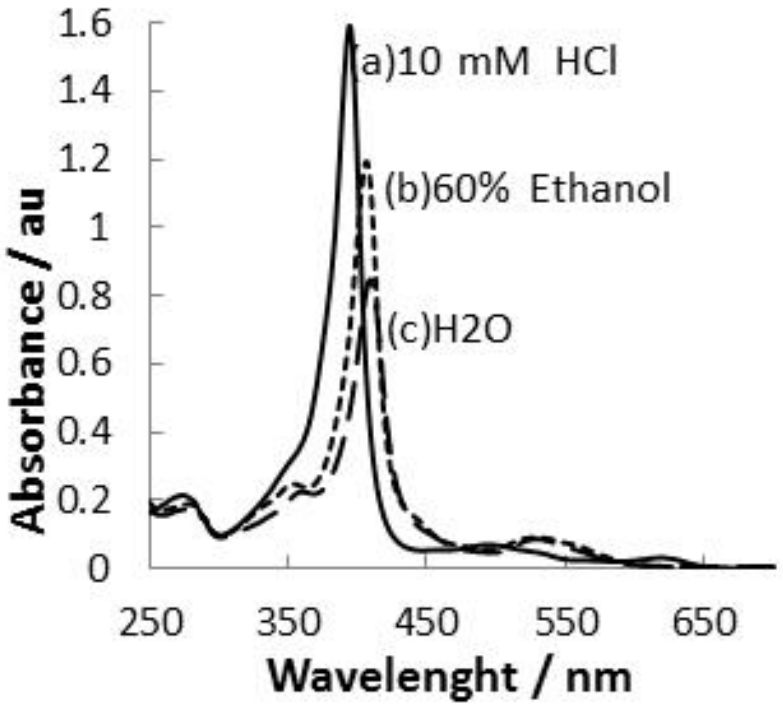

Figure 4 (b): UV/Vis absorbance spectra of 10 μM cyt *c* in (a) 10 mM HCl and (b) H_2O (18 MΩ cm)

6.4 Conclusions

The electroactivity of cytochrome *c* at the ITIES investigated using adsorptive stripping voltammetry. The optimum adsorption potential was determined to be 0.975 V, below 0.875 V no voltammetric response was obtained for cytochrome *c* due to insufficient amounts of adsorbed protein at the interface. The effects of adsorption time and bulk concentration of cytochrome *c* were investigated and it was shown that the voltammetric response for the desorption peak tends to reach a plateau indicating that there is a maximum of adsorbed protein possible due to a saturation of the interface. It was found that at longer adsorption times, which result in larger concentration of adsorbed protein, a single voltammetric response developed into a double and triple peak which corresponded to surface coverage's of 56 pmol cm^{-2}, 141 pmol

cm^{-2} and 420 pmol cm^{-2}. This result is attributed to the formation of polymeric complexes of cytochrome *c* which are induced by aggregation at the interface under denaturing conditions. These conditions where the protein is denatured and aggregation is induced are analogous to those needed to form amyloid fibrils. These results provide the basis for adsorptive stripping voltammetry to be used as a tool to investigate the formation of amyloid fibrils and the effects of protein aggregation.

Chapter 7

Conclusions and future perspectives

7.1 Conclusions

Ion transfer electrochemistry at the polarisable liquid – liquid interface has been successfully utilised to study the behaviour of biomolecules. The focus of the work presented can be divided into four significant topics.

(1) The investigation into the fundamental behaviour of a protein, myoglobin, at the ITIES.
(2) The development of techniques to achieve selective detection of a protein in more complex samples such as protein mixtures.
(3) Modification of the organic phase composition with addition of surfactant molecules and an investigation into their interactions with proteins.
(4) The potential dependant adsorption of a protein, cytochrome *c*, and electrochemical characterisation of its properties under varying adsorption conditions.

(1) Myoglobin was investigated using voltammetry and was shown to have a linear response to protein concentration from 1 – 6 μM. It was found that the protein produces an observable electrochemical response only when the pH of the aqueous phase is sufficiently low that the protein is cationic. The protein was shown to adsorb at the interface, which is indicated by its disruption of TEA^+ transfer across the interface. By increasing the ionic strength of the aqueous phase it was found that the protein peaks increase in magnitude and became more distinct, which is attributed to the salting out effect. It was found

that using a more hydrophobic organic anion shifts the peak potential for the protein response to a more positive value. UV/vis spectroscopy indicated that the protein was likely to be partially denatured at lower pH observed by loss of the Soret band from the spectra. These results illustrate an electrochemical characterisation of the behaviour of a model protein at the ITIES and provide a useful platform for which further investigations can be compared against.

(2) Three different approaches were investigated, with the aim to develop methods for selective detection of protein at the ITIES. The electroactivity of polypeptide amylin was investigated, where it was found that due to its iso-electric point it was positively charged at physiological pH. This allowed the detection of amylin at physiological pH, which has a slight reduction in sensitivity as compared to the analogous experiment when using a more acidic pH. Being cationic at pH 7.4 allowed for the selective detection of amylin in the presence of two proteins, haemoglobin and myoglobin.

The adsorptive stripping voltametry of insulin and albumin was investigated at the ITIES. It was found that the two proteins had adsorption maxima at different applied potentials of 0.9 V and 0.975 V respectively. It was found that at 0.9 V albumin showed a minimal electrochemical response. This allowed for the selective detection of insulin in the presence of albumin by applying a fixed adsorption potential of 0.9 V where only insulin will be adsorbed to the interface and undergo facilitated ion transfer resulting in the voltammetric peak. Insulin was detected from 1 – 6 μM in the presence of 1 μM albumin.

The final investigation into methods of selective protein detection involved incorporating antibodies into the aqueous phase. A characterisation of the behaviour of anti albumin and albumin at physiological pH resulted in no

observable electrochemical response. The anti-BSA also showed no significant response at low pH. At pH 2 the albumin gives a small but reproducible voltammetric peak. Interestingly when the anti albumin and albumin are combined at low pH an increase in peak current at ~ 0.9 V is observed, which increases over time. This may be due to non specific interactions between the antigen and antibody.

These results provide a several different approaches towards achieving selectivity at the ITIES.

(3) The effects of an anionic surfactant, present in the organic phase, on protein electrochemistry were investigated. The mechanism was probed by using the surfactant as a replacement for the conventional electrolyte anion, which showed a new adsorption process was achieved when the surfactant was present with the protein. When the surfactant was present as its sodium salt it was found to increase the peak currents for myoglobin 6-fold and the surface coverage increased 17-fold. This was attributed to enhanced adsorption of the protein in the presence of surfactant. Repeated cycling of CVs for cytochrome *c* showed successive increases in peak currents, whereas for myoglobin and haemoglobin the cycling produced relatively reproducible voltammetry.

(4) The adsorption behaviour of cytochrome *c* at the ITIES was investigated, in particular the effects of bulk concentration and adsorption times were studied. It was found that the peak currents tended towards a plateau in all cases. This is likely due to the ability of a finite amount of material to be adsorbed at the interface. It was found that when both the concentration and adsorption times are increased sufficiently high, new features in the voltammetry are observed, where a single peak evolves to a double peak, then

to a triple peak. This unusual result is possibly due to the formation of aggregates of polymeric protein compounds at the ITIES, which are induced by the low pH and high molecular packing of proteins under applied potentials.

7.2 Future perspectives

The use of electrochemistry at the ITIES as a method for biomolecular detection is one of the key driving forces behind the research presented in this thesis. In recent years there has been much development in this area, although further investigations and understanding of the processes which underlie electrochemistry at the ITIES are needed to put this technology in a position to compete with the more established methods for biomolecular detection. With that in mind there are a few important areas which would require attention.

Firstly, while knowledge of the fundamental behaviour of proteins at the electrified liquid – liquid interface has improved significantly since the concept was first introduced there is still further work to be done in this area. The current proposed mechanism for detection, which applies to most proteins, is the facilitated ion transfer mechanism. This utilises the interactions between the protein and the organic anion as the detection method in the electrochemical experiments. Little is known about the nature of these interactions and a more detailed knowledge could lead to the development of better anions to complex with the proteins, which perhaps could improve the sensitivity and selectivity for a protein.

Following from that, this leads to a key area relating to selective detection of proteins. A real challenge in the area of protein detection at the ITIES is detection of a protein in a complex mixture or real biological samples such as

blood. Presented in this thesis are several approaches towards selective detection, but there are improvements needed to successfully apply these techniques in real samples. The approaches centre around two concepts, tuning of the experimental conditions and addition of a molecule that will help attain selectivity. There are certainly many possible avenues which could be explored to attain chemical selectivity of a protein. Addition of ionophores, antibodies or antibody fragments, protein binding anions, surfactants, aptamers and cellular receptors are all merit exploration.

In terms of the experimental conditions it is clear that simple changes such as adjusting the pH or selection of an appropriate adsorption potential can dramatically change the observed electrochemistry. It must also be considered that no one technique or set of conditions will solve every problem. Each target biomolecule comes with its own unique properties and challenges, thus it is imperative that suitable target biomolecules are chosen based on their inherent properties, an example of which is amylin. Due to its physiochemical properties alone it was possible to detect amylin in the presence of a mixture of proteins at physiological pH.

The majority of work at the ITIES employs little to no sample preparation or pre-treatment and the ability to detect biomolecules without labelling provides scope for the use of this technique in point of care applications. However some challenges relating to selectivity and sensitivity may be addressed if the ITIES were used in combination with other techniques. Coupling electrochemistry at the ITIES with capillary electrophoresis, liquid chromatography or mass selective filtration steps has the potential to lead into new areas of research.

The other main attraction of the ITIES is that it can be used to understand fundamental processes which occur at the oil – water interface, which is essentially a simple model for half of a phospholipid bilayer membrane. A

better understanding of the fundamental processes which occur at the ITIES may help improve the understanding of the ion and electron transfer processes which occur across the cell membrane. It was shown that adsorption of the proteins at the ITIES can produce unusual voltammetry, which was proposed as formation of protein aggregates at the interface. There is further work to be done in this area to identify the nature of the protein molecules at the interface. It is unknown how the more highly crowded conditions of adsorbed layers at the interface affect the protein structure and protein – protein interactions. Further knowledge of these aggregated protein interactions could lead to a better understand of the conditions which lead to fibril formation.

References

1. Bard, A. J.; Faulkner, L. R., *Electrochemical methods : fundamentals and applications*. 2nd ed.; John Wiley & Sons, Inc: New York, 2001.
2. Zoski, C. G., *Handbook of Electrochemistry*. 1st ed.; Elsevier: Oxford, 2007.
3. Wang, J., *Analytical Electrochemistry*. 3rd ed.; John Wiley & Sons, Inc.: Ney jersey, 2006.
4. Samec, Z., Electrochemistry at the interface between two immiscible electrolyte solutions, 2004, *Pure and Applied Chemistry* **2004,** *76* (12), 2147-2180.
5. Arrigan, D. W. M., Bioanalytical Detection Based on Electrochemistry at Interfaces between Immiscible Liquids, 2008, *Analytical Letters* **2008,** *41* (18), 3233-3252.
6. Samec, Z.; Mareček, V.; Koryta, J.; Khalil, M. W., Investigation of ion transfer across the interface between two immiscible electrolyte solutions by cyclic voltammetry, 1977, *Journal of Electroanalytical Chemistry and Interfacial Electrochemistry* **1977,** *83* (2), 393-397.
7. Taylor, G.; Girault, H. H. J., Ion transfer-reactions across a liquid liquid interface supported on a micropipette tip, 1986, *Journal of Electroanalytical Chemistry* **1986,** *208* (1), 179-183.
8. Shao, Y.; Osborne, M. D.; Girault, H. H., Assisted ion transfer at micro-ITIES supported at the tip of micropipettes, 1991, *Journal of Electroanalytical Chemistry* **1991,** *318* (1-2), 101-109.
9. Sherburn, A.; Platt, M.; Arrigan, D. W. M.; Boag, N. M.; Dryfe, R. A. W., Selective silver ion transfer voltammetry at the polarised liquid vertical bar liquid interface, 2003, *Analyst* **2003,** *128* (9), 1187-1192.
10. Lillie, G. C.; Holmes, S. M.; Dryfe, R. A. W., Electrochemistry of cytochrome c at the liquid-liquid interface, 2002, *Journal of Physical Chemistry B* **2002,** *106* (47), 12101-12103.
11. Sugihara, T.; Hotta, H.; Osakai, T., Electrochemical control of glucose oxidase-catalyzed redox reaction using an oil/water interface, 2004, *Physical Chemistry Chemical Physics* **2004,** *6* (13), 3563-3568.
12. Koryta, J., Electrochemical polarization phenomena at the interface of two immiscible electrolyte solutions, 1979, *Electrochimica Acta* **1979,** *24* (3), 293-300.
13. Campbell, J. A.; Stewart, A. A.; Girault, H. H., Determination of the kinetics of facilitated ion transfer reactions across the micro interface between two immiscible electrolyte solutions, 1989, *Journal of the Chemical Society, Faraday Transactions 1: Physical Chemistry in Condensed Phases* **1989,** *85* (4), 843-853.

14. Campbell, J. A.; Girault, H. H., Steady state current for ion transfer reactions at a micro liquid interface, 1989, *Journal of Electroanalytical Chemistry* **1989,** *266* (2), 465-469.
15. Berduque, A.; Zazpe, R.; Arrigan, D. W. M., Electrochemical detection of dopamine using arrays of liquid-liquid micro-interfaces created within micromachined silicon membranes, 2008, *Analytica Chimica Acta* **2008,** *611* (2), 156-162.
16. Shao, Y.; Mirkin, M. V., Fast Kinetic Measurements with Nanometer-Sized Pipets. Transfer of Potassium Ion from Water into Dichloroethane Facilitated by Dibenzo-18-crown-6, 1997, *Journal of the American Chemical Society* **1997,** *119* (34), 8103-8104.
17. Sun, P.; Laforge, F. O.; Mirkin, M. V., Ion Transfer at Nanointerfaces between Water and Neat Organic Solvents, 2005, *Journal of the American Chemical Society* **2005,** *127* (24), 8596-8597.
18. Sun, P.; Laforge, F. O.; Mirkin, M. V., Role of Trace Amounts of Water in Transfers of Hydrophilic and Hydrophobic Ions to Low-Polarity Organic Solvents, 2007, *Journal of the American Chemical Society* **2007,** *129* (41), 12410-12411.
19. Scanlon, M. D.; Arrigan, D. W. M., Enhanced Electroanalytical Sensitivity via Interface Miniaturisation: Ion Transfer Voltammetry at an Array of Nanometre Liquid-Liquid Interfaces, 2011, *Electroanalysis* **2011,** *23* (4), 1023-1028.
20. Rimboud, M.; Hart, R. D.; Becker, T.; Arrigan, D. W. M., Electrochemical behaviour and voltammetric sensitivity at arrays of nanoscale interfaces between immiscible liquids, 2011, *Analyst* **2011,** *136* (22), 4674-4681.
21. Koryta, J.; Vanysek, P.; Brezina, M., Electrolysis with Electrolyte Dropping Electrode .2. Basic Properties of System, 1977, *Journal of Electroanalytical Chemistry* **1977,** *75* (1), 211-228.
22. Samec, Z.; Marecek, V.; Koryta, J.; Khalil, M. W., Investigation of Ion Transfer across Interface between 2 Immiscible Electrolyte-Solutions by Cyclic Voltammetry, 1977, *Journal of Electroanalytical Chemistry* **1977,** *83* (2), 393-397.
23. Sanchez Vallejo, L. J.; Ovejero, J. M.; Fernández, R. A.; Dassie, S. A., Simple Ion Transfer at Liquid | Liquid Interfaces, 2012, *International Journal of Electrochemistry* **2012,** *2012*, 34.
24. Shao, Y. H.; Mirkin, M. V., Voltammetry at micropipet electrodes, 1998, *Analytical Chemistry* **1998,** *70* (15), 3155-3161.
25. Vladimirova, E. V.; Dunaeva, A. A.; Petrukhin, O. M.; Shipulo, E. V., Study of the transfer of aminoglycoside antibiotics through the phase boundary water/o-nitrophenyl octyl ether by voltammetry at the interface of two immiscible electrolyte solutions, 2013, *Journal of Analytical Chemistry* **2013,** *68* (3), 253-260.

26. Vagin, M. Y.; Trashin, S. A.; Karyakin, A. A.; Mascini, M., Label-free detection of DNA hybridization at a liquid|liquid interface, 2008, *Analytical Chemistry* **2008,** *80* (4), 1336-1340.
27. Horrocks, B. R.; Mirkin, M. V., Cation Binding to DNA Studied by Ion-Transfer Voltammetry at Micropipets, 1998, *Analytical Chemistry* **1998,** *70* (22), 4653-4660.
28. Kivlehan, F.; Lefoix, M.; Moynihan, H. A.; Thompson, D.; Ogurtsov, V. I.; Herzog, G.; Arrigan, D. W. M., Interaction of acridine-calix[4]arene with DNA at the electrified liquid liquid interface, 2010, *Electrochimica Acta* **2010,** *55* (9), 3348-3354.
29. Ribeiro, J. A.; Miranda, I. M.; Silva, F.; Pereira, C. M., Electrochemical study of dopamine and noradrenaline at the water/1,6-dichlorohexane interface, 2010, *Physical Chemistry Chemical Physics* **2010,** *12* (46), 15190-15194.
30. Arrigan, D. W. M.; Ghita, M.; Beni, V., Selective voltammetric detection of dopamine in the presence of ascorbate, 2004, *Chemical Communications* **2004,** (6), 732-733.
31. Herzog, G.; McMahon, B.; Lefoix, M.; Mullins, N. D.; Collins, C. J.; Moynihan, H. A.; Arrigan, D. W. M., Electrochemistry of dopamine at the polarised liquid vertical bar liquid interface facilitated by an homo-oxo-calix 3 arene ionophore, 2008, *Journal of Electroanalytical Chemistry* **2008,** *622* (1), 109-114.
32. Faisal, S. N.; Pereira, C. M.; Rho, S.; Lee, H. J., Amperometric proton selective sensors utilizing ion transfer reactions across a microhole liquid/gel interface, 2010, *Physical Chemistry Chemical Physics* **2010,** *12* (46), 15184-15189.
33. Scanlon, M. D.; Berduque, A.; Strutwolf, J.; Arrigan, D. W. M., Flow-injection amperometry at microfabricated silicon-based mu-liquid-liquid interface arrays, 2010, *Electrochimica Acta* **2010,** *55* (14), 4234-4239.
34. Gohara, E.; Osakai, T., Flow-Injection On-line Electrochemical Separation/Determination of Ions Using a Two-Step Oil/Water-Type Flow Cell System, 2010, *Analytical Sciences* **2010,** *26* (3), 375-378.
35. Sisk, G. D.; Herzog, G.; Glennon, J. D.; Arrigan, D. W. M., Assessment of ion transfer amperometry at liquid-liquid interfaces for detection in CE, 2009, *Electrophoresis* **2009,** *30* (19), 3366-3371.
36. Wilke, S.; Schurz, R.; Wang, H. M., Amperometric ion detection in capillary zone electrophoresis by ion transfer across a liquid-liquid microinterface, 2001, *Analytical Chemistry* **2001,** *73* (6), 1146-1154.
37. Lee, H. J.; Girault, H. H., Amperometric ion detector for ion chromatography, 1998, *Analytical Chemistry* **1998,** *70* (20), 4280-4285.
38. Verwey, E. J. W.; Niessen, K. F., XL. The electrical double layer at the interface of two liquids, 1939, *Philosophical Magazine Series 7* **1939,** *28* (189), 435-446.

39. Gavach, C.; Seta, P.; Depenoux, B., Double-Layer and Ion Adsorption at Interface between 2 Non-Miscible Solutions .1. Interfacial-Tension Measurements for Water-Nitrobenzene Tetraalkylammonium Bromide Systems, 1977, *Journal of Electroanalytical Chemistry* **1977,** *83* (2), 225-235.
40. Girault, H. H.; Schiffrin, D. J., Thermodynamic surface excess of water and ionic salvation at the interface between two immiscible liquids, 1983, *Journal of Electroanalytical Chemistry* **1983,** *150* (1-2), 43-49.
41. Benjamin, I., Theoretical-study of the water 1,2-dichloroethane interface - structure, dynamics, and conformational equilibria at the liquid liquid interface, 1992, *Journal of Chemical Physics* **1992,** *97* (2), 1432-1445.
42. Strutwolf, J.; Barker, A. L.; Gonsalves, M.; Caruana, D. J.; Unwin, P. R.; Williams, D. E.; Webster, J. R. P., Probing liquid vertical bar liquid interfaces using neutron reflection measurements and scanning electrochemical microscopy, 2000, *Journal of Electroanalytical Chemistry* **2000,** *483* (1-2), 163-173.
43. Walker, D. S.; Richmond, G. L., Depth Profiling of Water Molecules at the Liquid−Liquid Interface Using a Combined Surface Vibrational Spectroscopy and Molecular Dynamics Approach, 2007, *Journal of the American Chemical Society* **2007,** *129* (30), 9446-9451.
44. Luo, G. M.; Malkova, S.; Yoon, J.; Schultz, D. G.; Lin, B. H.; Meron, M.; Benjamin, I.; Vanysek, P.; Schlossman, M. L., Ion distributions at the nitrobenzene-water interface electrified by a common ion, 2006, *Journal of Electroanalytical Chemistry* **2006,** *593* (1-2), 142-158.
45. Luo, G. M.; Malkova, S.; Yoon, J.; Schultz, D. G.; Lin, B. H.; Meron, M.; Benjamin, I.; Vanysek, P.; Schlossman, M. L., Ion distributions near a liquid-liquid interface, 2006, *Science* **2006,** *311* (5758), 216-218.
46. Nernst, W.; Riesenfeld, E. H., Ueber elektrolytische Erscheinungen an der Grenzfläche zweier Lösungsmittel, 1902, *Annalen der Physik* **1902,** *313* (7), 600-608.
47. Samec, Z.; Marecek, V.; Weber, J.; Homolka, D., Charge-Transfer between 2 Immiscible Electrolyte-Solutions - Advances in Method of Electrolysis with the Electrolyte Dropping Electrode (Ede), 1979, *Journal of Electroanalytical Chemistry* **1979,** *99* (3), 385-389.
48. Tatsumi, H.; Ueda, T., Ion transfer voltammetry of tryptamine, serotonin, and tryptophan at the nitrobenzene/water interface, 2011, *Journal of Electroanalytical Chemistry* **2011,** *655* (2), 180-183.
49. Quiroga, M. V. C.; Monzon, L. M. A.; Yudi, L. M., Interaction of triflupromazine with distearoylphosphatidylglycerol films studied by surface pressure isotherms and cyclic voltammetry at a 1,2-dichloroethane/water interface, 2010, *Electrochimica Acta* **2010,** *55* (20), 5840-5846.
50. Liu, S.; Li, Q.; Shao, Y., Electrochemistry at micro- and nanoscopic liquid/liquid interfaces, 2011, *Chemical Society reviews* **2011,** *40* (5), 2236-2253.

51. Liu, B.; Mirkin, M. V., Electrochemistry at microscopic liquid-liquid interfaces, 2000, *Electroanalysis* **2000,** *12* (18), 1433-1446.
52. Huang, X. J.; O'Mahony, A. M.; Compton, R. G., Microelectrode Arrays for Electrochemistry: Approaches to Fabrication, 2009, *Small* **2009,** *5* (7), 776-788.
53. Herzog, G.; Beni, V., Stripping voltammetry at micro-interface arrays: A review, 2013, *Analytica Chimica Acta* **2013,** *769*, 10-21.
54. Beni, V.; Arrigan, D. W. M., Microelectrode arrays and microfabricated devices in electrochemical stripping analysis, 2008, *Current Analytical Chemistry* **2008,** *4* (3), 229-241.
55. Stewart, A. A.; Taylor, G.; Girault, H. H.; Mcaleer, J., Voltammetry at Microities Supported at the Tip of a Micropipette .1. Linear Sweep Voltammetry, 1990, *Journal of Electroanalytical Chemistry* **1990,** *296* (2), 491-515.
56. Su, B.; Zhang, S.; Yuan, Y.; Guo, J. D.; Gan, L. B.; Shao, Y. H., Investigation of ion transfer across the micro-water/nitrobenzene interface facilitated by a fullerene derivative, 2002, *Analytical Chemistry* **2002,** *74* (2), 373-378.
57. Zazpe, R.; Hibert, C.; O'Brien, J.; Lanyon, Y. H.; Arrigan, D. W. M., Ion-transfer voltammetry at silicon membrane-based arrays of micro-liquid-liquid interfaces, 2007, *Lab on a Chip* **2007,** *7* (12), 1732-1737.
58. Peulon, S.; Guillou, V.; L'Her, M., Liquid vertical bar liquid microinterface. Localization of the phase boundary by voltammetry and chronoamperometry; influence of the microchannel dimensions on diffusion, 2001, *Journal of Electroanalytical Chemistry* **2001,** *514* (1-2), 94-102.
59. Vanýsek, P.; Reid, J. D.; Craven, M. A.; Buck, R. P., Properties of the Interface Between Two Immiscible Electrolytes in the Presence of Proteins, 1984, *Journal of the Electrochemical Society* **1984,** *131* (8), 1788-1791.
60. Vanýsek, P.; Sun, Z., Bovine serum albumin adsorption on a water/nitrobenzene interface, 1990, *Bioelectrochemistry and Bioenergetics* **1990,** *23* (2), 177-194.
61. Sawada, S.; Osakai, T., Hydrophobicity of oligopeptides: a voltammetric study of the transfer of dipeptides facilitated by dibenzo-18-crown-6 at the nitrobenzene/water interface, 1999, *Physical Chemistry Chemical Physics* **1999,** *1* (20), 4819-4825.
62. Georganopoulou, D. G.; Caruana, D. J.; Strutwolf, J.; Williams, D. E., Electron transfer mediated by glucose oxidase at the liquid/liquid interface, 2000, *Faraday Discussions* **2000,** *116* (0), 109-118.
63. Kakiuchi, T.; Chiba, M.; Sezaki, N.; Nakagawa, M., Cyclic voltammetry of the transfer of anionic surfactant across the liquid–liquid interface manifests electrochemical instability, 2002, *Electrochemistry Communications* **2002,** *4* (9), 701-704.

64. Kakiuchi, T., Electrochemical instability of the liquid liquid interface in the presence of ionic surfactant adsorption, 2002, *Journal of Electroanalytical Chemistry* **2002,** *536* (1–2), 63-69.
65. Vagin, M. Y.; Malyh, E. V.; Larionova, N. I.; Karyakin, A. A., Spontaneous and facilitated micelles formation at liquid vertical bar liquid interface: towards amperometric detection of redox inactive proteins, 2003, *Electrochemistry Communications* **2003,** *5* (4), 329-333.
66. Amemiya, S.; Yang, X. T.; Wazenegger, T. L., Voltammetry of the phase transfer of polypeptide protamines across polarized liquid/liquid interfaces, 2003, *Journal of the American Chemical Society* **2003,** *125* (39), 11832-11833.
67. Yuan, Y.; Amemiya, S., Facilitated protamine transfer at polarized water/1,2-dichloroethane interfaces studied by cyclic voltammetry and chronoamperometry at micropipet electrodes, 2004, *Anal. Chem.* **2004,** *76* (23), 6877-6886.
68. Kasahara, T.; Nishi, N.; Yamamoto, M.; Kakiuchi, T., Electrochemical instability in the transfer of cationic surfactant across the 1,2-dichloroethane/water interface, 2004, *Langmuir* **2004,** *20* (3), 875-881.
69. Kakiuchi, T., Electrochemical instability in facilitated transfer of alkaline-earth metal ions across the nitrobenzene water interface, 2004, *Journal of Electroanalytical Chemistry* **2004,** *569* (2), 287-291.
70. Guo, J. D.; Yuan, Y.; Amemiya, S., Voltammetric detection of heparin at polarized blood plasma/1,2-dichloroethane interfaces, 2005, *Analytical Chemistry* **2005,** *77* (17), 5711-5719.
71. Vagin, M. Y.; Trashin, S. A.; Ozkan, S. Z.; Karpachova, G. P.; Karyakin, A. A., Electroactivity of redox-inactive proteins at liquid|liquid interface, 2005, *Journal of Electroanalytical Chemistry* **2005,** *584* (2), 110-116.
72. Shinshi, M.; Sugihara, T.; Osakai, T.; Goto, M., Electrochemical extraction of proteins by reverse micelle formation, 2006, *Langmuir* **2006,** *22* (13), 5937-5944.
73. Trojánek, A.; Langmaier, J.; Samcová, E.; Samec, Z., Counterion binding to protamine polyion at a polarised liquid–liquid interface, 2007, *Journal of Electroanalytical Chemistry* **2007,** *603* (2), 235-242.
74. Kitazumi, Y.; Kakiuchi, T., Emergence of the electrochemical instability in transfer of decylammonium ion across the 1,2-dichloroethane|water interface formed at the tip of a micropipette, 2007, *Journal of Physics: Condensed Matter* **2007,** *19* (37), 375104.
75. Osakai, T.; Shinohara, A., Electrochemical aspects of the reverse micelle extraction of proteins, 2008, *Analytical Sciences* **2008,** *24* (7), 901-906.

76. Rodgers, P. J.; Jing, P.; Kim, Y.; Amemiya, S., Electrochemical-recognition of synthetic heparin mimetic at liquid/liquid microinterfaces, 2008, *Journal of the American Chemical Society* **2008,** *130* (23), 7436-7442.
77. Herzog, G.; Kam, V.; Arrigan, D. W. M., Electrochemical behaviour of haemoglobin at the liquid/liquid interface, 2008, *Electrochimica Acta* **2008,** *53* (24), 7204-7209.
78. Kivlehan, F.; Lanyon, Y. H.; Arrigan, D. W. M., Electrochemical study of insulin at the polarized liquid-liquid interface, 2008, *Langmuir* **2008,** *24* (17), 9876-9882.
79. Scanlon, M. D.; Jennings, E.; Arrigan, D. W. M., Electrochemical behaviour of hen-egg-white lysozyme at the polarised water/1,2-dichloroethane interface, 2009, *Physical Chemistry Chemical Physics* **2009,** *11* (13), 2272-2280.
80. Osakai, T.; Yuguchi, Y.; Gohara, E.; Katano, H., Direct Label-free Electrochemical Detection of Proteins Using the Polarized Oil/Water Interface, 2010, *Langmuir* **2010,** *26* (13), 11530-11537.
81. Herzog, G.; Roger, A.; Sheehan, D.; Arrigan, D. W. M., Ion-Transfer Voltammetric Behavior of Protein Digests at Liquid vertical bar Liquid Interfaces, 2010, *Analytical Chemistry* **2010,** *82* (1), 258-264.
82. Herzog, G.; Eichelmann-Daly, P.; Arrigan, D. W. M., Electrochemical behaviour of denatured haemoglobin at the liquid/liquid interface, 2010, *Electrochem. Commun.* **2010,** *12* (3), 335-337.
83. Kitazumi, Y.; Kakiuchi, T., A model of the electrochemical instability at the liquid|liquid interface based on the potential-dependent adsorption and Gouy's double layer theory, 2010, *Journal of Electroanalytical Chemistry* **2010,** *648* (1), 8-14.
84. Scanlon, M. D.; Strutwolf, J.; Arrigan, D. W. M., Voltammetric behaviour of biological macromolecules at arrays of aqueous vertical bar organogel micro-interfaces, 2010, *Physical Chemistry Chemical Physics* **2010,** *12* (34), 10040-10047.
85. Herzog, G.; Nolan, M. T.; Arrigan, D. W. M., Haemoglobin unfolding studies at the liquid-liquid interface, 2011, *Electrochemistry Communications* **2011,** *13* (7), 723-725.
86. Zhai, J.; Hoffmann, S. V.; Day, L.; Lee, T.-H.; Augustin, M. A.; Aguilar, M.-I.; Wooster, T. J., Conformational Changes of α-Lactalbumin Adsorbed at Oil–Water Interfaces: Interplay between Protein Structure and Emulsion Stability, 2011, *Langmuir* **2011**.
87. Hartvig, R. A.; van de Weert, M.; Ostergaard, J.; Jorgensen, L.; Jensen, H., Formation of Dielectric Layers and Charge Regulation in Protein Adsorption at Biomimetic Interfaces, 2012, *Langmuir* **2012,** *28* (3), 1804-1815.
88. Alvarez de Eulate, E.; Arrigan, D. W. M., Adsorptive stripping voltammetry of hen-egg-white-lysozyme via adsorption-desorption at an array

of liquid-liquid microinterfaces, 2012, *Analytical Chemistry* **2012,** *84* (5), 2505-2511.
89. Matsui, R.; Sakaki, T.; Osakai, T., Label-Free Amperometric Detection of Albumin with an Oil/Water-type Flow Cell for Urine Protein Analysis, 2012, *Electroanalysis* **2012,** *24* (5), 1164-1169.
90. Bates, R. G.; Macaskill, J. B., Standard Potential of the Silver-Silver Chloride Electrode, 1978, *Pure and Applied Chemistry* **1978,** *50* (11-1), 1701-1706.
91. Vanysek, P.; Ramirez, L. B., Interface between two immiscible liquid electrolytes: A review, 2008, *Journal of the Chilean Chemical Society* **2008,** *53* (2), 1455-1463.
92. Girault, H. H., Electrochemistry at the interface between two immiscible electrolyte solutions, 1987, *Electrochimica Acta* **1987,** *32* (3), 383-385.
93. Davies, T. J.; Ward-Jones, S.; Banks, C. E.; del Campo, J.; Mas, R.; Munoz, F. X.; Compton, R. G., The cyclic and linear sweep voltammetry of regular arrays of microdisc electrodes: Fitting of experimental data, 2005, *Journal of Electroanalytical Chemistry* **2005,** *585* (1), 51-62.
94. Beattie, P. D.; Delay, A.; Girault, H. H., Investigation of the kinetics of assisted potassium-ion transfer by dibenzo-18-crown-6 at the micro-ITIES by means of steady-state voltammetry, 1995, *Journal of Electroanalytical Chemistry* **1995,** *380* (1-2), 167-175.
95. Shao, Y. H.; Mirkin, M. V., Probing ion transfer at the liquid/liquid interface by scanning electrochemical microscopy (SECM), 1998, *Journal of Physical Chemistry B* **1998,** *102* (49), 9915-9921.
96. Arrigan, D. W. M., Nanoelectrodes, nanoelectrode arrays and their applications, 2004, *Analyst* **2004,** *129* (12), 1157-1165.
97. Saito, Y., A Theoretical Study on the Diffusion Current at the Stationary Electrodes of Circular and Narrow Band Types, 1968, *Review of Polarography* **1968,** *15* (6), 177-187.
98. Lee, H. J.; Beriet, C.; Ferrigno, R.; Girault, H. H., Cyclic voltammetry at a regular microdisc electrode array, 2001, *Journal of Electroanalytical Chemistry* **2001,** *502* (1–2), 138-145.
99. Fletcher, S.; Horne, M. D., Random assemblies of microelectrodes (RAM™ electrodes) for electrochemical studies, 1999, *Electrochemistry Communications* **1999,** *1* (10), 502-512.
100. Davies, T. J.; Compton, R. G., The cyclic and linear sweep voltammetry of regular and random arrays of microdisc electrodes: Theory, 2005, *Journal of Electroanalytical Chemistry* **2005,** *585* (1), 63-82.
101. Strutwolf, J.; Scanlon, M. D.; Arrigan, D. W. M., Electrochemical ion transfer across liquid/liquid interfaces confined within solid-state micropore arrays - simulations and experiments, 2009, *Analyst* **2009,** *134* (1), 148-158.

102. Wang, J., Stripping analysis at bismuth electrodes: A review, 2005, *Electroanalysis* **2005,** *17* (15-16), 1341-1346.
103. Paneli, M. G.; Voulgaropoulos, A., Applications of adsorptive stripping voltammetry in the determination of trace and ultratrace metals, 1993, *Electroanalysis* **1993,** *5* (5-6), 355-373.
104. Blanco, E.; Ruso, J. M.; Sabin, J.; Prieto, G.; Sarmiento, F., Thermal stability of lysozyme and myoglobin in the presence of anionic surfactants, 2007, *Journal of Thermal Analysis and Calorimetry* **2007,** *87* (1), 211-215.
105. Kendrew, J. C.; Bodo, G.; Dintzis, H. M.; Parrish, R. G.; Wyckoff, H.; Phillips, D. C., A three-dimensional model of the myoglobin molecule obtained by x-ray analysis, 1958, *Nature* **1958,** *181* (4610), 662-666.
106. Paulo, T. D.; Diogenes, I. C. N.; Abruna, H. D., Direct Electrochemistry and Electrocatalysis of Myoglobin Immobilized on L-Cysteine Self-Assembled Gold Electrode, 2011, *Langmuir* **2011,** *27* (5), 2052-2057.
107. Rajesh; Sharma, V.; Tanwar, V. K.; Mishra, S. K.; Biradar, A. M., Electrochemical impedance immunosensor for the detection of cardiac biomarker Myogobin (Mb) in aqueous solution, 2010, *Thin Solid Films* **2010,** *519* (3), 1167-1170.
108. Suprun, E.; Bulko, T.; Lisitsa, A.; Gnedenko, O.; Ivanov, A.; Shumyantseva, V.; Archakov, A., Electrochemical nanobiosensor for express diagnosis of acute myocardial infarction in undiluted plasma, 2010, *Biosensors & Bioelectronics* **2010,** *25* (7), 1694-1698.
109. McDonnell, B.; Hearty, S.; Leonard, P.; O'Kennedy, R., Cardiac biomarkers and the case for point-of-care testing, 2009, *Clinical Biochemistry* **2009,** *42* (7–8), 549-561.
110. Melanson, S. F.; Tanasijevic, M. J., Laboratory diagnosis of acute myocardial injury, 2005, *Cardiovascular Pathology* **2005,** *14* (3), 156-161.
111. Herzog, G.; O' Sullivan, S.; Ellis, J. S.; Arrigan, D. W. M., Sensing via Voltammetric Ion-Transfer at an Aqueous-Organogel Micro-Interface Array, 2011, *Sensor Letters* **2011,** *9*, 721-724.
112. Liu, S. J.; Li, Q.; Shao, Y. H., Electrochemistry at micro- and nanoscopic liquid/liquid interfaces, 2011, *Chemical Society reviews* **2011,** *40* (5), 2236-2253.
113. Scanlon, M. D.; Strutwolf, J.; Blake, A.; Iacopino, D.; Quinn, A. J.; Arrigan, D. W. M., Ion-Transfer Electrochemistry at Arrays of Nanointerfaces between Immiscible Electrolyte Solutions Confined within Silicon Nitride Nanopore Membranes, 2010, *Analytical Chemistry* **2010,** *82* (14), 6115-6123.
114. Cunnane, V. J.; Schiffrin, D. J.; Williams, D. E., micro cavity electrode - a new typre of liquid liquid microelectrode, 1995, *Electrochimica Acta* **1995,** *40* (18), 2943-2946.

115. Herzog, G.; Arrigan, D. W. M., Electrochemical strategies for the label-free detection of amino acids, peptides and proteins, 2007, *Analyst* **2007,** *132* (7), 615-632.
116. Jing, P.; Kim, Y.; Amemiya, S., Voltammetric Extraction of Heparin and Low-Molecular-Weight Heparin across 1,2-Dichloroethane/Water Interfaces, 2009, *Langmuir* **2009,** *25* (23), 13653-13660.
117. Ellis, J. S.; Xu, S. Q.; Wang, X.; Herzog, G.; Arrigan, D. W. M.; Thompson, M., Interaction of surface-attached haemoglobin with hydrophobic anions monitored by on-line acoustic wave detector, 2010, *Bioelectrochemistry* **2010,** *79* (1), 6-10.
118. Hartvig, R. A.; Mendez, M. A.; van de Weert, M.; Jorgensen, L.; Ostergaard, J.; Girault, H. H.; Jensen, H., Interfacial Complexes between a Protein and Lipophilic Ions at an Oil-Water Interface, 2010, *Analytical Chemistry* **2010,** *82* (18), 7699-7705.
119. Herzog, G.; Moujahid, W.; Strutwolf, J.; Arrigan, D. W. M., Interactions of proteins with small ionised molecules: electrochemical adsorption and facilitated ion transfer voltammetry of haemoglobin at the liquid vertical bar liquid interface, 2009, *Analyst* **2009,** *134* (8), 1608-1613.
120. Scanlon, M. D.; Herzog, G.; Arrigan, D. W. M., Electrochemical detection of oligopeptides at silicon-fabricated micro-liquid vertical bar liquid interfaces, 2008, *Analytical Chemistry* **2008,** *80* (15), 5743-5749.
121. Lee, H. J.; Beattie, P. D.; Seddon, B. J.; Osborne, M. D.; Girault, H. H., Amperometric ion sensors based on laser-patterned composite polymer membranes, 1997, *Journal of Electroanalytical Chemistry* **1997,** *440* (1–2), 73-82.
122. Osakai, T.; Kakutani, T.; Senda, M., A.C. Polarographic Study of Ion Transfer at the Water Nitrobenzene Interface, 1984, *Bulletin of the Chemical Society of Japan* **1984,** *57* (2), 370-376.
123. Dautrevaux, M.; Boulanger, Y.; Han, K.; Biserte, G., Structure covalente de la myoglobine de cheval, 1969, *European Journal of Biochemistry* **1969,** *11* (2), 267-277.
124. Evans, S. V.; Brayer, G. D., High-resolution study of the three-dimensional structure of horse heart metmyoglobin, 1990, *Journal of Molecular Biology* **1990,** *213* (4), 885-897.
125. Wang, J., 2000, *Analytical electrochemistry* **2000,** *2nd ed*, 209.
126. Perrenoud-Rinuy, J.; Brevet, P. F.; Girault, H. H., Second harmonic generation study of myoglobin and hemoglobin and their protoporphyrin IX chromophore at the water/1,2-dichloroethane interface, 2002, *Physical Chemistry Chemical Physics* **2002,** *4* (19), 4774-4781.
127. Maurus, R.; Bogumil, R.; Nguyen, N. T.; Mauk, A. G.; Brayer, G., Structural and spectroscopic studies of azide complexes of horse heart myoglobin and the His-64 -> Thr variant, 1998, *Biochemical Journal* **1998,** *332*, 67-74.

128. Yano, Y. F.; Uruga, T.; Tanida, H.; Terada, Y.; Yamada, H., Protein Salting Out Observed at an Air-Water Interface, 2011, *Journal of Physical Chemistry Letters* **2011,** *2* (9), 995-999.
129. Curtis, R. A.; Ulrich, J.; Montaser, A.; Prausnitz, J. M.; Blanch, H. W., Protein-protein interactions in concentrated electrolyte solutions - Hofmeister-series effects, 2002, *Biotechnology and Bioengineering* **2002,** *79* (4), 367-380.
130. Baldwin, R. L., How Hofmeister ion interactions affect protein stability, 1996, *Biophysical Journal* **1996,** *71* (4), 2056-2063.
131. Kuehner, D. E.; Engmann, J.; Fergg, F.; Wernick, M.; Blanch, H. W.; Prausnitz, J. M., Lysozyme net charge and ion binding in concentrated aqueous electrolyte solutions, 1999, *Journal of Physical Chemistry B* **1999,** *103* (8), 1368-1374.
132. Dumetz, A. C.; Snellinger-O'Brien, A. M.; Kaler, E. W.; Lenhoff, A. M., Patterns of protein - protein interactions in salt solutions and implications for protein crystallization, 2007, *Protein Science* **2007,** *16* (9), 1867-1877.
133. Zhang, Y. J.; Cremer, P. S., The inverse and direct Hofmeister series for lysozyme, 2009, *Proceedings of the National Academy of Sciences of the United States of America* **2009,** *106* (36), 15249-15253.
134. Dumetz, A. C.; Chockla, A. M.; Kaler, E. W.; Lenhoff, A. M., Effects of pH on protein-protein interactions and implications for protein phase behavior, 2008, *Biochimica Et Biophysica Acta-Proteins and Proteomics* **2008,** *1784* (4), 600-610.
135. Anderson, A. B.; Robertson, C. R., Absorption spectra indicate conformational alteration of myoglobin adsorbed on polydimethylsiloxane, 1995, *Biophysical Journal* **1995,** *68* (5), 2091-2097.
136. Rimington, C., Spectral-absorption coefficients of some porphyrins in the Soret-band region, 1960, *Biochem J* **1960,** *75* (3), 620-623.
137. Jones, C. M., Protein Unfolding of metMyoglobin Monitored by Spectroscopic Techniques, 1999, *Chem. Educator* **1999,** *4*, 94-101.
138. Walsh, D. M.; Selkoe, D. J., Deciphering the molecular basis of memory failure in Alzheimer's disease, 2004, *Neuron* **2004,** *44* (1), 181-193.
139. Cooper, G. J. S.; Willis, A. C.; Clark, A.; Turner, R. C.; Sim, R. B.; Reid, K. B. M., Purification and characterization of a peptide from amyloid-rich pancreases of type-2 diabetic-patients, 1987, *Proceedings of the National Academy of Sciences of the United States of America* **1987,** *84* (23), 8628-8632.
140. Castillo, M. J.; Scheen, A. J.; Lefebvre, P. J., Amylin Islet Amyloid Polypeptide - Biochemistry, Physiology, Pathophysiology, 1995, *Diabetes Metab.* **1995,** *21* (1), 3-25.
141. Nanga, R. P. R.; Brender, J. R.; Xu, J. D.; Hartman, K.; Subramanian, V.; Ramamoorthy, A., Three-Dimensional Structure and Orientation of Rat Islet Amyloid Polypeptide Protein in a Membrane Environment by Solution NMR Spectroscopy, 2009, *J. Am. Chem. Soc.* **2009,** *131* (23), 8252-8261.

142. Zhou, N.; Chen, Z. Y.; Zhang, D. M.; Li, G. X., Electrochemical assay of human islet amyloid polypeptide and its aggregation, 2008, *Sensors* **2008,** *8* (9), 5987-5995.
143. Herzog, G.; Arrigan, D. W., Electrochemical strategies for the label-free detection of amino acids, peptides and proteins, 2007, *Analyst* **2007,** *132* (7), 615-632.
144. Scanlon, M. D.; Strutwolf, J.; Arrigan, D. W. M., Voltammetric behaviour of biological macromolecules at arrays of aqueous-organogel micro-interfaces, 2010, *Phys. Chem. Chem. Phys.* **2010,** *12* (34), 10040-10047.
145. Vagin, M. Y.; Trashin, S. A.; Ozkan, S. Z.; Karpachova, G. P.; Karyakin, A. A., Electroactivity of redox-inactive proteins at liquid/liquid interface, 2005, *J. Electroanal. Chem.* **2005,** *584* (2), 110-116.
146. Yonemoto, I. T.; Kroon, G. J. A.; Dyson, H. J.; Balch, W. E.; Kelly, J. W., Amylin Proprotein Processing Generates Progressively More Amyloidogenic Peptides that Initially Sample the Helical State†, 2008, *Biochemistry* **2008,** *47* (37), 9900-9910.
147. Herzog, G.; Flynn, S.; Johnson, C.; Arrigan, D. W. M., Electroanalytical Behavior of Poly-L-Lysine Dendrigrafts at the Interface between Two Immiscible Electrolyte Solutions, 2012, *Analytical Chemistry* **2012,** *84* (13), 5693-5699.
148. O'Sullivan, S.; Arrigan, D. W. M., Electrochemical behaviour of myoglobin at an array of microscopic liquid–liquid interfaces, 2012, *Electrochimica Acta* **2012,** *77* (0), 71-76.
149. Alvarez de Eulate, E.; Arrigan, D. W. M., Adsorptive Stripping Voltammetry of Hen-Egg-White-Lysozyme via Adsorption–Desorption at an Array of Liquid–Liquid Microinterfaces, 2012, *Anal. Chem.* **2012,** *84* (5), 2505-2511.
150. Silberring, J.; Ciborowski, P., Biomarker discovery and clinical proteomics, 2010, *Trac-Trends in Analytical Chemistry* **2010,** *29* (2), 128-140.
151. Rusling, J. F.; Kumar, C. V.; Gutkind, J. S.; Patel, V., Measurement of biomarker proteins for point-of-care early detection and monitoring of cancer, 2010, *Analyst* **2010,** *135* (10), 2496-2511.
152. Issaq, H. J.; Waybright, T. J.; Veenstra, T. D., Cancer biomarker discovery: Opportunities and pitfalls in analytical methods, 2011, *Electrophoresis* **2011,** *32* (9), 967-975.
153. Wang, J., Electrochemical glucose biosensors, 2008, *Chemical Reviews* **2008,** *108* (2), 814-825.
154. Heller, A.; Feldman, B., Electrochemical glucose sensors and their applications in diabetes management, 2008, *Chemical Reviews* **2008,** *108* (7), 2482-2505.
155. Alberti, K. G. M. M.; Zimmet, P. Z., Definition, diagnosis and classification of diabetes mellitus and its complications. Part 1: diagnosis and

classification of diabetes mellitus. Provisional report of a WHO Consultation, 1998, *Diabetic Medicine* **1998,** *15* (7), 539-553.
156. Andersen, L.; Dinesen, B.; Jørgensen, P. N.; Poulsen, F.; Røder, M. E., Enzyme immunoassay for intact human insulin in serum or plasma, 1993, *Clinical Chemistry* **1993,** *39* (4), 578-582.
157. Xu, M.; Luo, X.; Davis, J. J., The label free picomolar detection of insulin in blood serum, 2013, *Biosensors and Bioelectronics* **2013,** *39* (1), 21-25.
158. Yang, M.; Chao, T.-C.; Nelson, R.; Ros, A., Direct detection of peptides and proteins on a microfluidic platform with MALDI mass spectrometry, 2012, *Analytical and Bioanalytical Chemistry* **2012,** *404* (6-7), 1681-1689.
159. Park, J.; Karsten, S. L.; Nishida, S.; Kawakatsu, H.; Fujita, H., Application of a new microcantilever biosensor resonating at the air-liquid interface for direct insulin detection and continuous monitoring of enzymatic reactions, 2012, *Lab on a Chip* **2012,** *12* (20), 4115-4119.
160. Tao, L.; Kennedy, R. T., On-Line Competitive Immunoassay for Insulin Based on Capillary Electrophoresis with Laser-Induced Fluorescence Detection, 1996, *Analytical Chemistry* **1996,** *68* (22), 3899-3906.
161. Guo, C.; Chen, C.; Luo, Z.; Chen, L., Electrochemical behavior and analytical detection of insulin on pretreated nanocarbon black electrode surface, 2012, *Analytical Methods* **2012,** *4* (5), 1377-1382.
162. de Eulate, E. A.; Serls, L.; Arrigan, D. W. M., Detection of haemoglobin using an adsorption approach at a liquid-liquid microinterface array, 2013, *Analytical and Bioanalytical Chemistry* **2013,** *405* (11), 3801-3806.
163. Helmerhorst, E.; Stokes, G. B., Self-Association of Insulin - Its Ph-Dependence and Effect of Plasma, 1987, *Diabetes* **1987,** *36* (3), 261-264.
164. Davies, D. R.; Padlan, E. A.; Sheriff, S., Antibody-Antigen Complexes, 1990, *Annual Review of Biochemistry* **1990,** *59*, 439-473.
165. Braden, B. C.; Poljak, R. J., Structural Features of the Reactions - between Antibodies and Protein Antigens, 1995, *Faseb Journal* **1995,** *9* (1), 9-16.
166. Davies, D. R.; Cohen, G. H., Interactions of protein antigens with antibodies, 1996, *Proceedings of the National Academy of Sciences of the United States of America* **1996,** *93* (1), 7-12.
167. Dejaegere, A.; Choulier, L.; Lafont, V.; De Genst, E.; Altschuh, D., Variations in antigen-antibody association kinetics as a function of pH and salt concentration: A QSAR and molecular modeling study, 2005, *Biochemistry* **2005,** *44* (44), 14409-14418.
168. Li, Q.; Gordon, M.; Cao, C.; Ugen, K.; Morgan, D., Improvement of a low pH antigen-antibody dissociation procedure for ELISA measurement of circulating anti-Abeta antibodies, 2007, *BMC Neuroscience* **2007,** *8* (1), 22.

169. Herzog, G.; Raj, J.; Arrigan, D. W. M., Immobilisation of antibody on microporous silicon membranes, 2009, *Microchimica Acta* **2009,** *166* (3-4), 349-353.
170. Emons, H.; Heineman, W. R., Influence of bovine immunoglobulin G on faradaic reactions at electrodes, 1990, *Analyst* **1990,** *115* (7), 895-897.
171. Emons, H.; Werner, G.; Heineman, W. R., Voltammetric behaviour of immunoglobulin G at stationary mercury electrodes, 1990, *Analyst* **1990,** *115* (4), 405-408.
172. Sargent, A.; Loi, T.; Gal, S.; Sadik, O. A., The electrochemistry of antibody-modified conducting polymer electrodes, 1999, *Journal of Electroanalytical Chemistry* **1999,** *470* (2), 144-156.
173. Gooding, J. J.; Wasiowych, C.; Barnett, D.; Hibbert, D. B.; Barisci, J. N.; Wallace, G. G., Electrochemical modulation of antigen-antibody binding, 2004, *Biosensors & Bioelectronics* **2004,** *20* (2), 260-268.
174. Wu, X. Z.; Huang, T. M.; Mullett, W. M.; Yeung, J. M.; Pawliszyn, J., Determination of isoelectric point and investigation of immunoreaction in peanut allergenic proteins-rabbit IgG antibody system by whole-column imaged capillary isoelectric focusing, 2001, *Journal of Microcolumn Separations* **2001,** *13* (8), 322-326.
175. Alvarez de Eulate, E.; O'Sullivan, S.; Fletcher, S.; Newsholme, P.; Arrigan, D. W. M., Ion-Transfer Electrochemistry of Rat Amylin at the Water–Organogel Microinterface Array and Its Selective Detection in a Protein Mixture, 2013, *Chemistry – An Asian Journal* **2013**, n/a-n/a.
176. A.L. Lehninger, D. L. N., M.M. Cox, Worth, NY, 1993., *Principles of Biochemistry, second ed.,* **Worth, NY, 1993.**
177. Giardina, B.; Messana, I.; Scatena, R.; Castagnola, M., The multiple functions of hemoglobin, 1995, *Critical Reviews in Biochemistry and Molecular Biology* **1995,** *30* (3), 165-196.
178. Treacher, D. F.; Leach, R. M., ABC of oxygen - Oxygen transport - 1. Basic principles, 1998, *British Medical Journal* **1998,** *317* (7168), 1302-1306.
179. Ow, Y. L. P.; Green, D. R.; Hao, Z.; Mak, T. W., Cytochrome c: functions beyond respiration, 2008, *Nature Reviews Molecular Cell Biology* **2008,** *9* (7), 532-542.
180. Matzke, S. F.; Creagh, A. L.; Haynes, C. A.; Prausnitz, J. M.; Blanch, H. W., Mechanisms of Protein Solubilization in Reverse Micelles, 1992, *Biotechnology and Bioengineering* **1992,** *40* (1), 91-102.
181. Jarudilokkul, S.; Poppenborg, L. H.; Stuckey, D. C., Backward extraction of reverse micellar encapsulated proteins using a counterionic surfactant, 1999, *Biotechnology and Bioengineering* **1999,** *62* (5), 593-601.
182. Hilhorst, R.; Sergeeva, M.; Heering, D.; Rietveld, P.; Fijneman, P.; Wolbert, R. B. G.; Dekker, M.; Bijsterbosch, B. H., Protein Extraction from an Aqueous-Phase into a Reversed Micellar Phase - Effect of Water-Content

and Reversed Micellar Composition, 1995, *Biotechnology and Bioengineering* **1995,** *46* (4), 375-387.
183. Hilhorst, R.; Fijneman, P.; Heering, D.; Wolbert, R. B. G.; Dekker, M.; Vantriet, K.; Bijsterbosch, B. H., Protein Extraction Using Reversed Micelles, 1992, *Pure and Applied Chemistry* **1992,** *64* (11), 1765-1770.
184. Ono, T.; Goto, M.; Nakashio, F.; Hatton, T. A., Extraction behavior of hemoglobin using reversed micelles by dioleyl phosphoric acid, 1996, *Biotechnology Progress* **1996,** *12* (6), 793-800.
185. Hu, N.; Rusling, J. F., Surfactant-intercalated clay films for electrochemical catalysis. Reduction of trichloroacetic acid, 1991, *Analytical Chemistry* **1991,** *63* (19), 2163-2168.
186. Hu, N. F.; Howe, D. J.; Ahmadi, M. F.; Rusling, J. F., Stable Films of Cationic Surfactants and Phthalocyaninetetrasulfonate Catalysts, 1992, *Analytical Chemistry* **1992,** *64* (24), 3180-3186.
187. Nassar, A.-E. F.; Rusling, J. F.; Kumosinski, T. F., Salt and pH effects on electrochemistry of myoglobin in thick films of a bilayer-forming surfactant, 1997, *Biophysical Chemistry* **1997,** *67* (1–3), 107-116.
188. Chattopadhyay, K.; Mazumdar, S., Direct electrochemistry of heme proteins: effect of electrode surface modification by neutral surfactants, 2001, *Bioelectrochemistry* **2001,** *53* (1), 17-24.
189. Rajbongshi, J.; Das, D. K.; Mazumdar, S., Direct electrochemistry of dinuclear Cu(A) fragment from cytochrome c oxidase of Thermus thermophilus at surfactant modified glassy carbon electrode, 2010, *Electrochimica Acta* **2010,** *55* (13), 4174-4179.
190. Johnson, D. L.; Conley, A. J.; Martin, L. L., Direct electrochemistry of human, bovine and porcine cytochrome P450c17, 2006, *Journal of Molecular Endocrinology* **2006,** *36* (2), 349-359.
191. Ho, H. L. T.; Dryfe, R. A. W., Transport of Neutral and Ionic Solutes: The Gel/Electrode and Gel/Electrolyte Interfaces, 2009, *Langmuir* **2009,** *25* (21), 12757-12765.
192. Lee, H. J.; Seddon, B. J.; Girault, H. H., Amperometric ion sensors based on laser patterned micro-interface polymer membranes, 1997, *Proceedings of the Symposium on Chemical and Biological Sensors and Analytical Electrochemical Methods* **1997,** *97* (19), 719-720

1100.
193. Avranas, A.; Papadopoulos, N.; Papoutsi, D.; Sotiropoulos, S., Adsorption of the neutral macromonomeric surfactant Tween-80 at the mercury/electrolyte solution interface as a function of electrode potential and time, 2000, *Langmuir* **2000,** *16* (14), 6043-6053.
194. Wilkins, D. K.; Grimshaw, S. B.; Receveur, V.; Dobson, C. M.; Jones, J. A.; Smith, L. J., Hydrodynamic radii of native and denatured proteins measured by pulse field gradient NMR techniques, 1999, *Biochemistry* **1999,** *38* (50), 16424-16431.

195. Strutwolf, J.; Manzanares, J. A.; Williams, D. E., Effect of self-assembled surfactant structures on ion transport across the liquidliquid interface, 1999, *Electrochemistry Communications* **1999,** *1* (3-4), 139-144.
196. Kontturi, A. K.; Kontturi, K.; Murtomaki, L.; Quinn, B.; Cunnane, V. J., Study of ion transfer across phospholipid monolayers adsorbed at micropipette ITIES, 1997, *Journal of Electroanalytical Chemistry* **1997,** *424* (1-2), 69-74.
197. Kakiuchi, T.; Kotani, M.; Noguchi, J.; Nakanishi, M.; Senda, M., Phase-transition and ion permeability of phosphatidylcholine monolayers at the polarized oil-water interface, 1992, *Journal of Colloid and Interface Science* **1992,** *149* (1), 279-289.
198. Kakiuchi, T.; Kondo, T.; Senda, M., Divalent cation-induced phase-transition of phosphatidylserine monolayer at the polarized oil-water interface and its influence on the ion-transfer processes, 1990, *Bulletin of the Chemical Society of Japan* **1990,** *63* (11), 3270-3276.
199. de Groot, N. S.; Ventura, S., Amyloid fibril formation by bovine cytochrome c, 2005, *Spectroscopy* **2005,** *19* (4), 199-205.
200. Taketa, M.; Komori, H.; Hattori, Y.; Nagao, S.; Hirota, S.; Higuchi, Y., Crystallization and preliminary X-ray analysis of dimeric and trimeric cytochromes c from horse heart, 2010, *Acta Crystallographica Section F-Structural Biology and Crystallization Communications* **2010,** *66*, 1477-1479.
201. Margoliash, E.; Lustgarten, J., Interconversion of horse heart cytochrome C monomer and polymers, 1962, *The Journal of biological chemistry* **1962,** *237*, 3397-3405.
202. Schejter, A.; Glauser, S. C.; George, P.; Margoliash, E., Spectra of cytochrome c monomer and polymers, 1963, *Biochimica et Biophysica Acta (BBA) - Specialized Section on Enzymological Subjects* **1963,** *73* (4), 641-643.
203. Hirota, S.; Hattori, Y.; Nagao, S.; Taketa, M.; Komori, H.; Kamikubo, H.; Wang, Z. H.; Takahashi, I.; Negi, S.; Sugiura, Y.; Kataoka, M.; Higuchi, Y., Cytochrome c polymerization by successive domain swapping at the C-terminal helix, 2010, *Proceedings of the National Academy of Sciences of the United States of America* **2010,** *107* (29), 12854-12859.
204. Chiti, F.; Dobson, C. M., Protein misfolding, functional amyloid, and human disease. In *Annual Review of Biochemistry*, Annual Reviews: Palo Alto, 2006; Vol. 75, pp 333-366.
205. Makin, O. S.; Atkins, E.; Sikorski, P.; Johansson, J.; Serpell, L. C., Molecular basis for amyloid fibril formation and stability, 2005, *Proceedings of the National Academy of Sciences of the United States of America* **2005,** *102* (2), 315-320.
206. Pulawski, W.; Ghoshdastider, U.; Andrisano, V.; Filipek, S., Ubiquitous Amyloids, 2012, *Applied Biochemistry and Biotechnology* **2012,** *166* (7), 1626-1643.

207. Mironova, L. N.; Goginashvili, A. I.; Ter-Avanesyan, M. D., Biological Functions of Amyloids: Facts and Hypotheses, 2008, *Molecular Biology* **2008,** *42* (5), 710-719.
208. Sunde, M.; Blake, C. C. F., From the globular to the fibrous state: protein structure and structural conversion in amyloid formation, 1998, *Quarterly Reviews of Biophysics* **1998,** *31* (1), 1-+.
209. Khoshnoodi, J.; Cartailler, J. P.; Alvares, K.; Veis, A.; Hudson, B. G., Molecular recognition in the assembly of collagens: Terminal noncollagenous domains are key recognition modules in the formation of triple helical protomers, 2006, *Journal of Biological Chemistry* **2006,** *281* (50), 38117-38121.
210. Caughey, B.; Lansbury, P. T., Protofibrils, pores, fibrils, and neurodegeneration: Separating the responsible protein aggregates from the innocent bystanders, 2003, *Annual Review of Neuroscience* **2003,** *26*, 267-298.
211. White, D. A.; Buell, A. K.; Knowles, T. P. J.; Welland, M. E.; Dobson, C. M., Protein Aggregation in Crowded Environments, 2010, *Journal of the American Chemical Society* **2010,** *132* (14), 5170-5175.
212. Dupr, S.; Brunori, M.; Greenwood, C.; Wilson, M. T., Kinetics of carbon monoxide binding and electron transfer by cytochrome c polymers, 1974, *Biochemical journal* **1974,** *141* (1), 299-304.
213. Konno, T., Conformational diversity of acid-denatured cytochrome c studied by a matrix analysis of far-UV CD spectra, 1998, *Protein Science* **1998,** *7* (4), 975-982.
214. Fang, M.; Wilson, S. R.; Suslick, K. S., A Four-Coordinate Fe(III) Porphyrin Cation, 2008, *Journal of the American Chemical Society* **2008,** *130* (4), 1134-1135.
215. Buell, A. K.; Blundell, J. R.; Dobson, C. M.; Welland, M. E.; Terentjev, E. M.; Knowles, T. P. J., Frequency Factors in a Landscape Model of Filamentous Protein Aggregation, 2010, *Physical Review Letters* **2010,** *104* (22).

Appendix A

Preparation of $BTPPA^+TPBCl^-$ and of $BTPPA^+TFPB^-$ electrolytes

Chemicals:

Potassium tetrakis(4-chlorophenyl-borate) (K^+TPBCl^-)

Bis(triphenylphosphoranylidiene)ammonium chloride ($BTPPA^+Cl^-$)

Sodium tetrakis(4-flourorophenyl) borate (Na^+TFPB^-)

De ionised water (H_2O)

Methanol (MeOH)

Acetone

Reaction:

$BTPPA^+Cl^- + K^+TPBCl^- \rightarrow BTPPA^+TPBCl^- + K^+Cl^-$

The reaction stoichiometry of the metathesis reaction is 1:1, where 1 mole of $BTPPA^+Cl^-$ reacts with 1 mole of K^+TPBCl^-.

Procedure:

- 1.157 g of $BTPPA^+Cl^-$ is dissolved in 10 mL of H_2O/MeOH (1:2 v/v) solution.
- 1 g of K^+TPBCl^- is dissolved in 20 mL of H_2O/MeOH (1:2 v/v) and stirred by magnetic stirrer on a hot plate.

- The solution of $BTPPA^+Cl^-$ is added dropwise to the K^+TPBCl^- solution, upon addition a white precipitate is formed.
- The product is filtered using a Buchner funnel and washed with 10 mL of H_2O/MeOH (1:2 v/v).
- The product $BTPPA^+TPBCl^-$ is placed in a dessicator overnight.
- Once dried the product is washed on a Buchner funnel with 10 mL of acetone and 10 mL of H_2O.
- The product is put into the dessicator overnight.
- The final product is stored in a glass vial covered in aluminium foil to prevent degradation by light and stored at 4 °C in a refrigerator.

Reaction:

$BTPPA^+Cl^- + Na^+TFPB^- \rightarrow BTPPA^+TFPB^- + Na^+Cl^-$

The reaction stoichiometry of the metathesis reaction is 1:1, where 1 mole of $BTPPA^+Cl^-$ reacts with 1 mole of Na^+TFPB^-.

Procedure:

- 1.275 g of $BTPPA^+Cl^-$ is dissolved in 10 mL of H_2O/MeOH (1:2 v/v) solution.
- 1 g of Na^+TFPB^- is dissolved in 20 mL of H_2O/MeOH (1:2 v/v) and stirred by magnetic stirrer on a hot plate.
- The solution of $BTPPA^+Cl^-$ is added dropwise to the K^+TPBCl^- solution, upon addition a white precipitate is formed.
- The product is filtered using a Buchner funnel and washed with 10 mL of H_2O/MeOH (1:2 v/v).
- The product $BTPPA^+TFPB^-$ is placed in a dessicator overnight.
- Once dried the product is washed on a Buchner funnel with 10 mL of acetone and 10 mL of H_2O.
- The product is put into the dessicator overnight.
- The final product is stored in a glass vial covered in aluminium foil to prevent degradation by light and stored at 4 °C in a refrigerator.

Appendix B

List of chemicals	Purity	Product number	Supplier
Acetone	99.5 %	1090	Univar
Albumin (from bovine serum)	> 98 %	A7906	Sigma - Aldrich
Amylin (from rat)	-	H-9475	Bachem
Bis(triphenylphosphoranylidiene) ammonium chloride	97 %	223832	Sigma -Aldrich
Cytochrome *c* (from equine heart)	> 95 %	C2506	Sigma -Aldrich
1,6 – dichlorohexane	98 %	D63809	Sigma -Aldrich
Haemoglobin (from equine heart)	-	H2500	Sigma -Aldrich
Hydrochloric acid	-	31087	Sigma -Aldrich
Iron (III) chloride	97 %	157740	Sigma -Aldrich
Lithium chloride	> 99 %	62478	Sigma -Aldrich
Methanol	99.8 %	1230	Univar
Myoglobin (from equine heart)	> 90 %	M1882	Sigma -Aldrich
Poly(vinyl chloride), low molecular weight	-	81388	Sigma -Aldrich
Phosphate buffer saline	-	79382	Sigma -Aldrich
Potassium tetrakis (4-chlorophenyl) borate	> 98 %	60591	Sigma -Aldrich
Sodium chloride	> 99.5 %	71380	Sigma -Aldrich
Sodium hydroxide	> 98 %	S5881	Sigma -Aldrich
Sodium tetrakis(4-flourorophenyl) borate	> 97 %	72014	Sigma -Aldrich

dihydrate			
Tetraethyl ammonium chloride	> 98 %	T2265	Sigma -Aldrich